SYNTHESIS AND STUDIES OF METAL COMPLEXES OF NEW AZAMACROCYCLIC LIGANDS

A thesis submitted for

the degree of

Doctor of Philosophy

by

Hadi Ali Ahmed Omar

Department of Chemistry

University of Warwick

September 1987

TO MY FAMILY

TABLE OF CONTENTS

LIST OF TABLES

ACKNOWLEDGEMENTS

I wish to express my sincere thanks to the following people. My supervisor, Dr. P. Moore, for his advice, help and invaluable encouragement throughout this work, Dr. N. W. Alcock for all x-ray determination, Drs. O. W. Howarth and A. T. Harrison for running 2-D n.m.r. spectra and their interpretation, and finally my partners in the "Macrocycles Group" Dr. K. P. Balakrishnan, Dr. R. J. Crowte and Mr. C. J. Reader, for help in ways too many to number.

The financial support from the University of Al-Fateh, Tripoli, Libya, is also gratefully acknowledged.

Finally, my thanks go to all members of the Department of Chemistry for their help and encouragement.

PUBLICATIONS

Parts of the work reported in this thesis have been published or accepted for publication in the scientific literature with the following references:

N. W. Alcock, H. A. A. Omar and P. Moore,
J. Chem. Soc., Chem. Commun., 1985, 1058

N. W. Alcock, K. P. Balakrishnan, P. Moore and H. A. A. Omar,
J. Chem. Soc., Dalton Trans., 1987, 545

N. W. Alcock, P. Moore and H. A. A. Omar,
J. Chem. Soc., Dalton Trans., 1987, 1107

N. W. Alcock, P. Moore, H. A. A. Omar and C. J. Reader,
J. Chem. Soc., Dalton Trans., (in press)

N. W. Alcock, P. Moore and H. A. A. Omar,
Acta Cryst., (in press)

SYMBOLS AND ABBREVIATIONS

u.v.	ultraviolet
λ	wavelength
nm	nanometre (10^{-9} m)
ϵ	molar extinction coefficient
i.r.	infra-red
ν	frequency of absorption maximum
n.m.r.	nuclear magnetic resonance
δ	chemical shift
p.p.m.	parts per million
TMS	tetramethylsilane
s	singlet
d	doublet
t	triplet
p	pentplet
br	broad
^{1}H	proton
^{13}C	carbon-13
e.i.	electron impact
f.a.b.	fast atom bombardment
DMSO	dimethylsulphoxide
DMF	N,N-dimethylformamide
THF	tetrahydrofuran
3,2,3-tet	1,5,8,12-tetraazadodecane
2,3,2-tet	1,4,8,11-tetraazaundecane

SUMMARY

The macrocycles referred to in this summary are identified in the frontispiece.

Ten new azamacrocyclic ligands have been synthesied and characterised, together with some of the metal complexes they form with the divalent metal ions Ni^{2+}, Cu^{2+}, Zn^{2+}, Pb^{2+}, and Cd^{2+}. The pyridine-containing tetra-azamacrocycle L^{1}, the related N-functionalised ligands L^{13} and L^{17}-L^{19}, the penta-azamacrocycles L^{5}-L^{7}, as well as the piperidine-containing tetra-azamacrocycle L^{4}, and the binucleating octa-azamacrocycle L^{10} were investigated.

Diamagnetic square-planar complexes, $[Ni(L)][ClO_4]_2$ (L = L^{1} and L^{4}), were isolated, and the three isomers formed by L^{1} were separated and characterised by ^{13}C n.m.r. The structure of unsymmetric $[Ni(L^{1})][ClO_4]_2$ was established by x-ray crystallography. Paramagnetic Ni^{2+} complexes of L^{1} were found which were either square-pyramidal $[Ni(L^{1})X]^{n+}$ (X = unidentate ligand; n = 1 or 2), or cis-octahedral $[(Ni(L^{1}))_2OX]^{2+}$ (OX = oxalate ion) with a tetradentate bridging oxalate group. Structures of the oxalato-complex, and the five-co-ordinate complexes with X = Cl^{-} and dimethyl sulphoxide (DMSO), were established by x-ray crystallography.

Five- and six-co-ordinate complexes of L^{5}-L^{7} were prepared of the type $[M(L)]^{2+}$ (M = Cu, L = L^{5}-L^{7}; M = Zn, L = L^{7}; M = Cd, Pb, L = L^{6}-L^{7}) and $[M(L)(DMSO)]^{2+}$ (M = Ni, L = L^{6} and L^{7}; M = Zn, L = L^{6}). A crystal structure of $[Zn(L^{7})][ClO_4]_2$ shows that the geometry around the zinc ion is a distorted trigonal bipyramid, with the pyridine N-atom in the trigonal plane, and with a C_2 rotation axis passing through the Zn and pyridine N-atoms, and bisecting the C-C bond furthest removed from the pyridine ring.

The large ring octa-azamacrocycle L^{10} forms homobinuclear complexes of the type $[M_2(L^{10})]^{4+}$ (M = Ni, Cu, Zn), and a heterobinuclear complex $[NiCu(L^{10})]^{4+}$ was also separated.

Of the complexes formed by the pendent-arm macrocycles L^{13} and L^{17}-L^{19}, the structures formed by two of them were established by x-ray crystallography. In $[Ni(L^{13})OClO_3][ClO_4]$ the Ni^{2+} ion is octahedral with co-ordinated perchlorate ion in a trans-position to the co-ordinated pendent-arm, and in $[Cu(L^{19}H_2)Cl]Cl$ the complex is a distorted trigonal bipyramid with only one of the two pendent carboxylate groups co-ordinated, and with the N-atom furthest from the pyridine ring protonated and non-co-ordinating.

The ligands and diamagnetic complexes were studied by ^{1}H and ^{13}C n.m.r., and in several cases evidence found for more than one isomer in solution. The Ni^{2+} and Cu^{2+} complexes were studied by u.v.-visible spectroscopy, and all of the complexes examined by fast atom bombardment (f.a.b.) mass spectroscopy. Magnetic moments of the paramagnetic complexes were measured at room temperature, and most of the compounds analysed for their elemental composition.

MACROCYCLIC LIGANDS DISCUSSED IN THIS THESIS

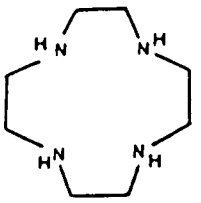

[12]aneN$_4$

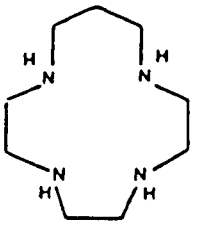

[13]aneN$_4$

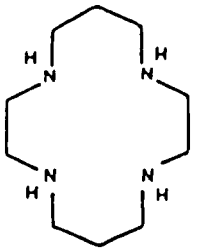

[14]aneN$_4$

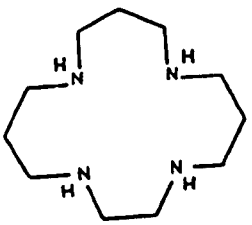

[15]aneN$_4$

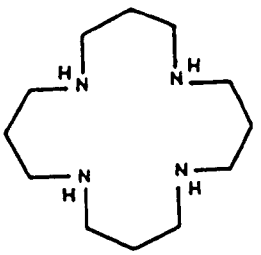

[16]aneN$_4$

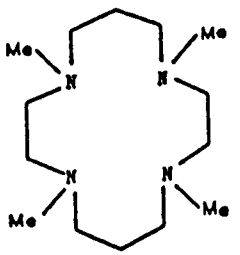

NMe$_4$-[14]aneN$_4$

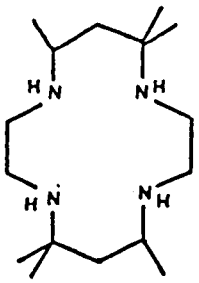

Me$_6$-[14]aneN$_4$

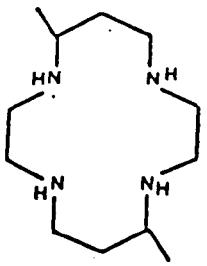

5,12-Me$_2$-[14]aneN$_4$

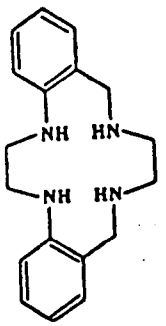

Dibenzo[14]aneN$_4$

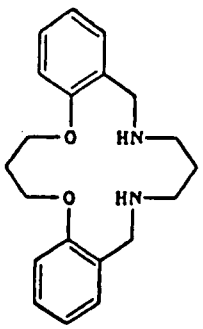

Dibenzo[16]aneN$_2$O$_2$

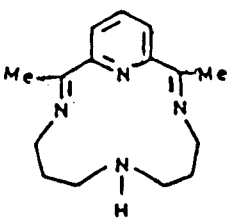

(CR)

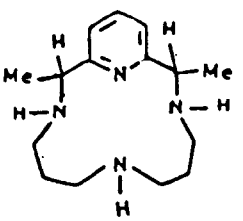

(CRH)

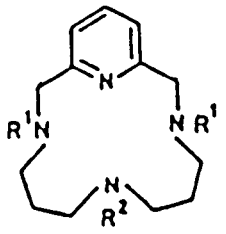

*L^1; $R^1 = R^2 = Me$

L^2; $R^1 = H$, $R^2 = Me$

L^3; $R^1 = -CH_2-C_6H_5$; $R^2 = H$

*L^{13}; $R^1 = H$, $R^2 = -CH_2CH_2-N$(pyrrolidine)

L^{14}; $R^1 = H$, $R^2 = -CH_2CH_2-NMe_2$

L^{15}; $R^1 = H$, $R^2 = -CH_2CH_2CH_2-NMe_2$

*L^{17}; $R^1 = -CH_2CN$, $R^2 = Me$

*L^{18}; $R^1 = -CH_2CN$, $-CH_2CONH_2$, $R^2 = Me$

*L^{19}; $R^1 = -CH_2CO_2^-$, $R^2 = Me$

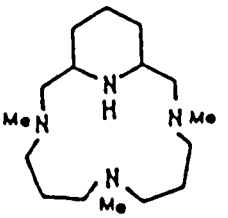

*L^4

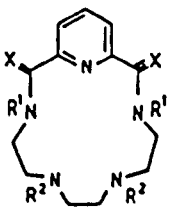

*L^5; $X = O$; $R^1 = H$, $R^2 = Me$

*L^6; $X = H_2$; $R^1 = H$, $R^2 = Me$

*L^7; $X = H_2$; $R^1 = R^2 = Me$

L^8; $X = Me$; H; $R^1 = R^2 = H$

*L^9; $X = H_2$; $R^1 = R^2 = H$

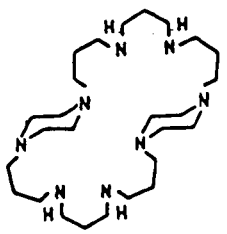

*L^{10}

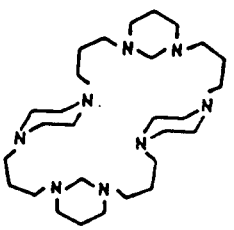

*L^{11}

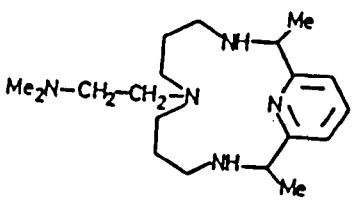

L^{12}

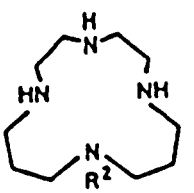

L^{16}; $R^2 = (CH_2)_2-NMe_2$

*These previously unreported compounds were synthesised as part of the work included in this thesis.

CHAPTER I

INTRODUCTORY CHAPTER

INTRODUCTION

The research described in this thesis is concerned with the synthesis of new azamacrocycles and studies of the complexes they form with metal ions such as copper(II), nickel(II), zinc(II) cadmium(II) and lead(II).

SECTION 1 MACROCYCLES (GENERAL)

Ever since the isolation of naturally occurring macrocyclic ligands such as those found in chlorophyll, haemoglobin, and other heme-containing units (e.g., cytochromes), co-ordination chemists have continued to develop new synthetic macrocycles and to explore their rich co-ordination chemistry. Although the initial interest can be traced to a desire to understand the naturally occurring systems, and to model their behaviour, it soon became evident that this class of compound had remarkable properties which warranted their careful investigation. Notable among the early discoveries were the especially robust phthalocyanines. Many of the complexes were found to have remarkable stability, and were often very inert to metal exchange and ligand substitution. Macrocyclic ligands were found to be capable of complexing a wide range of metal ions. For example, the unsaturated ring aza- and saturated thia-macrocycles were produced by the groups of Curtis[1] and Busch[2]. A recognition that the oxygen donor macrocyclic ligands are capable of complexing the alkali and alkaline earth metal ions led to the development of new ionophores, notably the crown-ethers first made by Pedersen[3], and the macrocyclic ligands of J. M. Lehn and co-workers[4], which were given the name of cryptands. Such work was parallel to the work on a recognition of the structures of the naturally occurring antibiotics

such as valinomycin and nonactin. The ability of such ligands to strongly complex the ions of group Ia and IIa is typical of the unusual behaviour often found in macrocyclic ligand chemistry. The progress so far has been well reviewed.[5-10] Notable among the discoveries made has been the ability to stabilise metal ions in uncommon oxidation states, both high and low (e.g., Cu^{3+}, Ni^{3+}, and Ni^{+}).[11,12] Important applications have already been found and no doubt many more will soon emerge. For example macrocycles find important uses in analytical chemistry (e.g., ion selective electrodes)[13], and crown ethers are useful in organic synthesis in enhancing the nucleophilicity of anions by 'freeing' them from cations in non-aqueous solvents.[14] New hydrometallurgical reagents are being developed[15], and new heterogeneous catalysts for selective oxidation chemistry (e.g., the use of metal phthalocyanines trapped in the cavities of zeolites).[16] It is, therefore necessary to discuss macrocyclic properties in some detail as outlined in the next sections.

SECTION 1.1 THE MATCHING OF MACROCYCLIC CAVITIES TO CATION DIAMETER

There is a close relationship between the cation size (ionic radius) for which maximum stability of a complex is found for a given macrocycle hole diameter.[17,18] This relationship has been extensively explored for polyether macrocycles, and some results are shown in Figure 1.1.[18,19,20]

One can draw four points from this figure.

(a) Monovalent cations show a small change in log K with the change in cationic radius.

(b) Polyether macrocyclic ligands have a sharp selectivity for certain cations over others which may be present in solution; for example differences in the stability constant values for Ca^{2+} and Pb^{2+} is about a factor of 10^5 in magnitude for the ligands in Figure 1.1.

(c) Stability constants increase with charge for cations which have approximately the same radius, e.g., K^+ (1.33 Å) forms less stable complexes than Ba^{2+} (1.35 Å) with the ligands in Figure 1.1.

(d) There are optimum stabilities for both monovalent and divalent cations. The "goodness of fit" of cations with a certain radius is well established by x-ray data.[18,20] It is also evident that as the hydration energy of the cations becomes predominant due to decreases in the cation size, the stability of macrocyclic complexes are diminished. Thermodynamic data for K^+, Rb^+ and Cs^+ has shown the dependence of log K on both ΔH^o and ΔS^o. Recently there has been an increased interest in determining the relationship between cavity size and cationic radius in saturated azamacrocyclic ligands, despite the difficulty caused by the way in which these ligands with different ring sizes may well adopt very different conformations around the metal ion.[21] Busch and co-workers[22] have reported a number of strain energy calculations for Co(III) and Ni(II) complexes of 12-16-membered tetraazamacrocycles coordinated in planar geometries, based on the visible spectroscopic parameter Dq. The ideal metal to nitrogen bond lengths for different macrocycles are shown from these calculations in Table 1.1. The ideal bond lengths fall in the range of 1.8-2.4 Å. For example, the copper-nitrogen bond distance ranges

FIGURE 1.1

(FROM REF. 19)

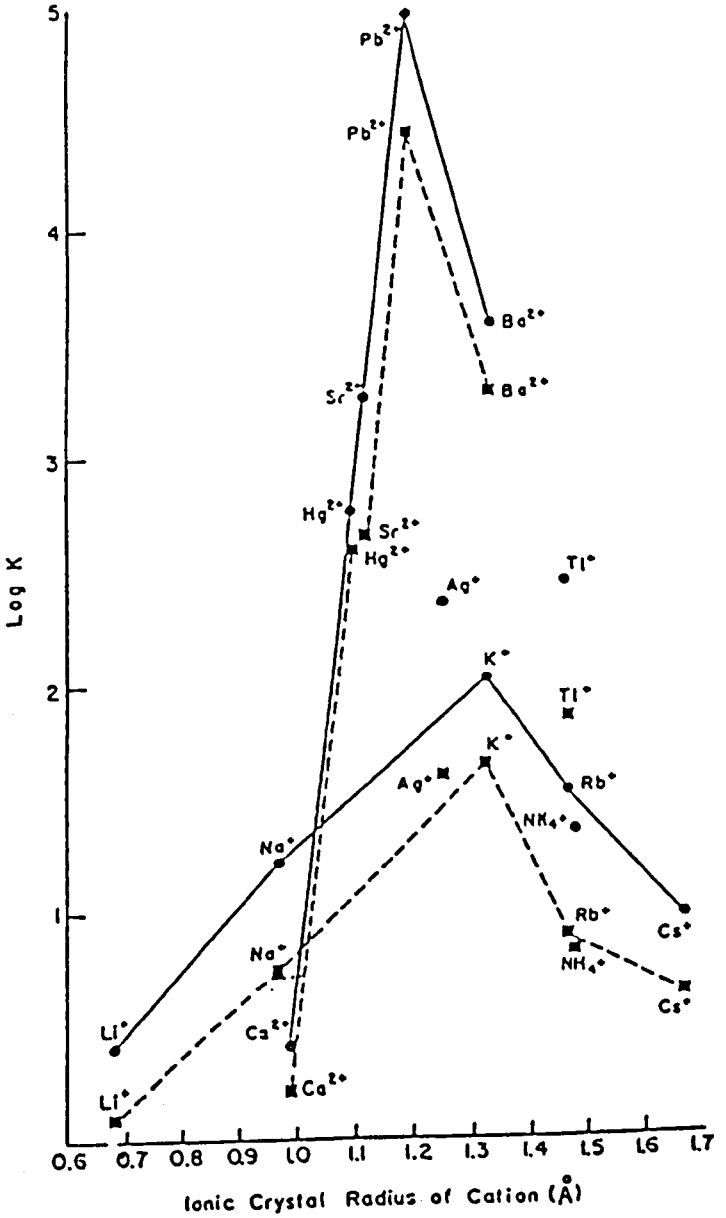

Plot of log K *vs* cation radius for the reaction in aqueous solution, $M^{n+} + L = ML^{n+}$ where L = dicyclohexyl-18-crown-6, isomer A (●), dicyclohexyl-18-crown-6 isomer B (■). T = 25°.

2.03-2.10 Å. According to these results, we can therefore conclude that the Cu^{2+} is the best ion to fit a [14]aneN_4 ligand. Similar work by Hancock, *et al.*[23-26] revealed that a large metal ion like Pb^{2+} prefers to complex the smaller macrocycle like [12]aneN_4(cyclen), while [14]aneN_4(cyclam) forms more stable complexes with smaller metal ions. It has been demonstrated recently by Tasker, *et al.*[27] that nickel(II) forms more stable complexes with [16]-ane-O_2N_2 macrocycle, Figure 1.2. This is because there is a reduction in the cavity size of the O_2N_2-macrocycle relative to its N_4 analogue by 0.04 Å. More recently the same group[21] has found that high spin nickel(II) (radius = 1.39 Å) is readily oxidised to low spin octahedral nickel(III) (radius = 1.30 Å) to fit dibenzo-14-ane-N_4 macrocycle with available cavity of 1.30 Å.

TABLE 1.1

IDEAL METAL-NITROGEN BOND LENGTHS AND DEVIATIONS FROM PLANARITY OF TETRAAZAMACROCYCLES (CALCULATED FROM STRAIN-ENERGY CALCULATIONS FOR SQUARE-PLANAR COORDINATION OF THE LIGAND; FROM REF. 22)

Ligand	Ideal M-N Length/A	Deviation from Ideal N_4 Plane
[12]-ane-N_4	1.83	± 0.41
[13]-ane-N_4	1.92	± 0.12
[14]-ane-N_4	2.07	0.00
[15]-ane-N_4	2.22	± 0.14
[16]-ane-N_4	2.38	0.00

FIGURE 1.2

(THE RELATIONSHIP BETWEEN HOLE SIZE AND THERMODYNAMIC STABILITY FOR NICKEL COMPLEXES OF O_2N_2 MACROCYCLES; FROM REF. 27)

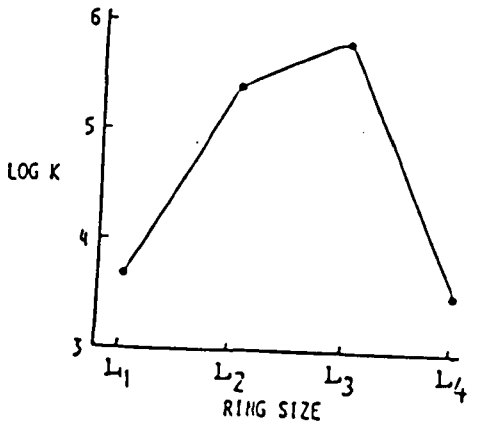

L_1-L_4 = [14], [15], [16] and [17]aneO_2N_2

SECTION 1.2 DONOR ATOM TYPE AND NUMBER

The stability of macrocyclic complexes is greatly affected by the type and number of ring donor atoms. Frensdorff[17] noted that substitution of nitrogen or sulfur for oxygen in 18-crown-6 (for nomenclature see Section 2.2) has a great effect, as shown by the data in Table 1.2, in producing macrocycles which have less affinity, or even no affinity, for alkali and alkaline earth metal ions (hard Lewis acids).[28] The stability constants of these metal complexes were found to decrease in order of the decreasing

electronegativity of the donor atoms, O > N > S. However, the effect of such substitution upon the complexation of silver(I) (a soft Lewis acid) was exactly the opposite. This may be due to the "soft" metal system providing some contribution to the covalent character of the metal-donor bond. An investigation of varying the number of ring donors without changing the ring size shows that 18-crown-5 is a much poorer donor for the *t*-butylammonium ion than 18-crown-6. Also, in the case of Ag^+ and Hg^{2+} an increase of complex stability is achieved by an increase in the number of donor atoms in the ring.[29]

TABLE 1.2

STABILITY CONSTANTS (LOG K) FOR THE FORMATION OF 1:1 COMPLEXES WITH THE LIGANDS $A(CH_2CH_2OCH_2CH_2OCH_2CH_2)_2B$; FROM REF. 17)

Polyether		Log K	
A	B	K^+ in MeOH	Ag in H_2O
O	O	6.10	1.60
NH	O	3.90	3.30
NH	NH	2.04	7.80
S	S	1.15	4.34

SECTION 1.3 THE MACROCYCLIC EFFECT

Macrocyclic ligands often form metal complexes which are considerably more stable than those of their open chain congeners. This extra stability is attributed to the so-called macrocyclic effect. Cabbiness and Margerum[30] in work on cyclic tetraamine ligands found that the macrocyclic effect is about ten times larger than the chelate effect observed for copper(II) complexes with multidentate open chain analogues. They employed visible absorption maxima (λ_{max}) to determine the approximate ΔH^{o} values for copper(II) cyclic tetraamine complexes. The value obtained was -126 kJ mol^{-1} which is clearly higher than ΔH^{o} values obtained for the related linear tetraamine complexes (Table 1.3). This is the case also in cyclic-polyethers, Frensdorff[17] observed that the stability constants of the cyclic polyether complexes are increased over those of noncyclic congeners by 3-4 log K units. This enhanced stability of macrocyclic complexes is believed to be based upon both enthalpy and entropy terms. Several attempts have been made to differentiate between the contributions from each term. Margerum and his co-workers[31,32] obtained a value of log K = 22.2 with, ΔH^{o} = -130 kJ mol^{-1} and ΔS^{o} = 8.4 J mol^{-1} K^{-1} using the temperature dependence of the equilibrium constant for Ni(II)-[14]-aneN_4 complex (Table 1.3). In the light of these results it is the enthalpy contributions which govern the macrocyclic effect. A similar conclusion was reached by Dei and Gori,[33] from their work on the copper(II) complexes of the same ligands. However, Kodama and Kimura[34] have reported values for the enthalpy of formation of the Cu(II) complexes with [12]-ane-N_4 of -77 K J mol^{-1} (ΔS^{o} = 216 J mol^{-1} K^{-1}), and by comparing these

TABLE 1.3

COMPARISON OF THERMODYNAMIC PARAMETERS FOR THE FORMATION OF 1:1 Cu^{II}, Ni^{II}, AMINE COMPLEXES IN AQUEOUS MEDIA

	log K	ΔH^o kJ mol^{-1}	ΔS^o J $K^{-1}mol^{-1}$	Ref.
$Ni(2,3,2\text{-tet})^{2+}$	15.3	-70.6	58.0	31
$Ni([14]aneN_4)^{2+}$	22.2	-130.0	-8.4	31
$Ni(5,12\text{-}Me_2\text{-}[14]\text{-}aneN_4)^{2+}$	21.9	-117.0	33.6	31
$Cu(2,3,2\text{-tet})^{2+}$	23.9	-116.0	24.4	38
$Cu(Me_6[14]aneN_4)^{2+}$	28.0	-126.0	113.0	30
$Cu([12]aneN_4)^{2+}$	24.8	-77.0	216.0	34
$Cu([12]aneN_4)^{2+}$	24.8	-95.3	152.0	37
$Cu([13]aneN_4)^{2+}$	29.1	-122.7	141.0	39
$Cu([14]aneN_4)^{2+}$	27.2	-127.7	95.0	40
$Cu([15]aneN_4)^{2+}$	24.4	-111.3	95.0	37

results with those obtained by Margerum's group, it is clear that in this case entropy has control of the macrocyclic effect. Also Paoletti and his collaborators[35,36] found that the entropy term was responsible primarily for the macrocyclic effect, using the same conditions as Kodama did. Moreover, they concluded that the relative magnitude of the enthalpy contribution is critically dependent on the match between cation and ligand cavity sizes for transition metals. This dichotomy regarding the origin of the macrocyclic effect has led to the conclusion that it is not simply defined, and that different systems may respond differently to stabilising factors.

SECTION 1.4 ELECTROCHEMICAL PROPERTIES

Macrocyclic ligands offer an unusual ability to stabilise a number of oxidation states of a coordinated metal ion. This character has received a great deal of attention in the past few years.[11,12,41-45] Fabbrizzi[46] demonstrated that both the high spin and low spin nickel(II) complexes of cyclam are oxidised more readily to nickel(III) species than the corresponding complexes of the open chain amine analogue (2,3,2-tet). The ring size has a great effect upon the redox properties of macrocyclic coordinated metals, and so the stability of unusual oxidation states of metal ions in such complexes basically depends upon the constrained metal-donor distance. This recognition led to extensive research into their electrochemistry to investigate the relationship between the ring size and the redox properties. Busch, *et al.*[43] in a comprehensive study, investigated the electrochemical behaviour of low-spin nickel(II) complexes of 27 tetraazamacrocycles. In this study they found that as the macrocyclic ring size decreases the Ni(II)/Ni(III) couple favours the trivalent state ($E_{1/2}$ = +1.3, +0.9, +0.69 volts, for [16], [15] and [14]-ane-N_4 respectively). Also the Ni(I)/Ni(II) couple shifts towards greater stability for the mono-valent ion as the ring size increases, ($E_{1/2}$ = -1.7, -1.57, -1.4 volts for [14], [15] and [16]-ane-N_4 respectively). Recently Suet, *et al.*[47] have reported the effect of changing the macrocyclic ring size on the disproportionation of the Ag(I) cation in rings of [14] to [20]-ane-N_4 macrocycles. This study reveals that the Ag(I) forms stable complexes with [18] and [20]-ane-N_4, whereas in the presence of [14] and [16]-ane-N_4, disproportionation to Ag^{2+} occurs. More recently, Sauvage and his co-workeres[48] have isolated and

characterised an air stable d^9 nickel(I) catenate complex, in which the metal oxidation state is stabilised by interlocking of two rings of this macrocycle. The conclusion one can draw from these studies is that the redox potentials are ring size dependent, and the simplest explanation of these properties is that the metal ion will tend to adjust its size (ionic radius) by oxidation or reduction to fit ideally a given ring size (see Section 1.1), so producing acceptable redox properties for the resulting complex.

SECTION 2 SYNTHESIS AND COMPARISON OF DIFFERENT MACROCYCLES

In the present decade numerous methods have been devised for the preparation of a vast array of macrocyclic ligands.[5,7,9,10,49] Ring sizes can be varied from nine to thirty-two members; donor atoms can include nitrogen, oxygen, sulfur, phosphorus and arsenic or any combination thereof; the number of donor atoms can be varied anywhere from three to nine; unsaturation in the ring can be regulated from completely saturated systems up to fully conjugated molecules; and ligand field strength can be controlled in a systematic manner. The most widely used synthetic routes are summarised in the next sections according to donor atom types, together with a discussion of some of the different characteristics of each type of macrocycle.

SECTION 2.1 POLYAZAMACROCYCLES

There is considerable interest in the preparation of nitrogen containing macrocycles, especially by transition metal chemists, because of their coordination behaviour to most of the first-row transition elements, and because they are more closely related to the naturally occurring macrocyclic ligands than those compounds with oxygen, sulfur and phosphorus donors. The synthetic routes to such compounds can be broadly classified as follows.

(1) STANDARD ORGANIC SYNTHESIS

Organic procedures employed in the synthesis of macrocycles are carried out in several steps to prepare linear amines followed by ring closure using high dilution techniques to avoid polymerisation side reactions (for more details see Chapter 3). The drawback of this procedure is that sometimes it gives very low

yields (< 10%).

(ii) Richman and Atkins[50] reported a useful procedure to prepare saturated polyazamacrocycles using deprotonated tosylated amines in dimethylformamide (DMF) solution at 100°C, without the need for high dilution, Scheme 1.1. The tosyl groups attached to the amines increase their acidity to make it easier to form the nucleophilic sodium salt *A*, which displaces the OTs leaving groups in *B*. This completes the cyclisation to give the fully protected macrocycle *C*; hydrolysis of *C* with concentrated sulfuric acid for 48 h gives the protonated amine macrocycle. This method has found application in preparing saturated macrocycles with pendent arms containing a donating group.[9,51,52] The pendent group is likely to be important since on axial co-ordination to a metal ion it may enhance the coordination of another group from the other side to complete an octahedral geometry. Such ligands may find application in the synthesis of an oxygen carrier, or in the chelation therapy of methyl-mercury(II) and other metal pollutants which are currently of environmental concern.[53,54]

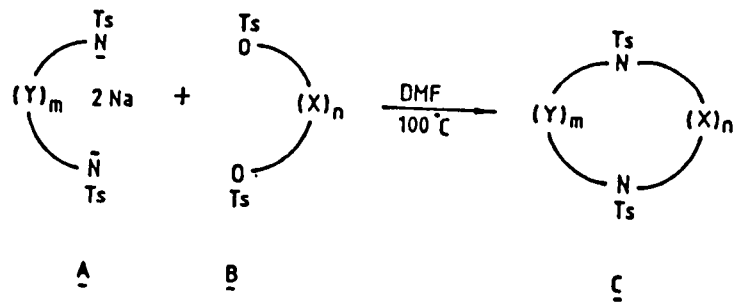

X = O or NTs
Y = X or pendent arm with donating group
m = n = 1 → 3
Ts = Toluene-p-sulphonate

SCHEME 1.1

(iii) The third approach[55,56] to the synthesis of azamacrocycles involves cyclisation by forming amide linkages, followed by reduction of the cyclic amide to give a simple saturated amine macrocycle, Scheme 1.2. This procedure has the advantage that it does not need a protecting tosyl group, which is often difficult to remove, and which tends to cause a reduction in the yield.

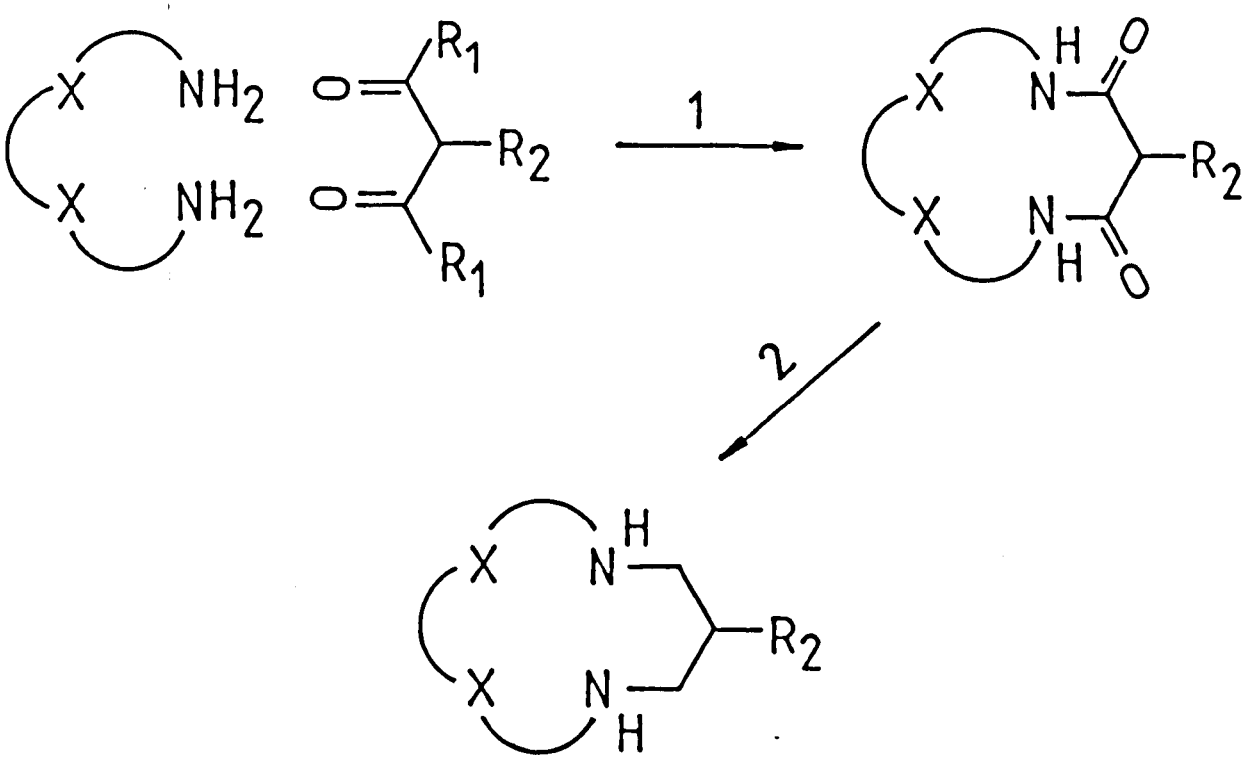

X = NH or O or S
R^1 = Cl or OEt
R_2 = any substituents

1 = reflux in EtOH
2 = $LiAlH_4$/THF
Reflux 24 h

SCHEME 1.2

(iv) The fourth procedure for the synthesis of azamacrocycles involves the use of metal ions *in situ* (template reactions); such metal ions control the steric course of a sequence of stepwise reactions by fixing the ligand geometry, i.e. by bringing the reactants into a favourable position to complete cyclisation and reduce the possibility of polymerisation. This procedure was first recognised by Curtis[57], who used the direct condensation between metal amine complexes and acetone to produce multi-substituted macrocycles of many sizes. A typical Curtis synthesis is shown in Scheme 1.3.

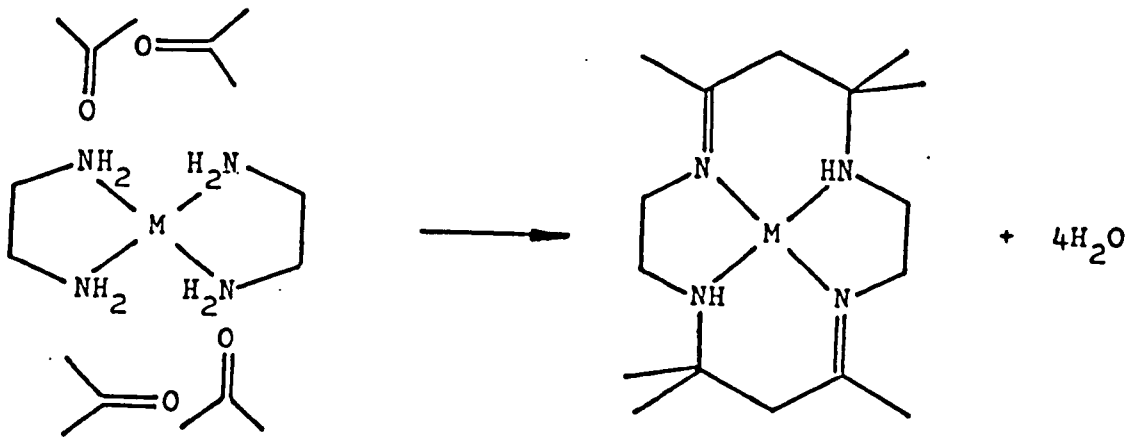

SCHEME 1.3

Barefield, *et al.*[58] prepared [14]-ane-N_4 (cyclam) using the template method, by condensation between the primary amine groups of the tetradentate ligand (3,2,3-tet) and glyoxal in the presence of Ni^{2+}, to produce a Schiff-base (diimine) *A*, Scheme 1.4. Reduction of the imine gave a good yield of the nickel(II) complex of the saturated amine *B*. The macrocycle is liberated by reaction of complex *B* with

excess NaCN in aqueous solution at high pH.

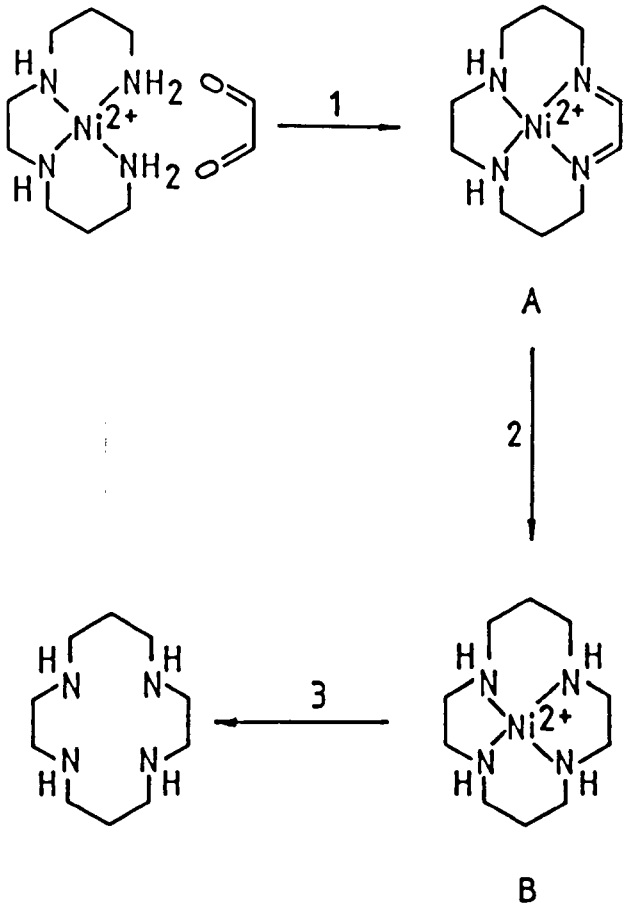

(1) H_2O, cool to 0°C, 4 h
(2) Reduction with $NaBH_4$ at 5°C
(3) Reaction with NaCN/NaOH

SCHEME 1.4

In situ reactions have been employed for the synthesis of a large number of macrocycles containing pyridine residues; these are prepared by a condensation reaction between 2,6-diacetylpyridine or pyridine-2,6-dicarbaldehyde and appropriate linear amine complexes, Scheme 1.5; for more details see Chapter 2, and reference 49.

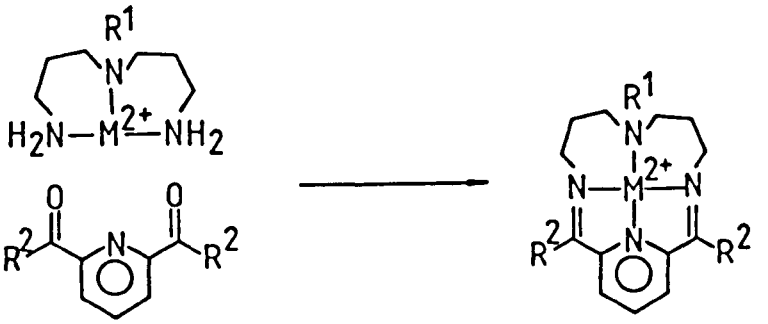

R^1 = R^2 or R^1 = pendent arm with donating group

R^2 = CH_3 or H

SCHEME 1.5

The metal ions most frequently employed for *in situ* macrocyclic synthesis are *d*-block metals. However, Drew *et al.*[59] and others have reported template syntheses of such ligands using s-block metal ions. The main advantage of *in situ* synthesis is normally the improved yields obtained by the addition of metal ions. This is due mainly to the substantial reduction of side reactions such as polymerisation. It is well known that Schiff-base macrocycles tend to be unstable in the uncomplexed state, and they are restricted to certain metals which are effective as templates. However, it has been found that the metal exchange is possible in such Schiff-base macrocyclic complexes with metals which are not useful in direct template routes.[60]

The syntheses of azamacrocycles have expanded to include cases in which two macrocycles can be linked together with hydrocarbon bridges either through the nitrogen donor or the carbon backbone. These new macrocycles are capable of incorporating two different metal ions at the same time.[61]

SECTION 2.2 CYCLIC POLYETHER LIGANDS

The first cyclic polyether "crown" was discovered accidentally by Pedersen in the late 1960's.[62] The name "crown" has been adapted for these compounds; examples are in Figure 1.3 which shows how the name is composed of the ring substituents, and the total number of atoms in the main ring. Since Pedersen's discovery, the chemistry of these compounds has grown rapidly because of the unusual property they have in forming stable complexes with alkali, alkaline-earth and toxic heavy metal ions.[63,64]

This exceptional stability arises from the close fitting of the metal ion into the hole in the centre of the ligand (Section 1.1). The "crown" ethers have found their application in organic synthesis to promote the solubility of alkali metal salts such as $KMnO_4$ and KOH in organic solvents, where solubility of these salts can improve the reaction yield.[14,65] Crystal structure determinations of complexes formed by naturally occurring antibiotics[66] and related synthetic macrocycles[18,20,67] reveal the basic similarity in their mode of co-ordination to alkali metal cations.

Synthesis of polyether macrocycles can be achieved either by a condensation reaction between two reactants using the high dilution method, or in most cases by both condensation and *in*

FIGURE 1.3

Polyethers "crown" shapes and nomenclature

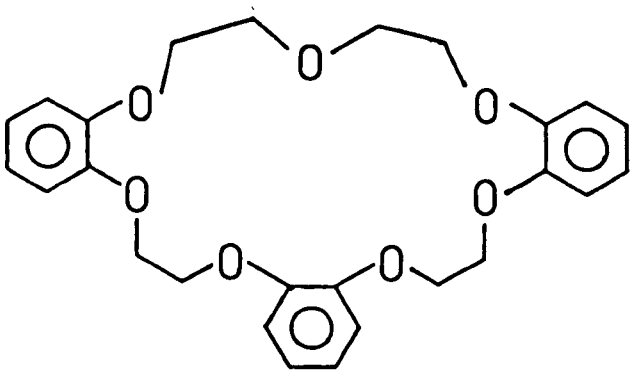

Tri-benzo-21-crown-7

Tri-benzo- describes the non-ethylene oxy-content; 21-describes the total number of atoms in the crown ring and 7- the number of hetero atoms in the ring.

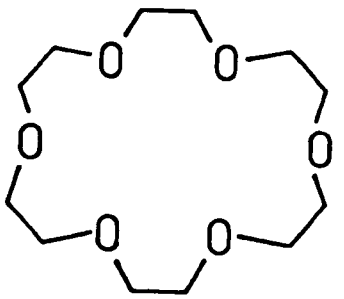

18-Crown-6

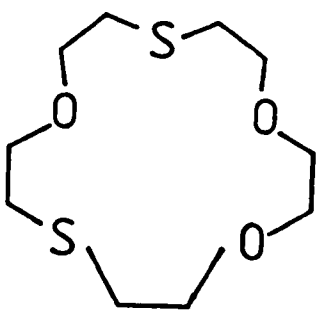

1,7-Dithia-15-crown-5

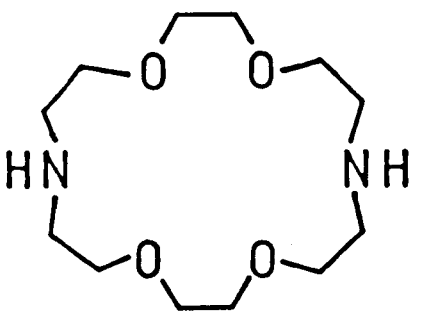

1,10-Diaza-18-crown-6

situ reactions at the same time. For example, using KOH as in reaction shown in Scheme 1.6, where the K^+ ion is also acting as a template to enhance the cyclisation process.[68]

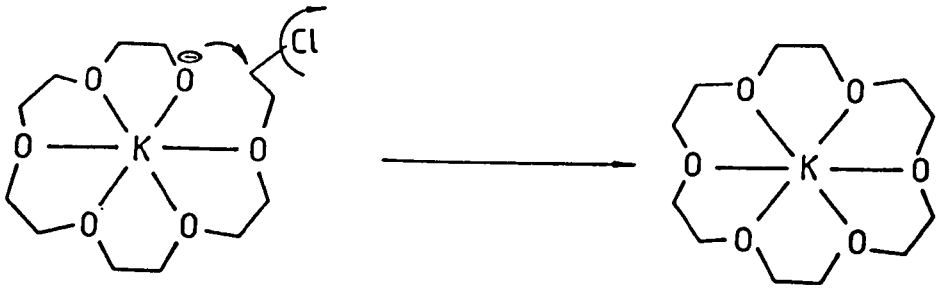

SCHEME 1.6

Another class of polyethers are three dimensional macrocycles, "cryptates"[2], Figure 1.4, which are bicyclic and contain nitrogen and oxygen donor atoms [e.g. $N(CH_2CH_2OCH_2CH_2OCH_2CH_2)_3N$]. These compounds have been developed by Lehn and his collaborators.[67] They can form more stable complexes with alkali metal ions than crown ethers[69], since the cation is contained inside the cavity of the cage (crypt). The cryptates are prepared by acylation of the diamino heterocycle to give a di-amide followed by hydride reduction as shown in Scheme 1.7.

FIGURE 1.4

The Cryptates and their nomenclature as designated in reference 67 by J. M. Lehn.

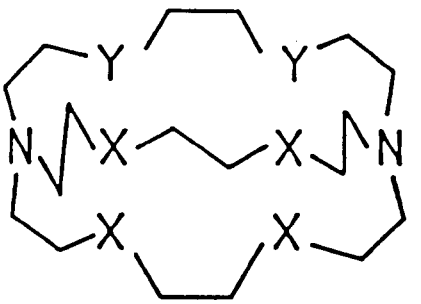

$[2_O.\ 2_O.\ 2_O]$ X = Y = O

$[2_O.\ 2_{OS}.\ 2_S]$ 3X = O; X + 2Y = S

$[2_O.\ 2_O.\ 2_N]$ X = O; Y = NCH_3

$[2.\ 2.\ 8_C]$ X = O; Y = CH_2

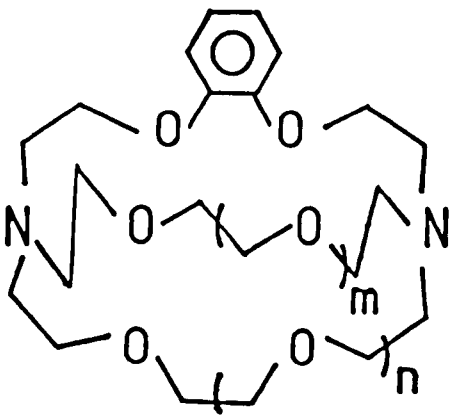

$[2_B.\ 1.\ 1]$ m = n = 0

$[2_B.\ 2.\ 1]$ m = 0; n = 1

$[2_B.\ 2.\ 2]$ m = n = 1

The symbol in brackets describes the nature of the hetero atoms and their numbers, and structure variations of the bridges.

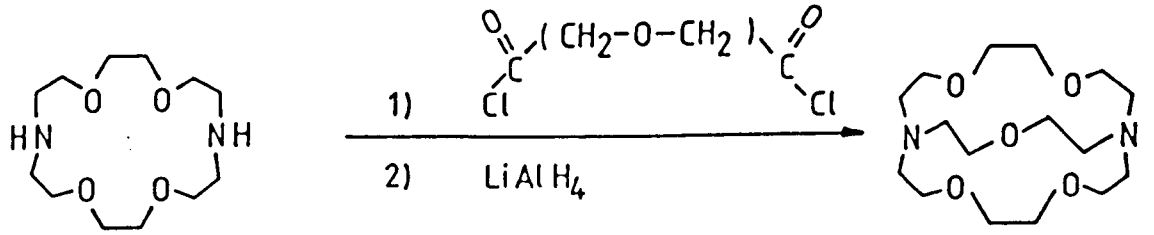

SCHEME 1.7

Again the chemistry of these ligands has been the subject of interesting research in which the hard oxygen donor is replaced with nitrogen or sulfur atoms to give new ligands capable of coordination to transition metal ions.[70,71] The coordination chemistry of these ligands have been investigated using x-ray crystallography,[20] i.r., n.m.r. spectroscopy[72] and f.a.b. mass spectroscopy.[64]

SECTION 2.3 CYCLIC POLYTHIAETHERS

Macrocycles containing sulfur donor atoms have not been as extensively investigated as those of analogous polyazamacrocycles and cyclic polyethers. This is partly due to synthetic difficulties arising from the preparation of precursor linear polydentate ligands, and the relatively poor yields afforded by ring closure using the high dilution technique. Also these compounds are much poorer in their coordinating ability compared with the analogous polyazamacrocycles. However, despite these problems macrocycles of this type have revealed interesting properties due to their flexibility. This is shown by the different modes of coordination they adopt with different classes of metal ion. For example, an

exo-conformation[73,74] with large metal ions, and an endoconformation[75] where the metal ion can fit the macrocyclic cavity. Cyclic thioethers have received much attention as simple models for blue copper proteins which are known to contain thiolate or thioether donors.[76,77]

Also, their ability to coordinate to "soft" (class b) metal ions has increased their importance in co-ordination chemistry. In addition to this, they have applications as solvent extractants for mercury(II) and silver(I), to increase the solubility of such metal ions in organic solvents.[78]

Gould and Schröder[79] have synthesised [9]-ane-S_3 and [18]-ane-S_6 by direct condensation of bis-(2-mercaptoethyl)sulphide and 1,2-dichloroethane, where the ring closure process takes place under the high dilution technique. The dicopper(I) complex of the large ring macrocycle was isolated and its x-ray crystal structure reported. Recently Wieghardt, *et al.*[80] reported an octahedral palladium(II) complex of [9]-ane-S_3. With each metal ion coordinated to two macrocycles. However, the introduction of template reactions in the preparation of cyclic polythiaether ligands has improved the reaction yield dramatically. For example, yields obtained for the preparation of 1,4,7-trithiacyclononane using a condensation reaction in a high dilution procedure was < 5%[81], whereas this compound can be obtained in yields up to 60% by involving a suitable metal ion.[82] Sellmann and Frank[83] have synthesised dibenzo-[18]-ane-S_6 in very good yield using an *in situ* reaction with routes summarised in Scheme 1.8.

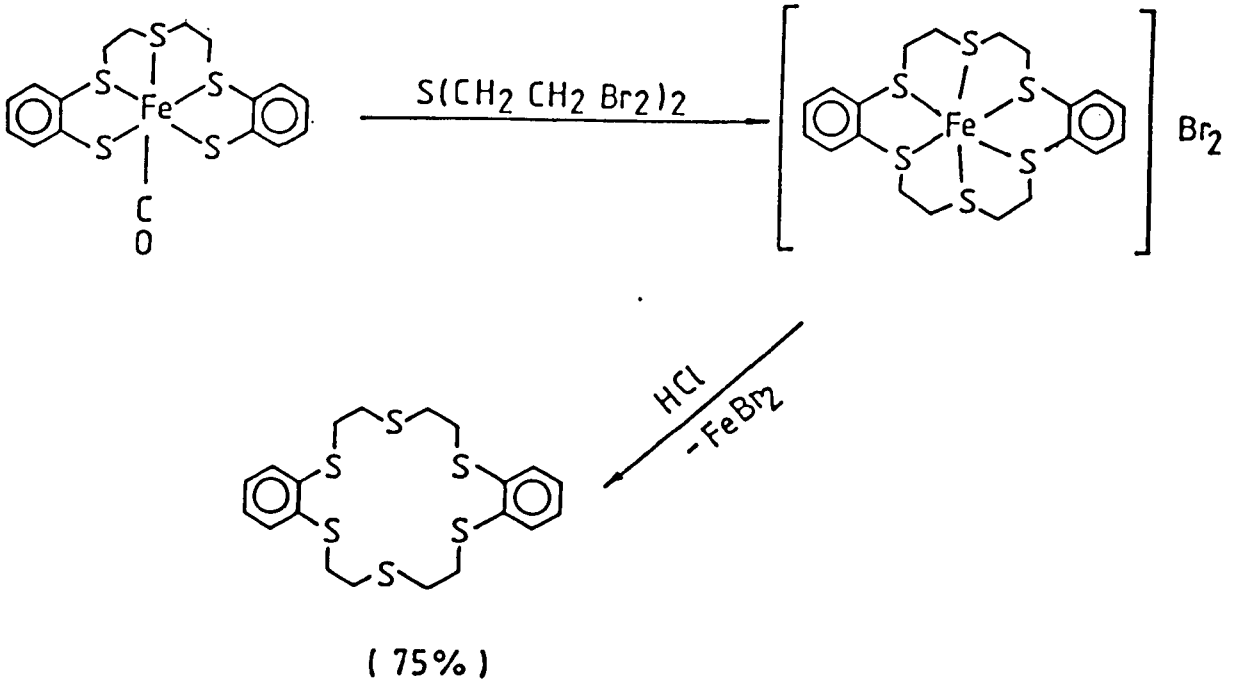

SCHEME 1.8

Synthesis of macrocycles containing exclusively sulfur and having unsaturation in the macrocyclic ring (similar to the pyridine containing macrocycles in Section 2.1) are relatively few. This is because unsaturation tends to lower the nucleophilicity of the sulfur atoms of thioethers by involving their lone pair of electrons in π-bonding. One such ligand based on a 2,5-thiophene linkage has been synthesised and its copper complex was isolated.[84] However, pyridine containing thioethers have been prepared recently by Lehn and his co-workers[85] using the condensation reaction between propane-1,3-dithiol with 2,6-di(bromomethyl)pyridine to give 1 + 1 and 2 + 2 adducts. Rhodium and palladium complexes of these

ligands have been reported. The chemistry of these ligands has been reviewed.[86,87]

SECTION 2.4 POLYPHOSPHORUS MACROCYCLES

The first metal complex containing a coordinated phosphino-group of a macrocycle was described in 1974.[88] Since that time considerable interest in the syntheses and complex formation reactions of polyphosphorus macrocycles has grown.[89-95] Phosphorus donors are well known for their properties of stabilising low oxidation state metal ions, and this, in combination with the macrocyclic effect discussed in Section 1.3, makes this area an attractive one. So far, most phosphorus macrocycles which have been reported contain other donors such as S, O, and N, Figure 1.5.

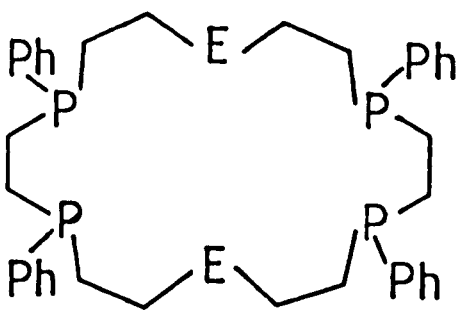

E = O or S or NH

FIGURE 1.5

Kyba, *et al*,[96] published the synthesis of tri- and tetra-phosphorus macrocycles using the high dilution procedure as shown in Scheme 1.9.

SCHEME 1.9

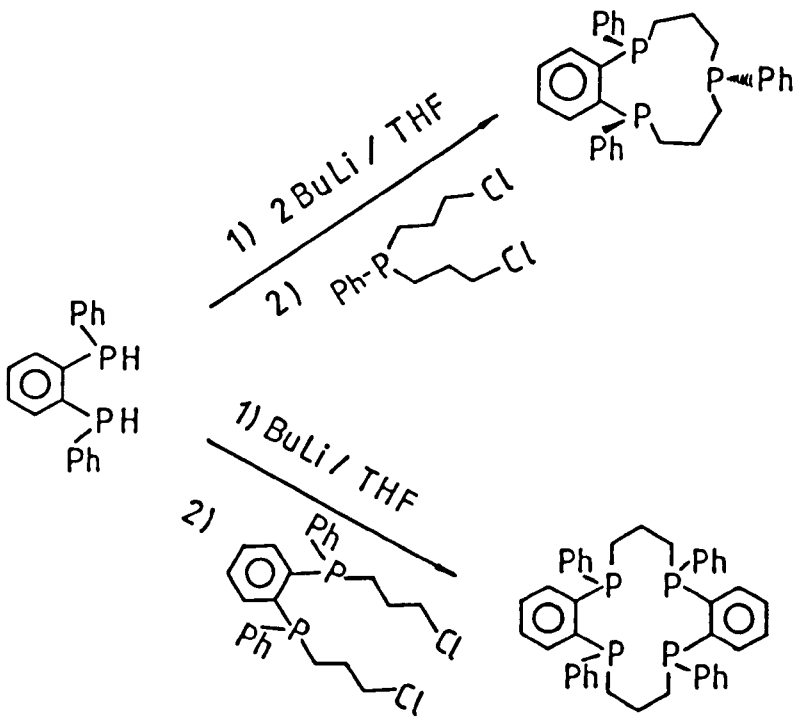

More recently[97] the same group have reported the preparation of macrocycles with secondary phosphino ligating sites in which alkylation to introduce pendent arms are possible. Molybdenum(0) and rhodium(I) complexes of the parent macrocycles have also been prepared. Use of the template reaction in the synthesis of polyphosphorus macrocycles was first introduced by Rosen,[98] who prepared a tetraphosphorus macrocycle by the reaction between the nickel(II) complex of tetradentate phosphorus chelate and α,α'-dibromo-o-xylene. This was followed by treatment of the complex with excess sodium cyanide to give the free ligand. The nickel(II) complex of this macrocycle was prepared and characterised after its purification. Nelson[99] and his group reported the effect of some metal ions to organise the *in situ* synthesis of pentadentate,

N_3P_2 macrocycles. From this study only silver(I) and cadmium(II) were found to be suitable for their template synthesis.

SECTION 2.5 POLYARSENIC MACROCYCLES

Although arsenic donors are well known for their ability to stabilise high oxidation states of coordination metals;[100] and its chelates have been known for a long time;[100,101] very few examples of arsenic macrocycles are reported in the literature.[102,103] This is probably due to the difficult synthesis of such macrocycles, and the poisonous nature of arsenic compounds. However, recently Kauffmann and Ennen[104] have published the syntheses of several arsenic macrocyclic ligands, most of them in poor yield, and no metal complexes have been reported. The preparation of some of these compounds is shown in Scheme 1.10.

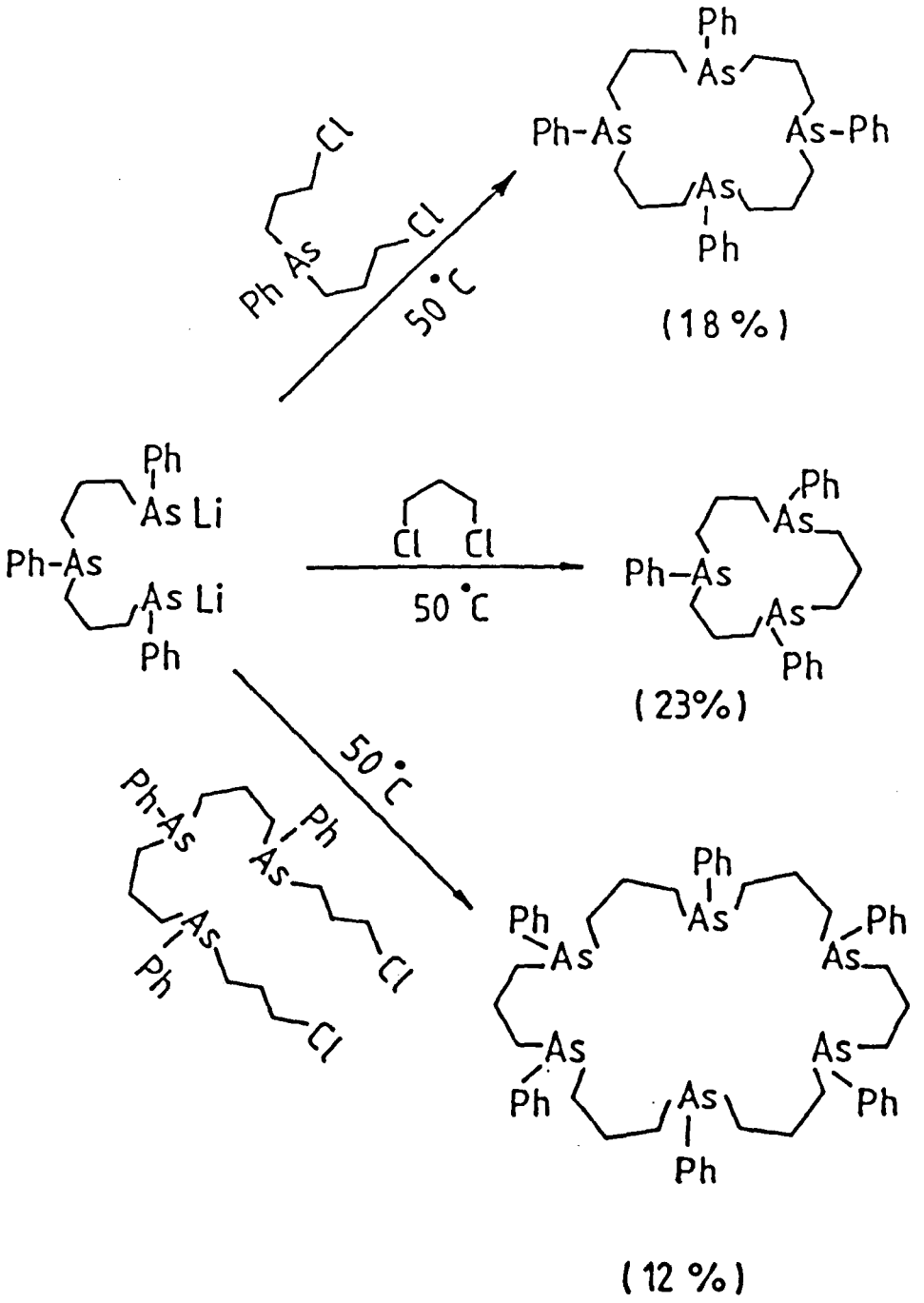
Ph
As
Ph-As
As-Ph
As
Ph
(18 %)
Cl
Cl
Ph As
50 °C
Ph
As Li
Ph-As
As Li
Ph
Cl Cl
50 °C
Ph
As
Ph-As
As
Ph
(23%)
50 °C
Ph-As
Ph
As
Cl
As
Ph
Cl
Ph
As
Ph
As
Ph
As
Ph
As
Ph
As
Ph
As
Ph
(12 %)

SCHEME 1.10

CHAPTER II

SYNTHESIS AND STUDY OF SOME TETRADENTATE AZAMACROCYCLES AND THEIR NICKEL(II), COPPER(II) AND ZINC(II) COMPLEXES

SECTION 1 INTRODUCTION

During recent years considerable interest has been shown in synthesis of tetradentate pyridine containing macrocycles and their metal complexes.[105-112] This is largely due to the relative ease of their synthesis. The synthesis, reduction and characterisation of some new quadridentate pyridine containing macrocycles and their nickel(II), copper(II) and zinc(II) complexes are reported in the next sections.

SECTION 2 RESULTS AND DISCUSSION

SECTION 2.1 SYNTHESIS OF 3,7,11-TRIMETHYL-3,7,11,17-TETRAAZA-BICYCLO[11.3.1]HEPTADECA-1(17),13,15-TRIENE, L^1

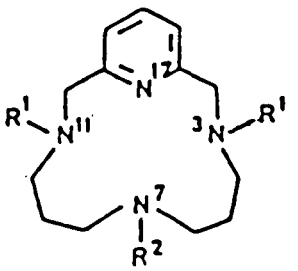

L^1 $R^1 = R^2 = Me$

L^2 $R^1 = H, R^2 = Me$

L^3 $R^1 = CH_2Ph, R^2 = H$

FIGURE 2.1

Nickel(II) ion was employed as a template to promote the condensation reaction between the readily available linear tridentate amine (5-methyl-1,9-diamino-5-azaheptane) and pyridine-2,6-dicarbaldehyde, to produce the Schiff's base shown in Scheme 2.1 (page 60). This product was reduced *in situ* using $NaBH_4$

in an aqueous ethanolic solution, and the cyclic amine L^2 (Figure 2.1) was liberated from the Ni^{2+} ion in 43% yield using sodium cyanide.[113] The trimethyl macrocycle L^1 (Figure 2.1) was prepared from L^2 using the method of Clarke, *et al.*[114] (formaldehyde and formic acid) to fully methylate the secondary amine groups:

$$R_2NH + CH_2O + HCO_2H \longrightarrow R_2NCH_3 + CO_2 + H_2O$$

Unlike L^2, which is a crystalline solid, L^1 is a pale yellow viscous oil at room temperature. This is almost certainly due to the introduction of the extra methyl groups, and the removal of the secondary amine groups, which removes the ligand's capability for intermolecular hydrogen bonding. The purity of L^1 was established by an elemental analysis (Table 2.1, page 55), and by the ^1H and ^{13}C n.m.r. (Table 2.2, page 56). The macrocycle L^1 (Figure 2.1) has a plane of symmetry through the pyridine and N-Me (R^2) atoms and shows the expected nine ^{13}C n.m.r. resonances. No impurity was evident in the ^{13}C n.m.r. spectrum.

SECTION 2.2 SYNTHESIS OF NICKEL(II) COMPLEXES OF LIGAND L^1

Section 2.2.1 Four Co-ordinate Nickel(II) Complexes

Four co-ordinate nickel(II) complexes of L^1 were prepared as described in the experimental Section 5.2 (page 59). There are four possible isomers for $[Ni(L^1)]^{2+}$ (Figure 2.2), two of which, (III) and (IV), are an enantiomeric pair. These isomers arise from the different positions of the coordinated N-Me groups, either above or below the macrocyclic plane.

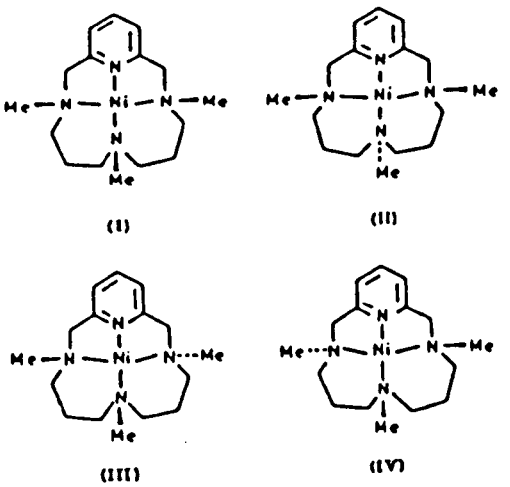

FIGURE 2.2

Possible isomers of the $[Ni(L^1)]^{2+}$ ion. Isomers (III) and (IV) are enantiomers.

The ^{13}C n.m.r. spectra of these three isomers are characteristically different as shown in Figure 2.3 (the chemical shifts are in Table 2.2, page 56). Isomer (I) can be prepared by mixing equimolar amounts of ethanolic solutions of $[Ni(H_2O)_6](ClO_4)_2$ and L^1, and the reaction mixture left to stir at room temperature overnight.

During this time the colour of the solution changes from green to blue, and finally a red solid precipitate. This observation is in close agreement with the recent related study by Barefield and his collaborators.[115]

In order to ascertain the conformation of isomer (I) two dimensional 400 MHz, ^1H n.m.r., and ^1H nuclear Overhauser enhancement studies were carried out. Referring to Figure 2.4 in which the aromatic protons are labelled *a* and *b* and the aliphatic protons c-j, the following assignments were made for the nickel(II) complex of L^1 based on chemical shifts, integrals, spin-spin coupling patterns, and coupling constants; δ 7.93 (*a*; t; 1H), 7.26

FIGURE 2.3

Proton decoupled ^{13}C n.m.r. of the three possible isomers of $[Ni(L^1)](ClO_4)_2$ in CD_3NO_2

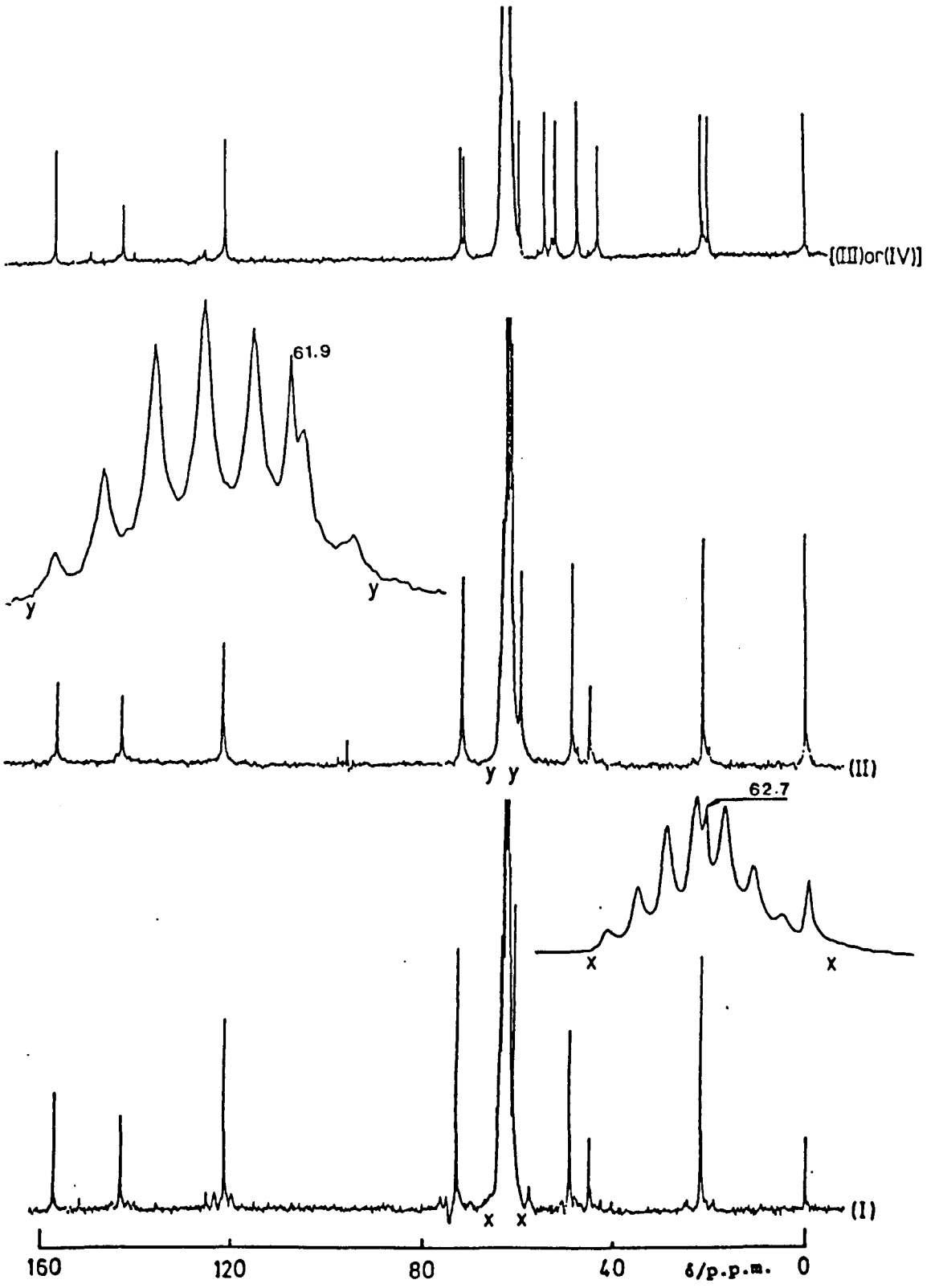

(*b*; d; 2H), 4.11 (*c*; d; 2H), 3.66 (*d*; d; 2H), 3.35 (1 + 2 equivalent *NMe*; overlapping, S and d; 8H), 2.89 (*f*; m; 2H), 2.53 (single *NMe*;*e* S; 3H), 2.18 (*g*; d; 2H), 1.85 (*h* and *i*; m; 4H), 1.68 (*j*; d; 2H).

N.O.e. difference spectra were recorded with irradiation at the frequencies of resonances *j*, *g*, *c*, *d*, 2 equivalent *NMe* + *e*, *f* and single *NMe*.

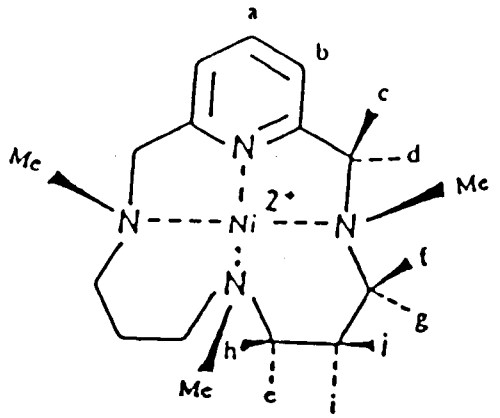

FIGURE 2.4

Labelling scheme for the protons in $[Ni(L^1)]^{2+}$ ion

The following proximal protons were revealed by each of these experiments (irradiated resonances first, followed by enhanced resonances in parentheses); *c* (*b*; *d*; 2 equivalent NMe_2 + *e*; *f*), *d* (*b*; *c*; 2 equivalent *NMe* + *e*; *g*), *f* (*c*; 2 equivalent *NMe* + *e*; *g*, *j*); single *NMe* (2 equivalent *NMe* + *e*, *h*, *i*). It is interesting to note that irradiation of the resonances from the 2 equivalent *NMe* groups enhanced the resonance from the third *NMe* and *vice versa*, showing undoubtedly that all three methyl groups are pointing on the same side of macrocyclic plane.

Addition of an ethanolic solution of an equimolar amount of $[Ni(DMSO)_6](ClO_4)_2$ to a solution of L^1 in ethanol gave a solid which when recrystallised from nitromethane-ethanol gave red crystals of $[Ni(L^1)](ClO_4)_2$, which were found by ^{13}C n.m.r. to be the pure symmetric isomer (II), Figure 2.2. The ^1H-decoupled ^{13}C n.m.r. spectrum in $[^2H]_3$-nitromethane of this isomer is compared with those of the other isomers in Figure 2.3, and chemical shifts are given in Table 2.2 (page 56). When this preparation was repeated, the product was found to be a mixture of the symmetric isomer (I) and asymmetric isomers [(III) and (IV)]. It is reported that isomer (I) readily isomerises to (III) and (IV), and (III) and (IV) equilibrate with largely (II) and some (I) in aqueous solution.[115] We found that when hydrated nickel(II) perchlorate was used in the preparation of $[Ni(L^1)](ClO_4)_2$ instead of the dimethyl sulphoxide solvate, the product obtained was the symmetric isomer (I), as described previously. We conclude that (II) is the preferred isomer in solutions of coordinating solvents (and other unidentate anionic ligands; Section 2.2.2), and that (I) is a kinetically formed first product.

To obtain the asymmetric isomers [(III) and (IV)], a sample of the symmetric complex (I) was dissolved in water and heated at 85°C for 20 h, and the solution was then slowly concentrated, when orange crystals of the asymmetric isomer of $[Ni(L^1)](ClO_4)_2$ precipitated. The structure of this isomer was confirmed by ^{13}C n.m.r. in solution (Figure 2.3 and Table 2.2) and by an x-ray crystallographic study (see Section 2.2.3).

The visible spectra of the $[Ni(L^1)](ClO_4)_2$ isomers in nitromethane solution are shown in Table 2.3 (page 57), and are as expected for diamagnetic square-planar nickel(II) complexes. The f.a.b. mass spectrum of $[Ni(L^1)](ClO_4)_2$ shows a cluster of peaks centred at m/z 433 as calculated for $[Ni(L^1)ClO_4]^+$. This behaviour is in the same as that observed in our previous studies.[113]

In earlier studies,[116] it has been shown how the rate of Me-N inversions can be accelerated in the $[Ni(tmc)]^{2+}$ ion (tmc = 1,4,8,11-tetramethyl-1,4,8,11-tetraazacyclotetradecane) by the addition of co-ordinating solvents such as DMSO, and it is not surprising, therefore to find a similar behaviour for the $[Ni(L^1)]^{2+}$ ions. Foster, *et al.*[115] reported the rate and equilibrium constants for the equilibration of (I) and (II) in aqueous sodium perchlorate solutions, and our synthetic observations confirm that this isomerisation occurs. In addition we have observed that when a solution of isomer (I) is held at 358 K in the non-coordinating solvent nitromethane, there is a slow equilibration with (III) and (IV). Approximate data for the rate of isomerisation is given in Table 2.4, based on integration of the ^{13}C n.m.r. resonances shown in Figure 2.5. The approximate rate constant for the approach to equilibrium (sum of the forward and reverse rate constants) is 1.82 x 10^{-7} s^{-1} at 358 K, and the approximate equilibrium constant, [(III + IV)/(I)] = 3.0.

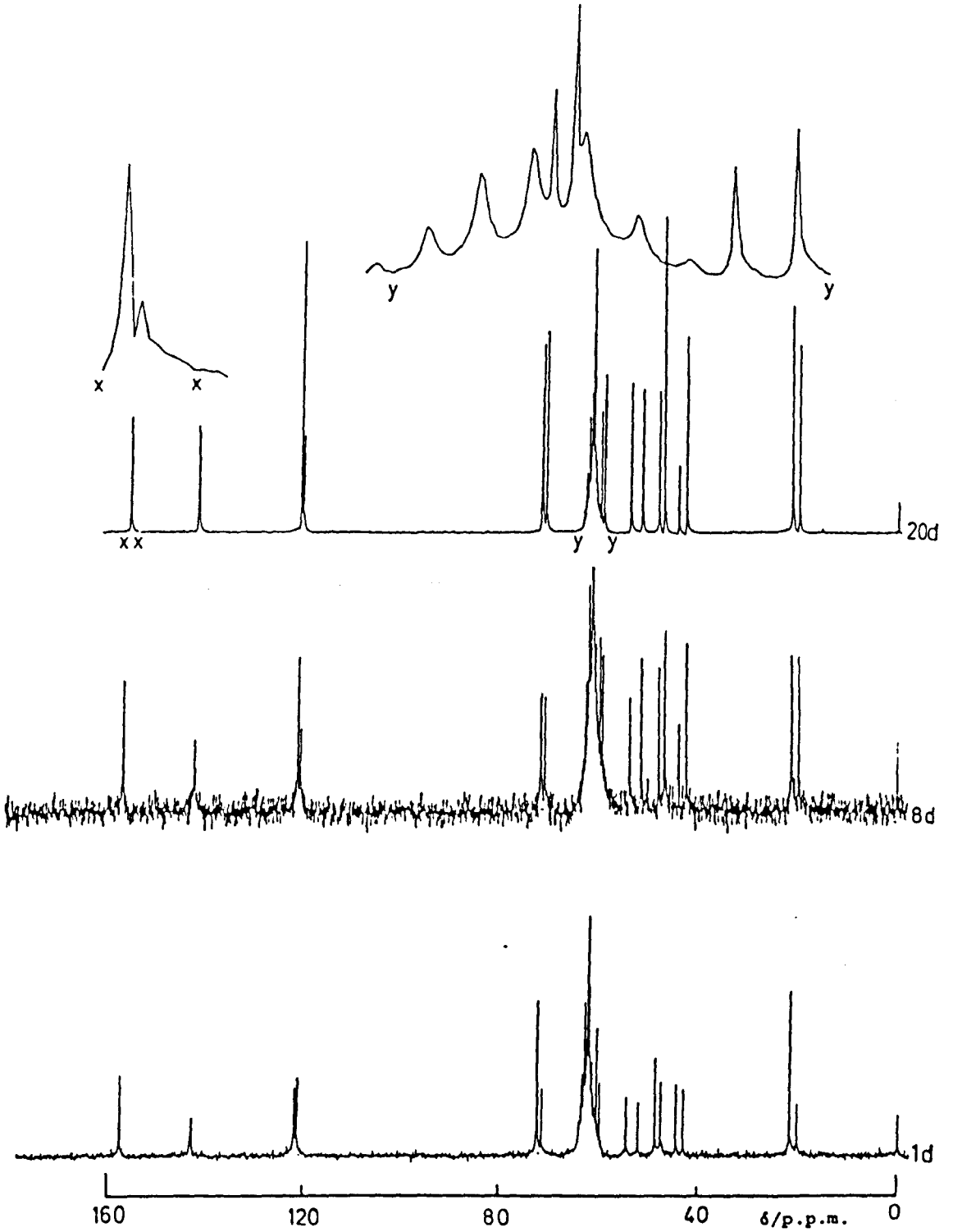

FIGURE 2.5

Variation of the proton decoupled ^{13}C n.m.r. spectrum of $[Ni(L^1)](ClO_4)_2$ isomer (1) held in nitromethane-d_3 at 358 K for 20 days.

TABLE 2.4

Variation of the relative amounts (%) of isomer (I) and (III) + (IV) with time in nitromethane solutions of $[Ni(L^1)](ClO_4)_2$ at 358 K (based on integrals of the Me-N ^{13}C n.m.r. resonances at δ 45.21 and 43.69 p.p.m.; Figure 2.3).

	t/d		
	1	8	20
(I)	52	34	25
(III) + (IV)	48	66	75

Section 2.2.2 Five and Six Coordinate Nickel(II) Complexes of L^1

In the presence of either coordinating solvents, or anions such as Cl^- or NCS^- or NO_2^-, the favoured isomers have the N-configuration of (II), Figure 2.2. This is shown by crystal structures of the aqua-[115]; DMSO (B) and chloro- (C) complexes (Section 2.2.3). The microanalytical data, visible spectra and magnetic moments are collected in Tables 2.1 and 2.3 (page 55 and page 57, respectively), and confirm that these complexes are five-coordinate paramagnetic species. With oxalate ion the visible spectrum and analytical data are consistent with a bridged *cis*-octahedral structure of the type found previously for the analogous complex of L^2.[113] The latter deduction is confirmed by a crystal structure of $[(L^1)Ni-(\mu-OX)-Ni(L^1)](ClO_4)_2$ (complex D) as shown in Section 2.2.3. The paramagnetic ^1H n.m.r. spectrum of $[Ni(L^1)Cl]ClO_4$ in $[^2H]_3$-nitromethane (recorded at 368 K) extends from *ca* + 247.15 to -16.57 p.p.m. The central protons of the propyl group (C $-CH_2-$C) appear upfield of tetra-methyl silane, at δ -16.57 and -5.72 p.p.m. (each of relative area 2), and the pyridine *para* proton at δ 7.64 p.p.m. (relative area 1), whereas *meta* protons are

at 10.49 p.p.m. (relative area 2). The CH_3-N group (relative area 3) appears at δ 90.44 p.p.m. and the two equivalent CH_3-N groups (relative area 6) apear at δ 111.26 p.p.m. The remaining six resonances of relative area 2 appear at δ 33.41, 47.31, 126.73, 136.63 and 247.15 p.p.m. with two resonances overlapping at δ 33.41 p.p.m. (relative area 4). The spectrum is entirely consistent with a single symmetric species and most likely isomer (II) (Figure 2.2). The f.a.b. mass spectra of $[Ni(L^1)X]^+$, with x = Cl^-, NCS^- and NO_2^- gave a cluster of parent ion peaks centred at m/z 369, 392, and 380 respectively. Complex (D) gave a cluster of peaks centred at m/z 858 as expected for $[(L^1)Ni(\mu\text{-}OX)Ni(L^1)ClO_4]^+$ (M + 1).

Section 2.2.3 Crystal and Molecular Structure of Four, Five and Six Coordinate Nickel(II) Complexes of L^1

Crystal data for $[Ni(L^1)](ClO_4)_2$ (A) [the asymmetric isomer (III) or (IV)], $[Ni(L^1)(DMSO)](ClO_4)_2$ (B), $[Ni(L^1)(Cl)]ClO_4$ (C) and $[(L^1)Ni\text{-}(\mu\text{-}OX)\text{-}Ni(L^1)](ClO_4)_2$ (D) are collected in Table 2.5; (B) and (C) were found to be five-coordinate complexes of the symmetric isomer (II), Figure 2.2, whereas the structure of complex (D) is *cis*-octahedral with the two macrocyclic units adopting the same N-Me chiralities around the nickel(II) ions as found for (B) and (C).

DESCRIPTION OF THE STRUCTURES

ISOMER (A): The Ni atom adopts a square-planar geometry, with no additional co-ordinated ligand. The methyl groups on N(2) and N(4) are on opposite sides of the macrocyclic ring (Figure 2.6); this arrangement reduces the ability of the macrocycle to fold, and hinders the entry of a fifth ligand into the inner coordination sphere. As expected for a low-spin d^8 system, in comparison to

high-spin systems, the Ni-N distances (Table 2.6, page 66) are significantly shorter than in (B), (C) or (D), though they have a relatively large spread of values. The Ni-N (pyridine) bond is shorter than the other Ni-N distances as found previously in related structures.[109]

COMPLEXES (B) AND (C): (Figures 2.7 and 2.8): The Ni^{2+} ion adopts a square-pyramidal geometry, sitting above the basal plane by *ca.* 0.37 Å, and with the unidentate ligand in the basal plane in a *trans*-

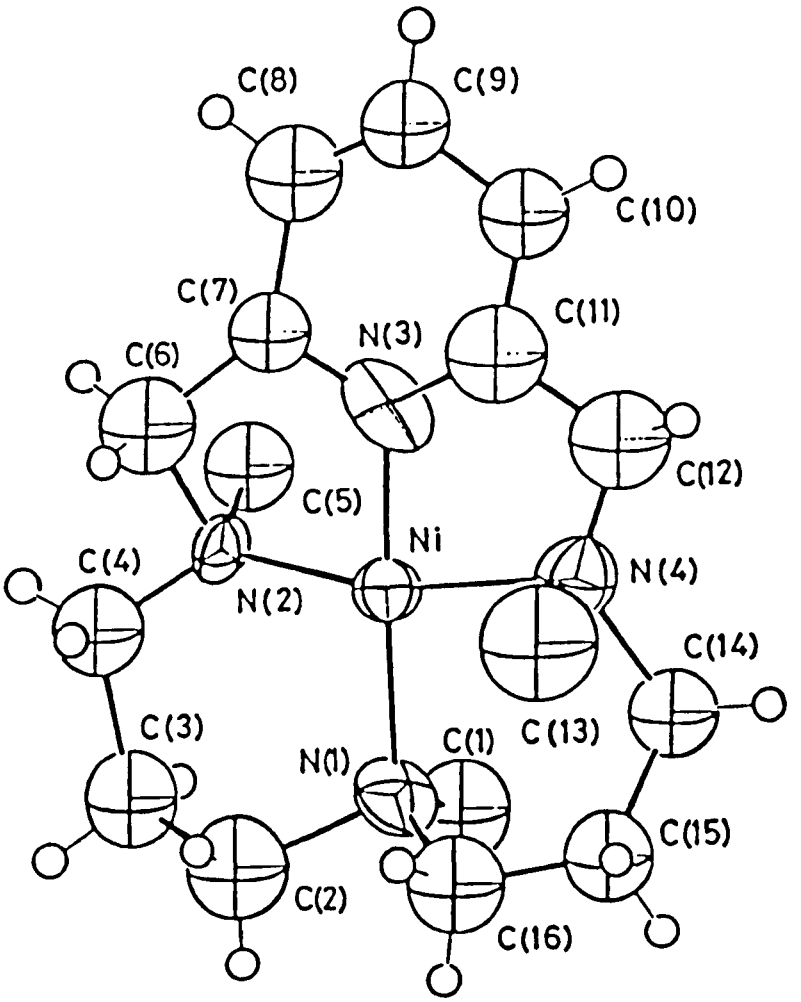

FIGURE 2.6

View of Molecule (A) Showing the Atomic Numbering

position to the pyridine-N atom; the macrocycle is folded about the N(2) to N(4) axis, and the apex is occupied by N(1) as shown in the sketch below.

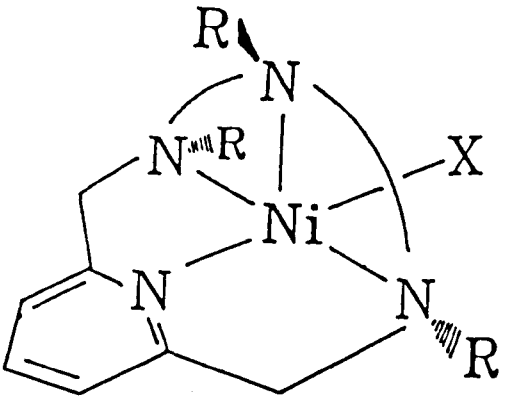

X = unidentate ligand such as DMSO or Cl

This conformation allows easier N-Me inversion at N(1) as observed. The Ni-N bond lengths are very similar in (B) and (C), with those to the pyridine N atom the shortest (1.97-1.98 Å). The bond angles are close to those of a regular square pyramid, with X-Ni-X angles across the basal plane of *ca.* 157°. As well as the aqua-complex,[115] this geometry has also been found in a related macrocyclic complex $[Ni(L^3)Cl]ClO_4$, (for the structure of L^3, see Figure 2.1, page 29).[117]

COMPLEX (D): The x-ray determination confirmed the expected structure, and shows that the oxalate ion is tetradentate forming a bridge between the two nickel atoms as shown in the following sketch.

TABLE 2.5

Crystal data for $[Ni(L^1)][ClO_4]_2$, (A); $[Ni(L^1)(DMSO)][ClO_4]_2$, (B); $[Ni(L^1)Cl]ClO_4$, (C); and $[(L^1)Ni\text{-}(\mu\text{-}OX)\text{-}Ni(L^1)][ClO_4]_2$, (D)

Compound	(A) $C_{16}H_{28}Cl_2N_4NiO_8$	(B) $C_{18}H_{34}Cl_2N_4NiO_8$	(C) $C_{18}H_{34}Cl_2N_4NiO_9S$	(D) $C_{34}H_{56}Cl_2N_8Ni_2O_{12}$
M	534.0	556.1	470.0	956
System	Monoclinic	Orthorhombic	Triclinic	Monoclinic
Space Group	Cc	$Pn2_1a$	pI	$P2_1/c$
Absences	hkl,h+k≠2n; h0l, l≠2n	hk0h ≠2n; 0kl,k+l≠2n	None	h0l,l≠2n,0k0,k≠2n
a/Å	10.043(3)	17.361(6)	7.425(2)	8.394(2)
b/Å	13.842(3)	12.169(3)	10.322(3)	20.270(9)
c/Å	15.473(9)	12.626(2)	13.933(4)	12.410(3)
$\alpha/^o$	90	90	83.53(2)	-
$\beta/^o$	91.65(4)	90	75.52(2)	101.2(2)
$\gamma/^o$	90	90	84.19(2)	-
U/A^{o3}	2150.2(1)	2667(1)	1024.3(5)	2071(1)
D_c/g cm^{-3}	1.65	1.38	1.52	1.53
Z	4	4	2	2
μ(Mo-K_α)cm^{-1}	12.1	10.2	12.4	11.09
F(000)	1112	1168	492	1004
Reflections;				
Total	1977	1855	3626	4025
[$I/\sigma(I) \geq 3.0$]				
Observed	975	711	2039	1978
$2\Theta_{max}/^o$	50	45	50	50
Range (2Θ) about $K_{\alpha1}$-$K_{\alpha2}/^o$	±1.2	+1.0 to -0.9	±0.9	±1.1
Speed $(2\Theta)/^o$ min^{-1}	1.5-29	1.5-29	1.2-29	3-29^o
Crystal dimensions/ mm	0.19 x 0.24 x 0.13	0.04 x 0.25 x 0.15	0.07 x 0.13 x 0.12	0.27 x 0.075 x 0.13
Final R(R^1)	0.090 (0.094)	0.084 (0.088)	0.043 (0.042)	0.071 (0.066)
Weighing factor g	0.007	0.003	0.0006	0.0017
Largest peak on ΔF map/e Å^{-3}	0.9 (near Ni)	0.8	0.4	0.9

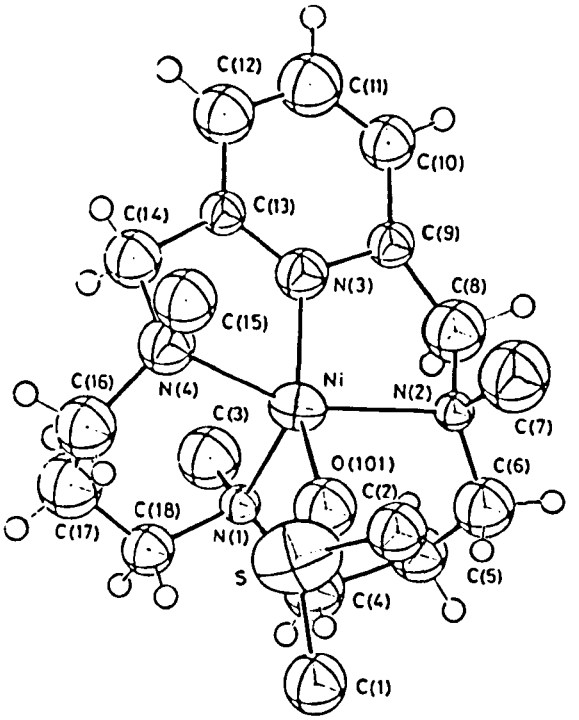

(i)

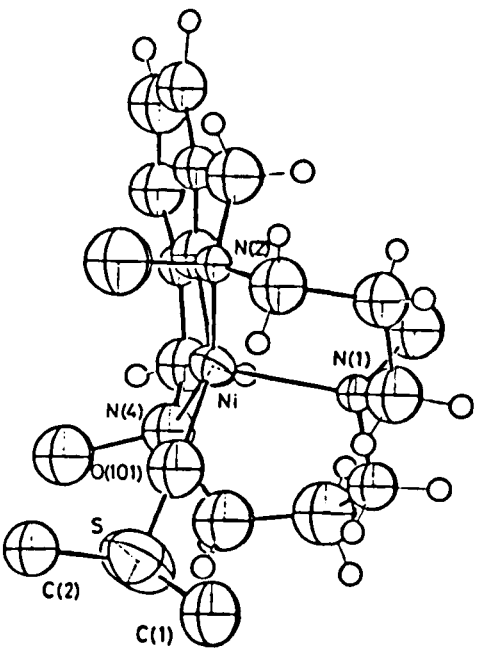

(ii)

FIGURE 2.7

Two views of molecule (B);
(i) showing the atomic numbering and general conformation,
(ii) showing the folded geometry.

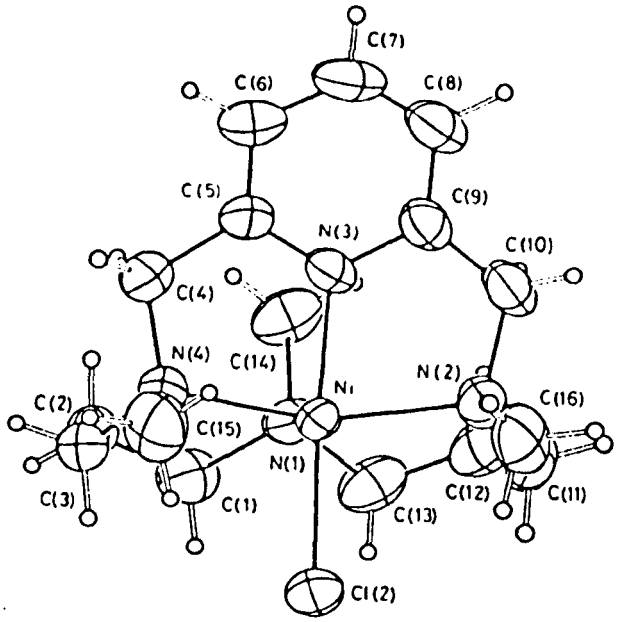

(i)

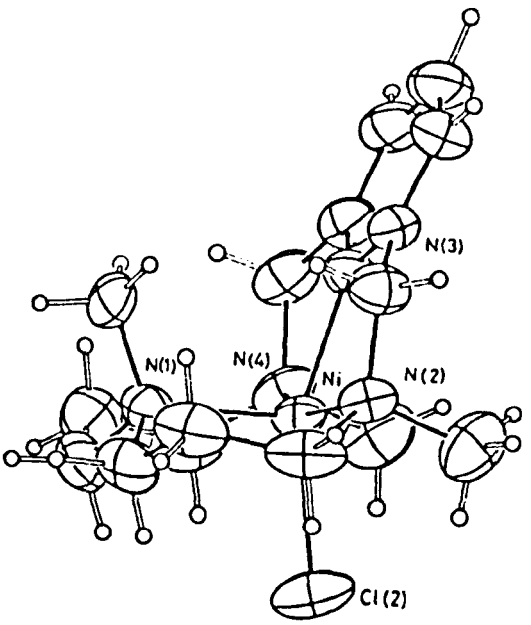

(ii)

FIGURE 2.8

Two views of molecule (C);
(i) showing the atomic numbering and general conformation,
(ii) showing the folded geometry

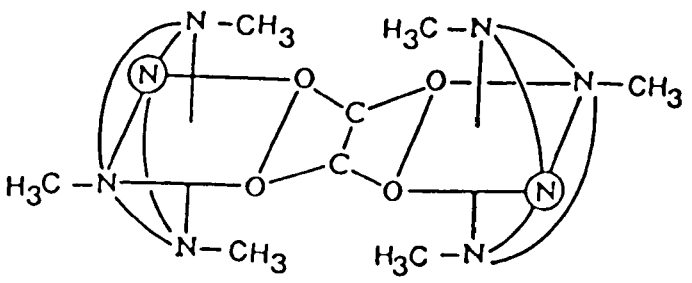

In the ortep picture (Figure 2.9) the geometry around the nickel(II) ion is *cis*-octahedral, and the structure has a plane of symmetry halfway between the carbon atoms of the oxalate group, with the two pyridine rings in *trans*-positions to each other. It is evident from the *trans*-angle N(2)-Ni-N(4) of only 158.2°(3) (Table 2.6, page 66), that the ligand is unable to accommodate the present geometry entirely satisfactorily. Another distortion arises as shown by the angle of 78.9°(2) between the oxygen atoms which is controlled by the bite of the oxalate ion. Ni-N and N-O distances are standard values for a high spin nickel(II) ion. The Ni-N(pyridine) distance is shorter than the others as is observed in complexes (A), (B) and (C). Einstein, *et al.*[118] have reported an x-ray structure of a dimeric nickel complex of [16]-ane-N_4 with an oxalate bridge, and the general mode of oxalate coordination is very similar to that found in complex (D).

SECTION 2.3 COPPER(II) AND ZINC(II) COMPLEXES OF L^1

In general copper(II) and zinc(II) complexes of L^1 were prepared by adding a solution of L^1 in ethanol to an equimolar amount of the DMSO or aquo-solvents of the metal perchlorates, or to

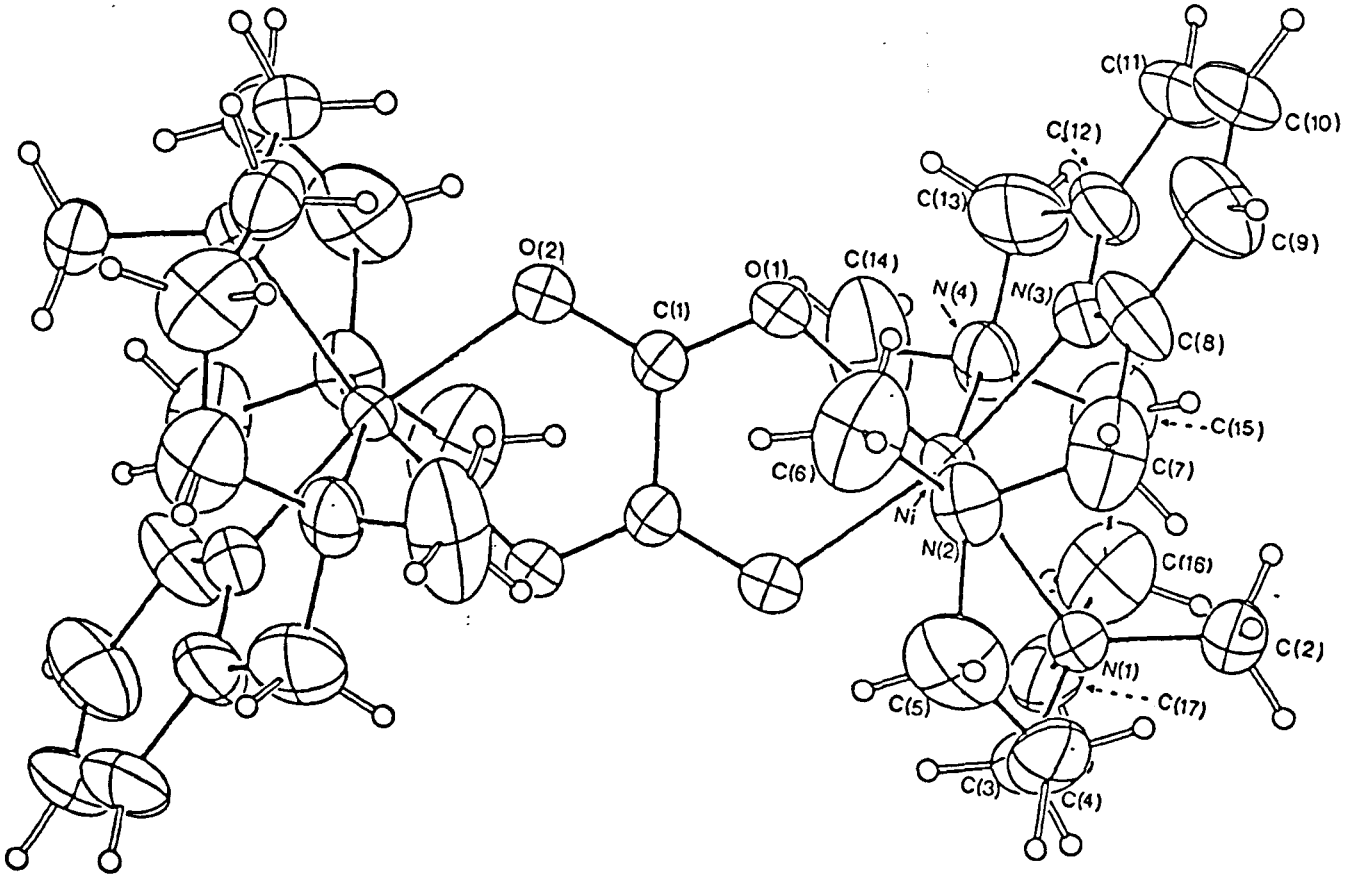

FIGURE 2.9

View of the cation, $[(L^1)Ni-(\mu-OX)-Ni(L^1)]^{2+}$ showing the atomic numbering. There is a centre of symmetry in the middle of the oxalate group.

$Zn(NO_3).6H_2O$; experimental details are given in Section 5.4. The copper(II) complex precipitates soon after the mixing, but in the case of the zinc(II) complexes dry diethyl ether was added dropwise to cause precipitation. Yields of the perchlorate salts were 80-90%, and starting from $Zn(NO_3)_2$ the yield was 65%. The products analysed as $[M(L^1)](ClO_4)_2.nH_2O$ (M = Cu, n = 1 or Zn, n = 0) and $[Zn(L^1)](NO_3)_2.H_2O$ (Table 2.1, page 55). The visible spectrum of $[Cu(L^1)](ClO_4)_2$ either in nitromethane or in dimethyl sulphoxide solvents (Table 2.3, page 57) are comparable to those found previously for analogous four coordinate systems.[113] The shoulder at 506 nm in nitromethane solution of $[Cu(L^1)](ClO_4)_2$ was resolved using Gaussian deconvolution as described in Section 3.2. The magnetic moments (Table 2.3) are in the range expected for a d^9 copper(II) complex. The f.a.b. mass spectrum of the $[Cu(L^1)](ClO_4)_2$ shows a cluster of peaks centred at m/z 438 as calculated for $[Cu(L^1)ClO_4]^+$ ion.

ZINC(II) COMPLEXES:

The ^{13}C n.m.r. spectral data are collected in Table 2.2, and show that in $[^2H]_3$-nitromethane solution $[Zn(L^1)](NO_3)_2$ is a mixture of symmetric and unsymmetric isomers, in a 1:3 ratio respectively, whereas $[Zn(L^1)DMSO](ClO_4)_2$ is a mixture of both symmetric species, in the ratio of 1:1, with an extra resonance at δ 39.95 p.p.m. attributed to coordinated dimethyl sulphoxide (the spectrum is shown in Figure 2.10). The structural deductions are based on the total number of carbon resonances observed, and the data are similar to those found in our earlier studies of $[Zn(L^2)]X_2$ (X = ClO_4 or NO_3).[113]

FIGURE 2.10

^{13}C N.m.r. spectrum of $[Zn(L^1)DMSO](ClO_4)_2$ in $[^2H]_3$-nitromethane recorded at 298 K.

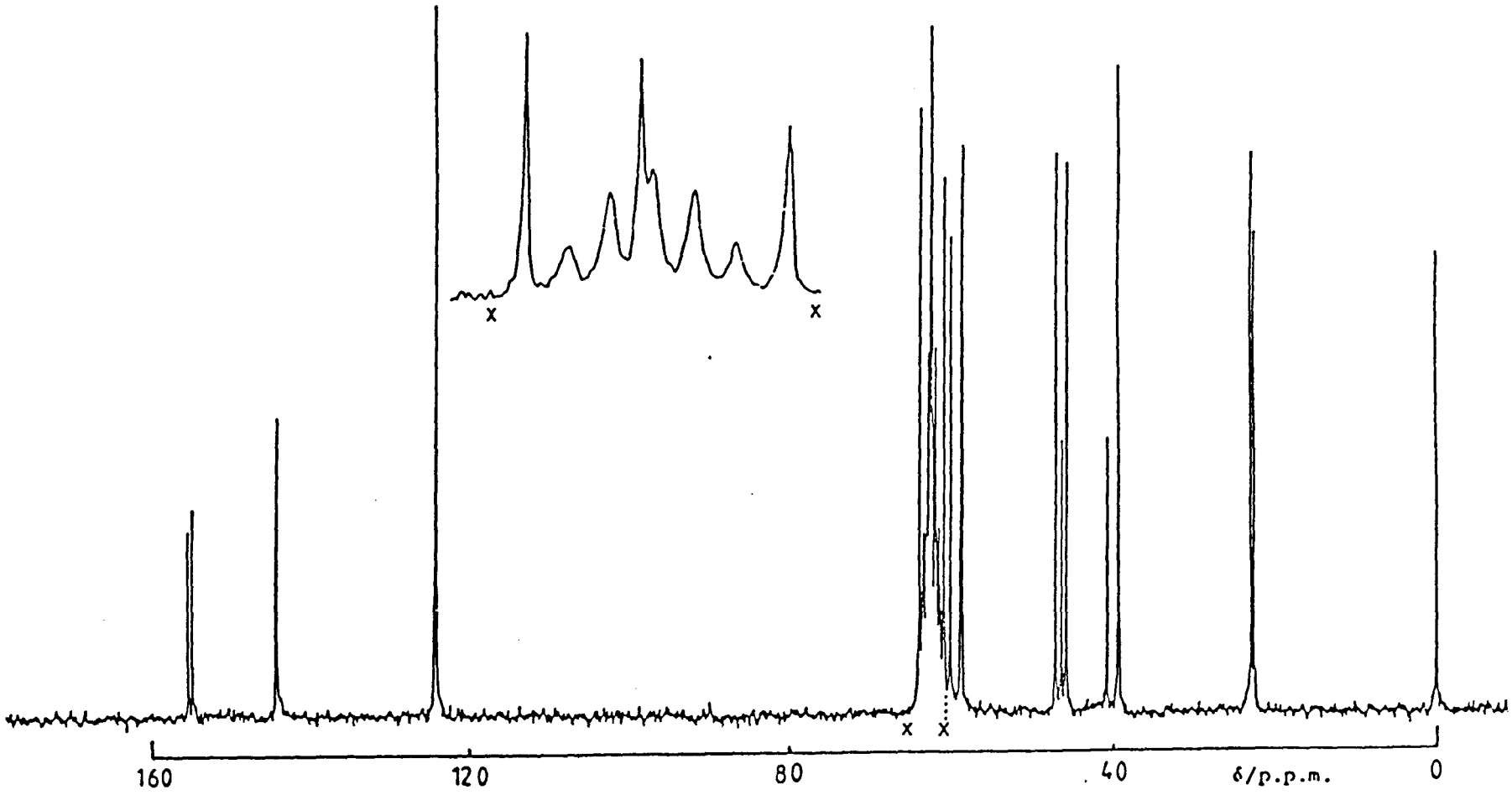

SECTION 3.1 SYNTHESIS OF 3,7,11-TRIMETHYL-3,7,11,17-TETRAAZA-BICYCLO[11.3.1]HEPTA DECANE (L^4)

The reduction of imine functions to produce secondary amine groups in a coordinated macrocyclic ligand is well known. A number of methods and reagents have been used for this reduction, including BH_4^-, and H_2 over heterogeneous catalysts such as platinum and Raney nickel. Recently Barefield[119] reported the reduction of a pyridine ring in the nickel(II) complex of the macrocycle (CRH). In this reduction the hydrogenation was carried out using a Parr hydrogenator (50 PSI H_2) and Raney nickel (W-2) as catalyst. However, in our earlier studies[113] we found that this method gave only partial reduction of the pyridine ring of $[Ni(L^2)]^{2+}$ after 24 h. Therefore, the reduction of $[Ni(L^2)]^{2+}$ was carried out by increasing the hydrogen pressure, and the temperature, to give a fully saturated macrocyclic nickel(II) complex. The reduction of the pyridine ring in $[Ni(L^1)]^{2+}$ was accomplished by using freshly prepared Raney nickel (W-2) catalyst with an increase in the hydrogen pressure and temperature, and even longer reaction time. The macrocycle (L^4) was liberated from nickel(II) complex by reacting the aqueous solution of $[Ni(L^4)]^{2+}$ with excess NaCN, and the ligand extracted with dichloromethane. L^4 is a colourless low melting solid. The ^1H decoupled ^{13}C n.m.r. spectrum in $[^2H]_3$-nitromethane of the free macrocycle (Figure 2.11), shows nine resonances, as expected, with three of them located in the upfield region.

^1H n.m.r. assignments for L^4 was greatly facilitated by use of two dimensional homonuclear correlation spectroscopy (COSY). The COSY spectrum is shown in Figure 2.12 which allows for easier

FIGURE 2.11

^{13}C N.m.r. of L^4 in $[^2H]_3$-nitromethane.

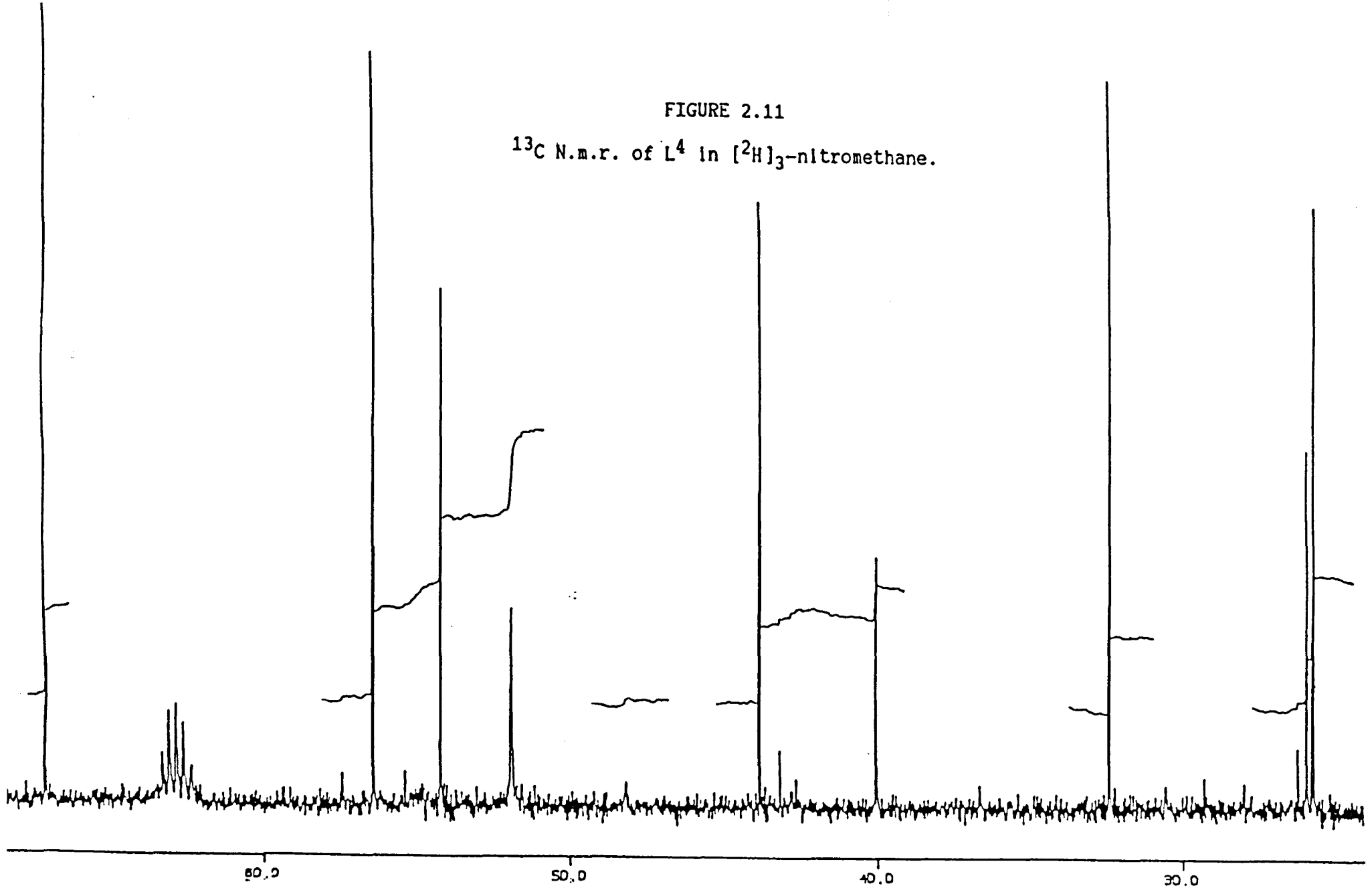

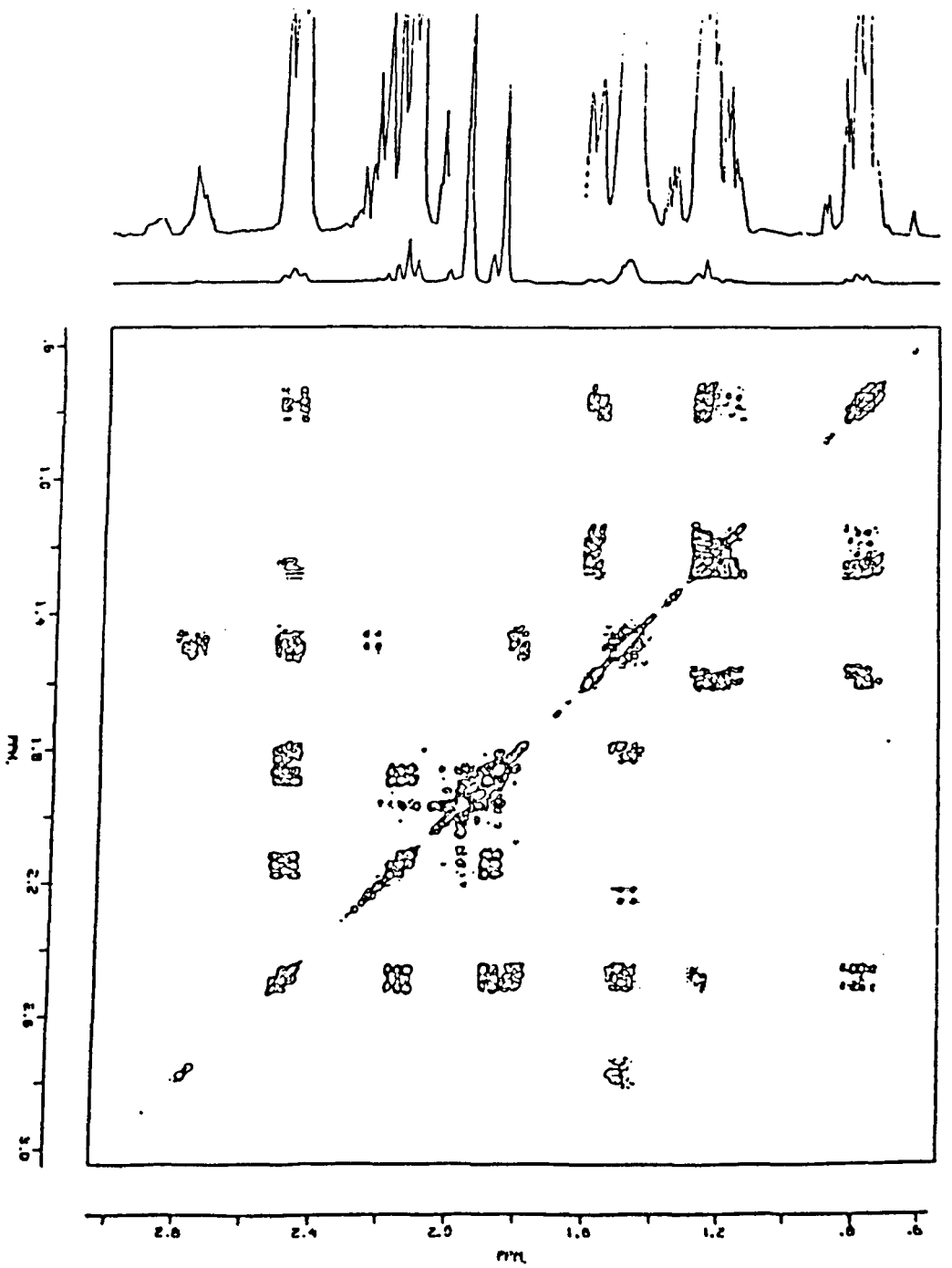

FIGURE 2.12

COSY spectrum of L^4 in $[^2H]_3$-nitromethane.

identification of the spin coupling network of the individual proton signals. According to structure 2.13 shown below, in which the protons are labelled *a-m*, the following assignments were made;

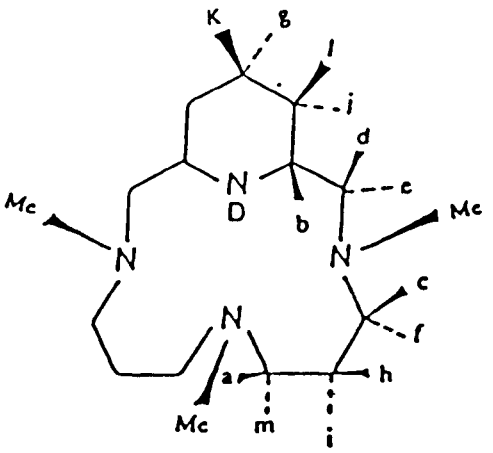

FIGURE 2.13

δ 0.78 (*l;* m; 2H), 1.2-1.29 (*j* + *k;* m; 3H), 1.50 (*h* + *i;* m; 4H), 1.60 (*g;* m; 1H), 1.80 (*f;* m; 2H), 1.89 (single *NMe;* s; 3H), 1.90 (*e;* d; 2H), 2.00 (2 equivalent *NMe;* s; 6H), 2.17 (*d;* t; 2H); 2.51 (*b* + *c* + *m;* m; 6H), 2.8 (*a;* m; 2H).

^{1}H nuclear Overhauser enhancement (n.O.e.) difference experiments were carried out to ascertain the conformation of the free macrocycle (L^4) and to obtain further information concerning the geometry of piperidine ring in this new macrocycle. N.O.e. difference spectra were recorded with irradiation of the frequencies of resonances *d, b/c, l* and the 2 equivalent *N-Me* groups. The following proximal protons were revealed by each of these experiments (irradiated resonance first, followed by enhanced

resonances in parentheses); *d (e, b/c, l,* 2 equivalent *N-Me) b/c (l, f, a, h, j, k); l(j, k, g, d, b/c),* 2 equivalent *NMe (d, b/c, h/i).* It is interesting to note that irradiation of the resonances from *b* or *d* enhanced the resonance from *l* and *vice versa,* showing that the piperidine ring is in the chair form.

Several attempts were made to prepare potentially quinquedentate macrocycles by attacking the NH group of the piperidine ring of L^4 with 2-picolyl chloride, acrylonitrile and formaldehyde/cyanide. However, these attempts failed probably because of steric hindrance.

SECTION 3.2 COPPER(II), NICKEL(II) AND ZINC(II) COMPLEXES OF L^4

The metal complexes of L^4 were obtained following the general procedure described previously (see Sections 2.2 and 2.3). The complexes gave the expected microanalyses (Table 2.1). The f.a.b. mass spectra of $[Ni(L^4)](ClO_4)_2$ and $[Cu(L^4)](ClO_4)_2$ show a cluster of peaks centred at m/z = 440 and 445 as calculated for $[Ni(L^4)ClO_4]^+$ and $[Cu(L^4)ClO_4]^+$ respectively. In addition, a strong peak is observed at m/z = 383 from both complexes, attributed to the protonated ligand $[L^4.H_2ClO_4]^+$, and indicating that the metal complexes of L^4 are not that stable (a sample spectrum is shown in Figure 2.14 for $[Cu(L^4)ClO_4]^+$). Protonated ligand peaks are not observed in the f.a.b. mass spectra of more stable complexes such as $[M(L^1)]^{2+}$, M = Ni, or Cu.

The ^{13}C n.m.r. spectra in $[^2H]_3$-nitromethane of the low spin nickel(II), and zinc(II) complexes reveal the presence of two symmetric species in a 1:1 ratio in both cases. These observations are similar to those reported previously for an analogous system.[113]

The visible spectrum of $[Cu(L^4)](ClO_4)_2$ in nitromethane solvent

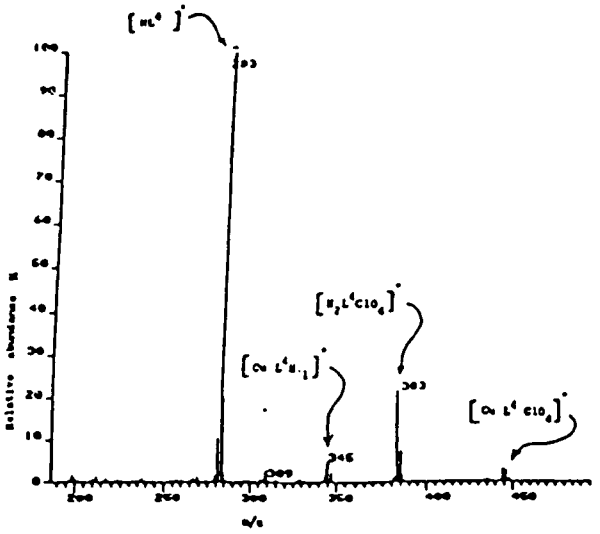

FIGURE 2.14

Fast atom bombardment mass spectrum of $[Cu(L^4)ClO_4]^+$ [in a matrix of *erythro*-1,4-dimercapto-2,3-butanediol and *threo*-1,4-dimercapto-2,3-butane diol in a ratio of 1:5; 8 KeV xenon plasma].

shows a major band at 573 nm, and a shoulder at 492 nm; the spectrum was resolved using Gaussian regression analysis to find the two overlapping wavelengths (see Appendix).

It is interesting to note that the visible spectrum of $[Ni(L^4)](ClO_4)_2$ in nitromethane (a non-coordinating solvent) and in dimethyl sulphoxide, pyridine, acetonitrile and water (normally coordinating solvents) are almost identical. The colour of the complex in solution is red in all solvents, and no change in the spectra and the colour was observed even after two weeks. This behaviour contrasts with that observed for $[Ni(L^1)](ClO_4)_2$ (Section 2.2), in which the colour of the complex in solution is blue and greenish-blue in water and dimethyl sulphoxide respectively; for $[Ni(L^1)](ClO_4)_2$ the visible spectra in coordinating solvents are typical of those for five-coordinate species. The different visible spectra of the nickel(II) complexes of L^1 and L^4 must be related to steric effects. To fully understand the observed effect, we can

refer to the x-ray structure of the nickel(II) complex of the reduced pyridine macrocycle (L^2) reported in our earlier study.[113] The macrocycle in its nickel(II) complex has a configuration in which the two nonpiperidine N-H groups, the N-CH_3 group, and hydrogen atoms at asymmetric carbons, point above the plane of macrocycle, whilst the N-H of the piperidine is located below this plane. If we assume this is the case also in the structure of $[Ni(L^4)](ClO_4)_2$, with all methyl groups pointing to the same side of the macrocyclic plane, strong steric interactions occur with solvent molecules entering on axis, thereby preventing their binding. In $[Ni(L^1)](ClO_4)_2$, which readily isomerises to structure (II) (Figure 2.2) in the presence of donor molecules, the solvent can easily co-ordinate without any steric hindrance.

TABLE 2.1

Combustion analyses (%), observed values in parentheses

Compound	Formula	C	H	N
L^1	$C_{16}H_{28}N_4$	69.5(69.2)	10.2(10.1)	20.3(20.1)
$[Ni(L^1)](ClO_4)_2$	$C_{16}H_{28}Cl_2N_4NiO_8$	36.0(35.7)	5.3(5.0)	10.5(10.3)
$[Ni(L^1)DMSO](ClO_4)_2$	$C_{18}H_{34}Cl_2N_4NiO_9S$	35.3(35.4)	5.6(5.6)	9.2(9.1)
$[Ni(L^1)Cl]ClO_4$	$C_{16}H_{28}Cl_2N_4NiO_4$	40.9(40.8)	6.0(5.9)	11.9(11.8)
$[Ni(L^1)(NCS)]ClO_4$	$C_{17}H_{28}ClN_5NiO_4S$	41.5(41.7)	5.7(5.7)	14.2(14.4)
$[Ni(L^1)(NO_2)]ClO_4$	$C_{16}H_{28}ClN_5NiO_6$	40.0(40.0)	5.9(5.9)	14.6(14.5)
$[L^1Ni(\mu\text{-}OX)NiL^1](ClO_4)_2$	$C_{34}H_{56}Cl_2N_8Ni_2O_{12}$	42.7(42.4)	5.9(5.9)	11.7(11.6)
$[Cu(L^1)](ClO_4)_2.H_2O$	$C_{16}H_{30}Cl_2CuN_4O_9$	34.5(34.5)	5.4(5.4)	10.1(9.9)
$[Zn(L^1)](NO_3)_2.H_2O$	$C_{16}H_{30}N_6O_7Zn$	39.7(40.1)	6.3(5.9)	17.4(17.1)
$[Zn(L^1)](ClO_4)_2$	$C_{16}H_{28}Cl_2N_4O_8Zn$	35.5(35.7)	5.2(5.8)	10.4(10.8)
$[Ni(L^4)](ClO_4)_2$	$C_{16}H_{34}Cl_2N_4NiO_8$	35.6(36.4)	6.3(6.8)	10.4(10.4)
$[Cu(L^4)](ClO_4)_2.1\frac{1}{2}H_2O$	$C_{16}H_{36}Cl_2N_4NiO_9$	33.7(33.9)	6.5(6.3)	9.8(9.7)
$[Zn(L^4)](ClO_4)_2$	$C_{16}H_{34}Cl_2N_4O_8Zn$	35.2(35.5)	6.3(6.4)	10.3(10.2)

TABLE 2.2

^{13}C N.m.r. Chemical Shifts (δ/p.p.m.; reference, $SiMe_4$) at 298 K in CD_3NO_2 solution unless specified otherwise (relative populations in parentheses)

Compound	Isomer[a]	Pyridine			Py-CH_2-N	N-CH_2-C				N-CH_3		C-CH_2-C		
		Ortho	Para	Meta										
L^1[b]		159.19(2)	137.13(1)	123.26(2)	64,67(2)	55.82(2)		53.82(2)		44.05(2)	43.13(1)	25.64(2)		
L^1[c]		157.91(2)	136.34(1)	122.56(2)	64.08(2)	54.87(2)		53.33(2)		44.02(2)	43.46(1)	25.09(2)		
$[Ni(L^1)](ClO_4)_2$	(I)	158.70(2)	143.77(1)	121.87(2)	73.02(2)	62.70(2)		60.95(2)		49.32(2)	45.17(1)	21.96(2)		
	(II)	157.66(2)	143.68(1)	122.49(2)	72.07(2)	61.90(2)		59.83(2)		49.24(2)	45.46(1)	21.68(2)		
	(III) or (IV)	158.62	144.14(1)	122.56(2)	72.89(1)	62.62(1)		60.49(1)		48.35(1)	48.19(1)	22.07(1)		
					72.17(1)	55.16(1)		52.83(1)		43.91(1)		20.59(1)		
$[Zn(L^1)](NO_3)_2$	(I) or (II)	155.18(2)	143.80(1)	124.93(2)	64.60(2)	60.69(2)		60.50(2)		46.82(2)	41.13(1)	23.61(2)		
	(III) or (IV)	155.77(2)	143.09(1)	124.57(2)	64.60(1)	61.32(1)		60.69(1)		45.86(1)	45.24(1)	23.61(1)		
					64.60(1)	59.05(1)		56.94(1)		45.24(1)		22.69(1)		
$[Zn(L^1)DMSO](ClO_4)_2$[d]	(I) or (II)	154.98(2)	144.26(2)	124.90(2)	62.83(2)	60.39(2)		59.01(2)		46.26(2)	41.26(1)	22.92(2)		
	(I) or (II)	155.61(2)	144.33(1)	124.96(2)	64.31(2)	61.25(2)		59.15(2)		47.57(2)	46.88(1)	23.41(2)		
L^4[e]						66.94(2)	56.30(2)	54.20(2)	51.89(2)	43.74(2)	40.02(1)	32.35(2)	25.90(1)	25.69(2)
$[Ni(L^4)](ClO_4)_2$	First Isomer					71.92(2)	61.22(2)	56.76(2)	56.84(2)	45.87(2)	44.79(1)	26.80(2)	22.77(1)	21.67(2)
$[Ni(L^4)](ClO_4)_2$	Second Isomer					63.96(2)	60.71(2)	54.15(2)	51.99(2)	42.12(2)	41.70(1)	30.55(2)	24.28(1)	22.34(2)
$[Zn(L^4)](ClO_4)_2$	First Isomer					67.42(2)	65.07(2)	61.72(2)	54.26(2)	45.22(2)	43.51(1)	30.39(2)	24.07(2)	22.35(1)
$[Zn(L^4)](ClO_4)_2$	Second Isomer					66.41(2)	64.67(2)	54.08(2)	46.82(2)	40.17(2)	39.25(1)	30.08(2)	23.09(2)	22.87(1)

[a]For assignment of isomers see Figure 2.2

[b]In CD_3NO_2

[c]In $CDCl_3$

[d]Coordinated dimethyl sulphoxide (DMSO) at δ = 39.95 p.p.m.

[e]In CD_3NO_2solution at 290 K

TABLE 2.3

U.v.-Visible Spectra [λ_{max}/nm (ϵ/dm^3 mol^{-1} cm^{-1})] and Magnetic Moments of Ni^{2+} and Cu^{2+} Complexes of L^1 and L^4

Complex	Isomer	Colour	Magnetic[c] Moments B.M.	$\lambda_{max}(\epsilon)$ [a]Nitromethane	[a]Water	[a]Dimethyl Sulphoxide	Reference
$[Ni(L^1)](ClO_4)_2$	(III) or (IV)	Orange		478(215)			This work
$[Ni(L^1)](ClO_4)_2$	"	"		473(233)			115
$[Ni(L^1)](ClO_4)_2$	(I)	Red		498(215)			This work
$[Ni(L^1)](ClO_4)_2$	(I)	Red		502(239)			115
$[Ni(L^1)](ClO_4)_2$	(II)[d]	Green-blue				372(sh), 606(61), 768(43), 898(35)	This work "
$[Ni(L^1)](ClO_4)_2$	(II)	Blue			372(sh), 592(37), 769(25), 898(35)		" "
$[Ni(L^1)Cl]ClO_4$	(II)	Green	3.0	397(170), 632(61), 828(36), 916(24)			"
$[Ni(L^1)NCS]ClO_4$	(II)	Blue	3.1	372(351), 586(78), 780(55), 908(33)			"
$[Ni(L^1)NO_2]ClO_4$	(II)	Blue	3.0	375(70), 598(36), 824(25), 916(33)			"
$[(L^1)Ni\text{-}(\mu\text{-}OX)Ni(L^1)](ClO_4)_2$		Blue	3.1	378(83), 606(45), 808(sh), 980(67)			"
$[Cu(L^1)](ClO_4)_2$		Purple	1.7	506(sh), 584(331)			"
$[Cu(L^1)](ClO_4)_2$		Blue			602(228)	607(262)	"
$[Ni(L^4)](ClO_4)_2$[e]		Red		510(238)	498(226)	515(213)	"
$[Cu(L^4)](ClO_4)_2$		Purple	1.7	492(sh), 573(401)			"
$[Cu(L^4)](ClO_4)_2$		Blue				540(sh), 594(340)	"

[a]Solvents

[b]$[Ni(L^1)](ClO_4)_2$ Isomer (I) has λ_{max} = 498 in the solid phase

[c]Determined by the Evans method (ref. 120) in nitromethane solution

[d]Paramagnetic five coordinate DMSO complex of isomer (II) (see crystal structure)

[e]λ_{max} at 512 (217) in pyridine solvent and λ_{max} at 508 (222) in acetonitrile solvent

SECTION 4 EXPERIMENTAL

The experimental techniques and instrumentation are described in Chapter 7.

CHEMICALS AND SOLVENTS

All chemicals used in the preparation were reagent grade and were used without further purification. Deuterated solvents (99.9% [^{2}H]) were used as supplied, or dried over 4A molecular sieves when necessary. AR solvents were used to run u.v.-visible spectra. These solvents, and Nujol mulls for i.r. samples, were dried over 4A molecular sieves. Elemental analyses were obtained commercially. $[M(DMSO)_n](ClO_4)_2$, M = Ni, Cu n = 6; M = Zn, n = 4 were prepared as described in the literature.[121] The catalyst Raney nickel (W-2) was prepared from nickel-aluminium catalyst alloy using a published procedure.[122]

SECTION 5.1 PREPARATION OF 3,7,11-TRIMETHYL-3,7,11,17-TETRAAZABICYCLO[11.3.1]HEPTADECA-1(17),13,15-TRIENE (L^1)

7-Methyl-3,7,11,17-tetraazabicyclo[11.3.1] hepta deca 1(17), 13,15-triene (L^2) (6.0 g, 24.9 mmol; prepared as described[113], Scheme 2.1 overleaf) was dissolved in 98% formic acid (20 cm^3) and formaldehyde (20 cm^3 of 40% aqueous solution) was added. After heating at 90°C for 24 h, the solution was cooled to room temperature, and then basified to pH 12 with 15% aqueous NaOH. The product was extracted with dichloromethane (5 x 100 cm^3), the combined extracts dried with anhydrous $MgSO_4$, filtered, and the solvent removed with a rotary evaporator to leave a yellow oil. The oil was distilled with a Kugelrohr apparatus to give a pale yellow oil (5.07 g, 18.36 mmol; 75% yield; b.p. 95-98°C at 0.01 mm Hg); ^1H n.m.r. ($CDCl_3$; ref. $Si(CH_3)_4$ at δ = 0.00) 1.50 (4H, pentet), 2.00 (3H, s), 2.24 (4H, t), 2.34 (4H, t), 2.42 (6H, s), 3.69 (4H, s), 7.13 (2H, d) and 7.58 (1H, t) p.p.m. The combustion analyses are in Table 2.1 and the ^{13}C n.m.r. chemical shifts are in Table 2.2. I.r. (thin film); no N-H stretch. Electron impact mass spectrum, m/z 276 (calc. 276 for M^+).

SECTION 5.2 PREPARATION OF THE NICKEL(II) COMPLEXES OF L^1

(i) $[Ni(L^1)](ClO_4)_2$; Isomer (I):

A solution of L^1 (1.0 g, 3.62 mmol) in ethanol (10 cm^3) was added to a solution of $[Ni(H_2O)_6](ClO_4)_2$ (1.32 g, 3.62 mmol) in ethanol (15 cm^3), to give a green solution. This was left to stir at room temperature overnight, and during this time the solution changed colour to blue, and finally red crystals of isomer (I) precipitated. These were collected by filtration and washed with

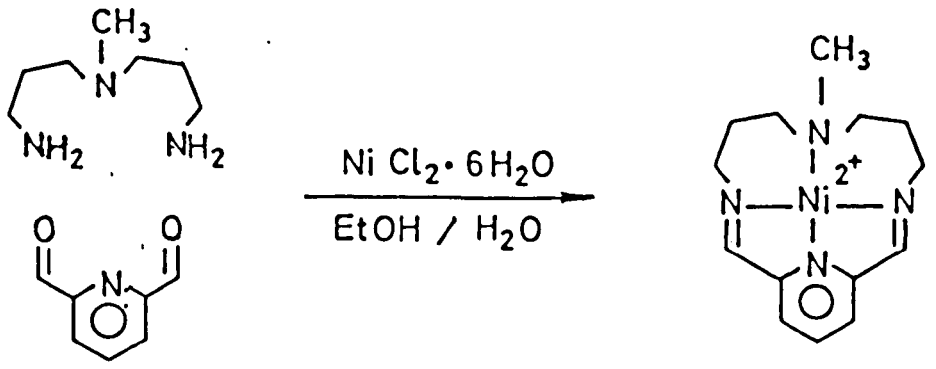

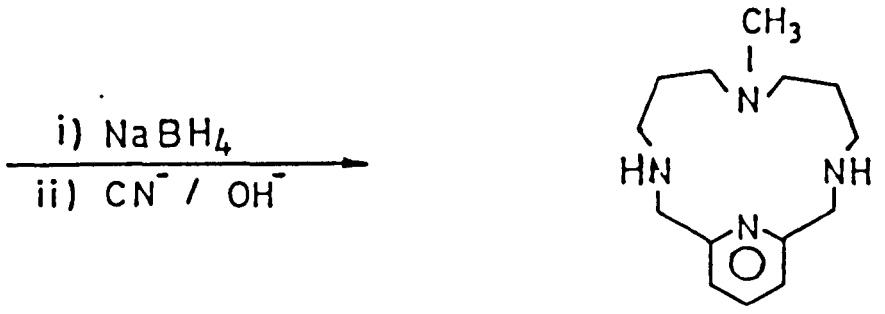

L^2

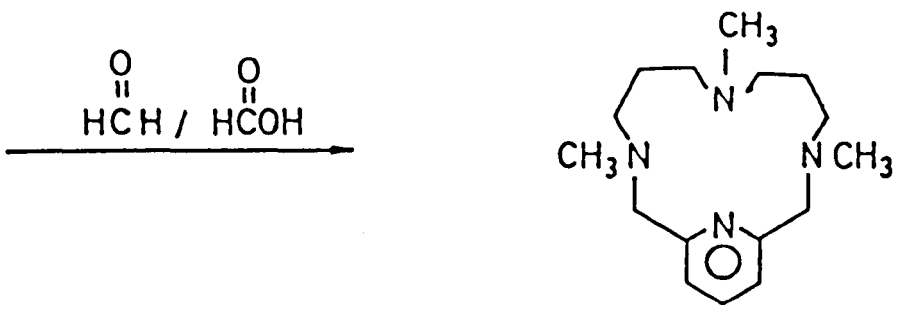

L^1

SCHEME 2.1

ethanol (3 x 5 cm^3) and diethyl ether respectively. The yield was (1.6 g, 3.0 mmol; 83%). The structure of the complex was confirmed by two-dimensional ^1H n.m.r. (Section 2.2.1, page 30).

(ii) $[Ni(L^1)](ClO_4)_2$; Isomer (II):

L^1 (1.0 g, 3.62 mmol) in ethanol (10 cm^3) was added to $[Ni(DMSO)_6](ClO_4)_2$ (2.63, 3.62 mmol) in ethanol (20 cm^3) to give a mixture of a blue and red solid. This was filtered and recrystallised twice from a mixture of nitromethane and ethanol (20 cm^3; 1:3), to give red crystals which were found by ^{13}C n.m.r. to be the symmetric isomer (II) (60% yield). The ^{13}C n.m.r. spectrum is shown in Figure 2.3, page 32.

(iii) $[Ni(L^1)](ClO_4)_2$; Isomer (III or IV):

A sample of the symmetric complex isomer (I) (1.0 g, 0.187 mmol) was dissolved in water (25 cm^3) and heated at 85°C for 20 h, and the solution was then slowly concentrated to *ca.* (5 cm^3), when orange crystals [isomer (III) or (IV)] precipitate. These were collected by filtration, washed with ethanol (3 x 10 cm^3) and diethyl ether respectively, to give the product 250 mg in 25% yield. The structure of the complex was confirmed by ^{13}C n.m.r. and x-ray crystallographic studies (Sections 2.2.1, page 30, and Section 2.2.3, page 38, respectively).

(iv) $[Ni(L^1)DMSO](ClO_4)_2$: DMSO = dimethyl sulphoxide:

$[Ni(L^1)](ClO_4)_2$ (200 mg, 0.37 mmol) was added to a solution of dimethyl sulphoxide (117 mg, 1.5 mmol) in nitromethane (3 cm^3). The product precipitated as a blue solid upon addition of ethanol (5 cm^3), and this was filtered and washed with diethyl ether (3 x 5 cm^3) to give $[Ni(L^1)DMSO](ClO_4)_2$ (210 mg, 0.34 mmol) in 92% yield.

(v) $[Ni(L^1)NCS]ClO_4$:

To a stirred solution of $[Ni(L^1)](ClO_4)_2$ (250 mg, 0.47 mmol) in ethanol (5 cm^3) was added a solution of NaSCN (76 mg, 0.937 mmol) in ethanol (5 cm^3), and the mixture was left to stir overnight at room temperature. The resulting blue solid was filtered and recrystallised from nitromethane/diethyl ether (1:3; 16 cm^3) to give $[Ni(L^1)NCS]ClO_4$, (200 mg, 0.41 mmol) in 87% yield.

(vi) $[Ni(L^1)NO_2]ClO_4$:

$[Ni(L^1)](ClO_4)_2$, (200 mg, 0.37 mmol) was dissolved in water (10 cm^3) at 100°C and added to a solution of sodium nitrite (509 mg, 7.4 mmol) in water (5 cm^3). The reaction mixture was heated at 100°C for 30 minutes, and on cooling blue crystals precipitated. These were collected, washed with cold water (3 cm^3), ethanol (3 x 5 cm^3) and dried under vacuum to give $[Ni(L^1)NO_2]ClO_4$, (100 mg, 0.21 mmol) in 56% yield.

(vii) $[Ni(L^1)Cl]ClO_4$:

A solution of $[Ni(L^1)](ClO_4)_2$ (500 mg; mixture of symmetric and asymmetric isomers) in water (25 cm^3) was carefully transferred to a column (300 x 25 mm) packed with Sephadex C-25 resin (10 g) which had been swelled in distilled water. Elution with 0.4 mol dm^{-3} aqueous NaCl moved a green band (chloro-complex of symmetric isomer) followed by an orange-red band (asymmetric isomer) which were collected separately. Slow evaporation of the water over a long period of time (1 week) afforded green crystals from both bands. These were recrystallised from chloroform, and found to have identical analyses and visible spectra. We conclude that the unsymmetric isomer slowly isomerises to the chloro-complex of the symmetric isomer in aqueous chloride media.

(viii) $[(L^1)Ni(\mu\text{-}OX)Ni(L^1)](ClO_4)_2$: (OX = oxalate ion)

To a stirred solution of $[Ni(L^1)](ClO_4)_2$ (250 mg, 0.47 mmol) in hot water (50 cm^3) was added a solution of Na_2OX (188 mg, 1.4 mmol) in water (2.5 cm^3). The mixture was heated to 100°C for 30 minutes, then allowed to cool slowly, whereupon blue crystals of the product precipitated.These were filtered, washed with a little cold water, and air dried to give $[(L^1)Ni(\mu\text{-}OX)Ni(L^1)](ClO_4)_2$, (185 mg, 0.19 mmol) in 83% yield.

SECTION 5.3 CRYSTALLOGRAPHY

For all compounds data were collected with a Syntex $P2_1$ four-circle diffractometer; reflections were scanned around the $K_{\alpha 1}$-$K_{\alpha 2}$ angles, with variable scan speed depending on the intensity of a 2-S pre-scan; backgrounds were measured at each end of the scan for 0.25 of the scan time. All data were taken at 290 K. Three standard reflections were monitored every 200 reflections; in each case they showed a slight decrease during data collection; the data were rescaled to correct for this. Unit cell dimensions and standard deviations were obtained by a least-squares fit to 15 high-angle reflections. Reflections with $I/\sigma(I) \geq 3.0$ were used in refinement, and corrected for Lorentz polarisation but not absorption effects. For each structure (except as noted below) the heavy atom was located by Patterson techniques and the light atoms were then found on successive Fourier syntheses. Hydrogen atoms were given fixed isotropic thermal parameters, U = 0.07 $Å^2$. Those defined by the molecular geometry were inserted at calculated positions and not refined; methyl groups [included only for (C) and (D)] were treated as rigid CH_3 units with their initial orientation

taken from the strongest peak on a difference Fourier synthesis. Final refinement was by cascaded least-squares methods, with anisotropic thermal parameters for all atoms other than hydrogen in (C), but in (A), (B) and (D) also nitrogen atoms were kept isotropic, in view of the limited number of strong reflections. A weighting scheme of the form $W = 1/[\sigma^2(F) + gF^2]$ (for g see Table 2.5) was used, and in all cases was shown to be satisfactory by a weight analysis. Computing was with the SHELXTL system[123] on a Data General DG30. Scattering factors in the analytical form and anomalous dispersion factors were taken from ref. 124. Specific points were as follows.

FOR (A) The crystals were small pink blocks obtained from slow liquid diffusion of *ca.* (1:4; 10 cm^3) CH_3NO_2:EtOH solution. The crystals bounded by {110} and {001}, which diffracted only weakly. The systematic absences indicate either space group $C2/c$ or Cc. The former would require two-fold molecular symmetry, unlikely on chemical grounds, and therefore the latter was chosen initially and shown to be correct by the successful refinement. Structure solution was somewhat difficult because of the false symmetry of Ni atom; the ClO_4^- ions were described as rigid tetrahedral (Cl-O 1.40 Å), but the high thermal parameters strongly suggest partial disorder. In view of this, and the weak diffraction the relatively high R value was considered satisfactorily; it is possible that some further disorder affects the $(CH_2)_3$ chains, as the bond lengths were rather far from standard values. No attempts were made to define the absolute configuration of the chosen crystal.

FOR (B) The crystals were obtained as small blue flakes by slow liquid diffusion of a solution of $[Ni(L^1)](ClO_4)_2$ in a mixture of DMSO:CH_3NO_2 (1:2) into EtOH 5 parts. Systematic absences

indicated either space group *Pnma* or $Pn2_1a$ (non-standard setting of $Pna2_1$). The automatic Patterson solution routine of SHELXTL applied in both space groups gave successful results for $Pn2_1a$ but not for *Pnma*. Starting from one Ni and one Cl position the full structure was built up by successive Fourier syntheses; the pseudo-symmetry caused some problems that were resolved by the removal and insertion of suspect atoms when necessary. The ClO_4^- ions were treated as rigid bodies (Cl-O 1.4 Å), allowing for shrinkage due to high thermal motion. The largest peak on the final difference synthesis (0.8 $eÅ^{-3}$) lay near to the S atom and suggested possible disorder of the CH_3 groups in the DMSO ligand. Other peaks are concentrated around Cl(1), and in view of the high thermal parameters for O(11)-O(14) they may also have a second partially occupied position. The small number of reflections made it impossible to investigate this further.

FOR (C) The crystals are small green prisms, and were obtained by a slow evaporation of a chloroform solution of the complex. It was excellently behaved in data collection, structure solution and refinement.

FOR (D) The crystals were obtained as blue needles by slow diffusion of ethanol (4 cm^3) into a nitromethane solution of the complex (2 cm^3). The crystals have a tendency to twin, but after some searching a small untwinned crystal was found. The crystals were monoclinic; systematic absences indicated space group $P2_1/c$.

Principal bond lengths and angles for (A)-(D) are given in Table 2.6 and atomic coordinates in Table 2.7.

TABLE 2.6
Principal bond lengths (Å) and angles (°) for
(A), (B), (C) and (D)

(A) $[Ni(L^1)](ClO_4)_2$

Ni-N(1)	1.99(2)	Ni-N(2)	1.86(2)	Ni-N(3)	1.82(2)
Ni-N(4)	2.09(3)				
N(1)-Ni-N(2)	98.7(1.3)	N(2)-Ni-N(4)	164.5(1.2)	N(2)-Ni-N(3)	86.0(1.3)
N(1)-Ni-N(4)	96.7(1.3)	N(1)-Ni-N(3)	175.2(1.3)	N(3)-Ni-N(4)	78.8(1.4)

(B) $[Ni(L^1)(DMSO)](ClO_4)_2$

Ni-N(1)	2.04(3)	Ni-N(2)	2.18(3)	Ni-N(3)	1.97(3)
Ni-N(4)	2.08(3)	Ni-O(10)	2.01(2)	O(101)-S	1.44(3)
S-C(1)	1.72(4)	S-C(2)	1.84(4)		
N(1)-Ni-N(2)	98.5(1.0)	Ni-O(101)-S	150.1(1.6)	N(3)-Ni-N(4)	80.7(1.1)
N(1)-Ni-N(4)	100.4(1.1)	O(101)-S-C(2)	108.0(1.7)	N(4)-Ni-O(101)	98.5(1.0)
N(2)-Ni-N(3)	83.3(1.1)	N(1)-Ni-N(3)	105.7(1.0)	O(101)-S-C(1)	105.9(1.7)
N(2)-Ni-O(101)	90.5(1.0)	N(1)-Ni-O(101)	97.0(1.0)	C(1)-S-C(2)	99.3(1.8)
N(3)-Ni-O(101)	157.1(1.0)	N(2)-Ni-N(4)	157.9(1.0)		

(C) $[Ni(L^1)Cl]ClO_4$

Ni- N(1)	2.027(4)	Ni-N(2)	2.119(5)	Ni-N(3)	1.976(3)
Ni-N(4)	2.119(5)	Ni-Cl(2)	2.300(1)		
N(1)-Ni-N(2)	98.8(2)	N(3)-Ni-Cl(2)	156.6(1)	N(2)-Ni-N(4)	156.0(2)
N(1)-Ni-N(4)	98.9(2)	N(1)-Ni-N(3)	104.2(2)	N(3)-Ni-N(4)	79.7(2)
N(2)-Ni-N(3)	80.4(2)	N(1)-Ni-Cl(2)	99.3(1)	N(4)-Ni-Cl(2)	96.0(1)
N(2)-Ni-Cl(2)	96.9(1)				

(D) $[(L^1)Ni(\mu\text{-}OX)Ni(L^1)](ClO_4)_2$

Ni-O(1)	2.124(6)	Ni-N(1)	2.157(7)	Ni-N(2)	2.187(7)
Ni-N(3)	1.989(7)	Ni-N(4)	2.200(7)	Ni-O(2)	2.069(3)
O(1)-C(1)	1.245(9)	O(2)-C(1)	1.275(10)	C(1)-C(1a)	1.503(15)
O(1)-Ni-N(1)	167.9(2)	O(1)-Ni-N(2)	92.9(3)		
N(1)-Ni-N(2)	91.9(3)	O(1)-Ni-N(3)	88.8(3)		
N(1)-Ni-N(3)	103.1(3)	N(2)-Ni-N(3)	79.1(3)		
O(1)-Ni-N(4)	87.0(3)	N(1)-Ni-N(4)	92.6(3)		
N(2)-Ni-N(4)	158.2(3)	N(3)-Ni-N(4)	79.1(3)		
O(1)-Ni-O(2)	78.9(2)	N(1)-Ni-O(2)	89.4(2)		
N(2)-Ni-O(2)	99.4(2)	N(3)-Ni-O(2')	167.5(3)		
N(4)-Ni-O(2')	102.0(2)				

TABLE 2.7
Atomic co-ordinates (x 10^4) for complexes (A), (B), (C) and (D)

Atoms	x	y	z	Atoms	x	y	z
(A)							
Ni	5000	1493(2)	7500	C(1)	3813(32)	3270(21)	7934(19)
Cl(1)	1618(11)	1000(6)	9102(6)	C(2)	5241(34)	3341(25)	6574(21)
O(11)	2553	1700	8672	C(3)	4095(30)	3065(22)	5910(18)
O(12)	2280	82	8880	C(4)	4300(30)	1842(21)	5708(18)
O(13)	1969	1132	9995	C(5)	2509(29)	1069(23)	6627(19)
O(14)	471	1084	8860	C(6)	4441(36)	375(23)	6042(20)
Cl(2)	8446(8)	1057(5)	5896(5)	C(7)	4754(32)	-321(23)	6797(19)
O(21)	7815	384	5350	C(8)	4682(33)	-1415(23)	6956(23)
O(22)	8971	1802	5398	C(9)	5105(38)	-1818(19)	7645(19)
O(23)	7529	1438	6466	C(10)	5464(29)	-1236(22)	8363(19)
O(24)	9478	605	6369	C(11)	5575(46)	-273(33)	8189(28)
N(1)	5072(35)	2928(11)	7550(23)	C(12)	5698(37)	331(24)	8934(20)
N(2)	3992(24)	1359(17)	6477(14)	C(13)	7479(57)	1413(32)	8462(31)
N(3)	5050(32)	179(12)	7520(22)	C(14)	5807(30)	2247(19)	9247(18)
N(4)	6057(37)	1240(23)	8663(21)	C(15)	6496(32)	3091(22)	8861(18)
				C(16)	6352(32)	3291(23)	7928(20)
(B)							
Ni	7066(3)	5000	4353(3)	C(2)	9020(21)	7157(33)	3422(26)
Cl(1)	3517(7)	4700(9)	4247(10)	C(3)	5904(25)	4518(31)	6065(29)
O(11)	3281	4051	3392	C(4)	7172(22)	5287(28)	6657(26)
O(12)	4202	4276	4662	C(5)	7615(21)	4191(27)	6748(27)
O(13)	2947	4692	5029	C(6)	8217(19)	4042(33)	5872(26)
O(14)	3637	5778	3904	C(7)	8523(25)	3783(36)	4082(32)
Cl(2)	9543(7)	509(8)	4380(9)	C(8)	7448(22)	2757(29)	4807(27)
O(21)	9912	-118	3602	C(9)	6887(17)	2670(24)	3969(22)
O(22)	9814	1589	4355	C(10)	6459(22)	1722(28)	3491(26)
O(23)	9697	65	5379	C(11)	5886(22)	1916(34)	2845(28)
O(24)	8748	498	4203	C(12)	5582(22)	2937(27)	2657(29)
O(101)	7851(13)	6206(20)	4443(18)	C(13)	5932(19)	3816(25)	3172(23)
S	8108(8)	7293(11)	4159(10)	C(14)	5638(18)	4986(32)	3089(26)
N(1)	6550(16)	5288(20)	5778(21)	C(15)	6673(23)	6072(30)	2283(29)
N(2)	7920(18)	3806(22)	4873(21)	C(16)	5972(22)	6813(31)	3853(26)
N(3)	6552(16)	3695(22)	3771(20)	C(17)	5689(22)	6696(35)	4901(28)
N(4)	6289(19)	5766(22)	3342(21)	C(18)	6195(19)	6364(27)	5790(26)
C(1)	8455(23)	7871(32)	5308(28)				

Atoms	x	y	z	Atoms	x	y	z
(C)							
Ni	2770.2(8)	2048.8(7)	2179.9(5)	C(4)	4(7)	116(5)	2347(4)
CL(1)	7415(2)	6761(1)	3250(1)	C(5)	-512(7)	778(5)	3288(4)
O(11)	7812(10)	6795(7)	2239(4)	C(6)	-1944(7)	455(6)	4084(4)
O(12)	8954(8)	7104(5)	3549(5)	C(7)	-2352(8)	1226(7)	4861(4)
O(13)	7188(8)	5479(6)	3665(5)	C(8)	-1359(7)	2278(6)	4841(4)
O(14)	5919(8)	7566(7)	3581(5)	C(9)	91(7)	2552(5)	4026(4)
Cl(2)	5869(2)	1755(2)	1375(1)	C(10)	1244(7)	3698(5)	3850(4)
N(1)	1861(5)	3289(4)	1136(3)	C(11)	3820(8)	4654(6)	2567(5)
N(2)	3080(5)	3437(4)	3127(3)	C(12)	2795(9)	5263(6)	1809(5)
N(3)	503(5)	1789(4)	3261(3)	C(13)	2954(8)	4469(6)	926(4)
N(4)	1988(5)	276(4)	1827(3)	C(14)	-161(7)	3689(6)	1420(4)
C(1)	2291(8)	2662(6)	172(4)	C(15)	3155(9)	-798(6)	2210(5)
C(2)	1453(8)	1372(7)	200(4)	C(16)	4409(8)	2797(7)	3709(5)
C(3)	2284(8)	208(7)	736(4)				
(D)							
Ni	1135.1(12)	942.9(5)	487.9(6)	C(3)	4728(11)	830(5)	4110(8)
Cl	4924(4)	1358(1)	9070(2)	C(4)	5080(12)	1379(6)	4955(9)
O(11)	5981(31)	1029(7)	6699(19)	C(5)	3884(15)	1429(7)	5666(9)
O(12)	3361(20)	1225(9)	8821(15)	C(6)	1198(16)	1592(7)	5976(8)
O(13)	5145(20)	1485(12)	10065(9)	C(7)	2116(15)	2270(5)	4653(8)
O(14)	5020(20)	1965(6)	8567(15)	C(8)	535(15)	2335(5)	3771(8)
O(1)	-940(7)	713(3)	4433(4)	C(9)	-290(17)	2921(5)	3488(9)
O(2)	-1813(7)	-45(3)	5491(4)	C(10)	-1615(15)	2909(6)	2642(11
C(1)	-773(9)	191(4)	4973(6)	C(11)	-2087(14)	2346(7)	2092(11
N(1)	3378(8)	960(3)	3158(5)	C(12)	-1187(12)	1778(5)	2413(9)
N(2)	2132(10)	1602(4)	5125(5)	C(13)	-1677(14)	1093(6)	2004(10
N(3)	88(8)	1791(4)	3220(5)	C(14)	-993(20)	-19(6)	2080(10
N(4)	-283(9)	636(4)	2163(5)	C(15)	555(14)	794(6)	1273(7)
C(2)	3830(12)	1536(4)	2519(8)	C(16)	2170(14)	410(6)	1338(8)
				C(17)	3299(12)	364(5)	2432(8)

SECTION 5.4 PREPARATION OF COPPER(II) AND ZINC(II) COMPLEXES OF L^1

(i) $[Cu(L^1)](ClO_4)_2.H_2O$

L^1 (100 mg, 0.36 mmol) was dissolved in ethanol (5 cm^3) and added to $[Cu(H_2O)_6](ClO_4)_2$ (133 mg, 0.36 mmol) in ethanol (8 cm^3). A purple solid precipitated, and was filtered, washed with diethyl ether (3 x 5 cm^3) and dried under vacuum (yield 180 mg, 0.32 mmol, 90%).

(ii) $[Zn(L^1)](NO_3)_2.H_2O$

L^1 (100 mg, 0.36 mmol) was dissolved in ethanol (5 cm^3) and $Zn(NO_3)_2.6H_2O$ (107 mg, 0.36 mmol) in ethanol (5cm^3) was added. The mixture was stirred for 30 minutes under dry dinitrogen, and then dry diethyl ether (20 cm^3) was added to precipitate the product as an oily solid. This was stirred in a mixture of dry dichloromethane and diethyl ether (15 cm^3, 1:2) under dinitrogen overnight to give a white solid. The solid was filtered in a dry box and vacuum dried to give the product (113 mg, 0.23 mmol in 65% yield). The ^{13}C n.m.r. chemical shifts are in Table 2.2 (page 56).

(iii) $[Zn(L^1)DMSO](ClO_4)_2$; DMSO = dimethyl sulphoxide

This was prepared in 75% yield as described for the nitrate salt using $[Zn(DMSO)_4](ClO_4)_2$. Diethyl ether was again required to precipitate the product which analysed as $[Zn(L^1)](ClO_4)_2$. The presence of coordinated (DMSO) was confirmed by ^{13}C n.m.r. spectrum (Figure 2.10). Recrystallisation of the product from nitromethane diethyl ether gave the unsolvated complex as shown by analytical data (Table 2.1, page 55).

SECTION 6.1 PREPARATION OF 3,7,11-TRIMETHYL-3,7,11,17-TETRAAZA-BICYCLO[11.3.1] HEPTA DECANE (L^4)

The ligand was prepared following the synthetic routes outlined in Scheme 2.2 overleaf; $[Ni(L^1)](ClO_4)_2$ (2.0 g, 3.75 mmol) was dissolved in water (100 cm^3) and hydrogenated over freshly prepared Raney-nickel (W-2) (*ca.* 6 g) at 120 atm H_2 (Scheme 2.2). The reaction mixture was placed in a 200 cm^3 autoclave, and the temperature of the reaction was gradually increased to 65° (24 h), 85°C (2 h) and finally allowed to cool to room temperature for 24 h. The catalyst was removed by filtration and the solution evaporated to a volume of *ca.* 50 cm^3. To the orange solution a NaCN (5 g) was added, and the reaction mixture kept in an oil bath at 80°C for 1 h. The solution was then basefied and extracted with dichloromethane (5 x 100 cm^3), dried with anhydrous $MgSO_4$, filtered and the solvent removed to give the product as very viscous oil. This was left in the refrigerator to give colourless crystals. M.P. 87°C (0.83 g, 2.94 mmol) in 78% yield. The ^{13}C n.m.r. spectrum is shown in Figure 2.11 (page 49), and the geometry of the macrocycle (L^4) was established by two dimensional ^1H n.m.r. (Section 3.1, page 48).

SECTION 6.2 PREPARATION OF METAL COMPLEXES OF L^4

(i) $[Ni(L^4)(ClO_4)_2$

To a stirred solution of $[Ni(DMSO)_6](ClO_4)_2$ (257 mg, 0.355 mmol) in ethanol (10 cm^3), a solution of the (L^4) (100 mg, 0.355 mmol) in ethanol (5 cm^3) was added. Orange-red crystals precipitated and these were filtered, washed with diethyl ether and air dried to give $[Ni(L^4)](ClO_4)_2$ (160 mg, 0.297 mmol) in 84% yield. ^{13}C n.m.r. chemical shifts are in Table 2.2 and the analytical data

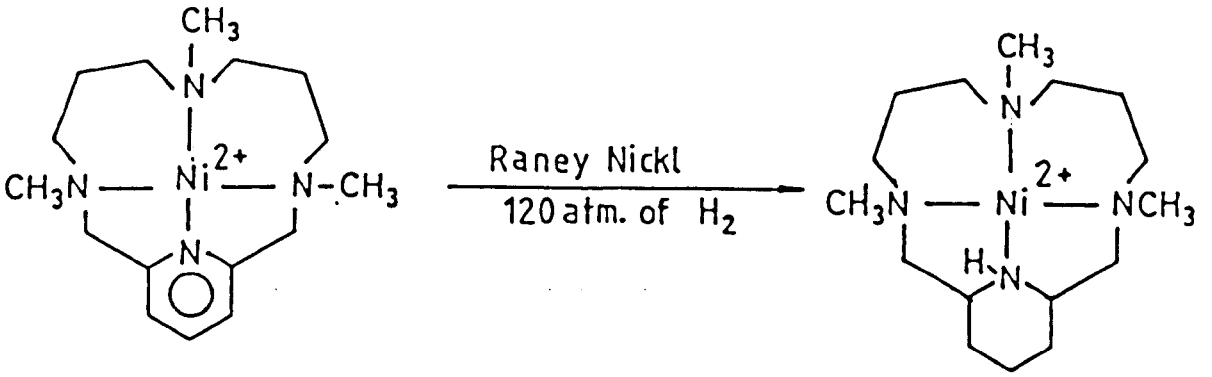
CH3
N
CH3N
Ni2+
N-CH3
N
Raney Nickl
120 atm. of H2
CH3
N
CH3N
Ni2+
NCH3
H
N

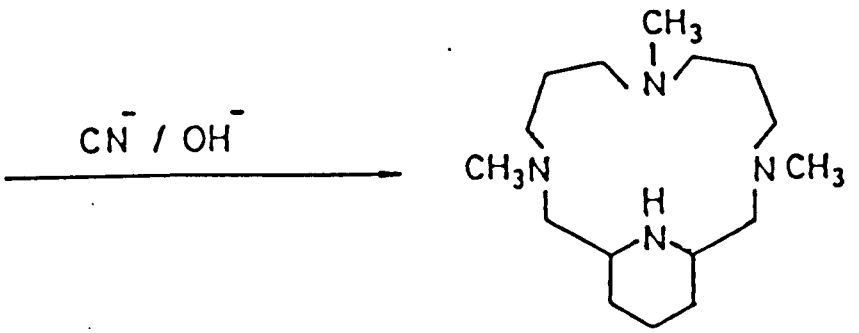
CN- / OH-
CH3
N
CH3N
N CH3
H
N

L^4

SCHEME 2.2

are in Table 2.1.

(ii) $[Cu(L^4)](ClO_4)_2.1\frac{1}{2}H_2O$

L^4 (50 mg, 0.177 mmol) was dissolved in ethanol (5 cm^3) and added to an ethanolic solution of $[Cu(DMSO)_6](ClO_4)_2$ (129 mg, 0.177 mmol). The resulting purple precipitate was filtered, washed with diethyl ether and dried under vacuum to give the product (70 mg, 0.121 mmol) in 68% yield. Analytical data are in Table 2.1 (page 55).

(iii) $[Zn(L^4)](ClO_4)_2$

$[Zn(DMSO)_4](ClO_4)_2$ (204 mg, 0.355 mmol) was dissolved in ethanol (10 cm^3) and added to a solution of (L^4) (100 mg, 0.355 mmol) in ethanol (5 cm^3) under dry dinitrogen. The product precipitated as a white moisture sensitive solid by the addition of dry diethyl ether (10 cm^3). Filtration under dinitrogen, and drying in vacuum gave the product (140 mg, 0.225 mmol) in 63% yield. Combustion analyses and ^{13}C n.m.r. chemical shifts are in Table 2.1 and 2.2 respectively.

CHAPTER III

SYNTHESIS AND STUDY OF PENTAAZAMACROCYCLIC LIGANDS AND THEIR NICKEL(II), COPPER(II), ZINC(II), CADMIUM(II) AND LEAD(II) COMPLEXES

SECTION 1 INTRODUCTION

Attempts to prepare macrocyclic Schiff's base complexes by the condensing of 2,6-diacetylpyridine with diamines such as $(NH_2CH_2CH_2XCH-)_2$ (X = NH, O or PPh) in the presence of template metal ions such as Ni^{2+} and Cu^{2+} were unsuccessful.[125] However, successful template syntheses have been achieved using other metal ions (e.g., Mn^{2+}, Fe^{2+}, Fe^{3+}, Co^{2+}, Mg^{2+}, Zn^{2+}, Cd^{2+}, Hg^{2+}, Ag^{2+}, Pb^{2+} and Sn^{4+}).[126-130] Busch and co-workers[130] succeeded in obtaining the saturated pentaazamacrocycle L^8 (Figure 3.1), by reduction of the Mn^{2+} complex of the corresponding Schiff's base macrocycle with nickel aluminium alloy in aqueous base.

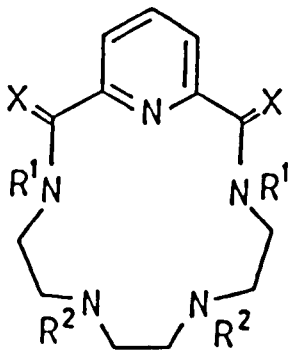

L^5; X = O; R^1 = H, R^2 = Me

L^6; X = H_2; R^1 = H, R^2 = Me

L^7; X = H_2; R^1 = R^2 = Me

L^8; X = Me,H; R^1 = R^2 = H

L^9; X = H_2; R^1 = R^2 = H

FIGURE 3.1

Our attempts to prepare the corresponding macrocycle L^9 (Figure 3.1) in an analogous way, starting from pyridine-2,6-dicarbaldehyde and $(NH_2CH_2CH_2NHCH_2-)_2$, gave very low yields (5-10%). Therefore, a better route to 15-membered ring pentaazamacrocycles was sought.

In this Chapter the synthesis of three related pentaazamacrocycles, L^5-L^7, are reported using high dilution technique. The Ni^{2+} and Cu^{2+} complexes of L^5 and the Ni^{2+}, Cu^{2+}, Zn^{2+}, Cd^{2+} and Pb^{2+} complexes of L^6 and L^7 were also isolated, and characterised by elemental analyses, fast atom bombardment (f.a.b.) mass spectrometry and ^{13}C n.m.r. for the diamagnetic Cd^{2+}, Pb^{2+} and Zn^{2+} complexes. The Ni^{2+} and Cu^{2+} complexes were investigated further by u.v.-visible spectroscopy and magnetic moment measurements. The crystal and molecular structure of $[Zn(L^7)](ClO_4)_2$ is also reported.

SECTION 2 RESULTS AND DISCUSSION

SECTION 2.1 LIGAND SYNTHESES

As mentioned previously, syntheses of pyridyl containing pentaazamacrocycles have mainly been achieved by template methods, although Kimura, *et al.*,[131] obtained a 16-membered ring diamide macrocycle in unspecified yield from refluxing (3d) the diethyl ester of pyridine-2,6-dicarboxylic acid and 3,7-diazanonane-1,9-diamine in ethanol solution. In this study, the high dilution method was employed to give the 15-membered ring diamide macrocycle L^5 (Figure 3.1) in 24% yield, in a rapid reaction between pyridine-2,6-dicarboxylic acid dichloride and 3,6-dimethyl-3,6-diazaoctane-1,8-diamine (see Scheme 3.1, page 93). Although this route gives only moderate yields, the starting materials are relatively cheap and readily available. However, the synthesis requires the use of an open chain amine in which only the terminal amino-groups are capable of being attacked by diacid chloride [i.e., R^2 in L^5 (Figure 3.1) must be alkyl or aryl, and not hydrogen].

Reduction of the amide groups of L^5 to give L^6 proceeds in good yield (> 80%) using BH_3.thf, and methylation of the secondary amine groups of L^6 with formaldehyde formic acid gives L^7 in *ca.* 88% yield. The ligands were characterised by their ^1H n.m.r., mass spectra, ^{13}C n.m.r. chemical shifts (Table 3.4), and by the analytical data for their metal complexes (Table 3.1).

SECTION 3 METAL COMPLEX SYNTHESES

SECTION 3.1 SYNTHESIS OF METAL COMPLEXES OF L^5

Reaction of L^5 with an equimolar amount of copper or nickel acetate in methanol under reflux gave the neutral complexes of formula $[ML_{-2}]$, M = Cu^{II} and Ni^{II}. The complexes are nonelectrolytes in methanol, and their f.a.b. mass spectra show a cluster of peaks, centred at m/z 367 for the copper complex and 362 for the nickel complex, attributed to $[M(LH_{-2})]^+$, (M + 1), M = Cu^{II} and Ni^{II} (Table 3.3). The solid thin film infrared spectrum (for sample preparation method see Chapter VII) of L^5 shows an amide band ν(C=O) at 1676 cm^{-1}, and that of the solid copper(II) complex has bands at 1638 cm^{-1} and 1600 cm^{-1}, and the nickel(II) complex has bands at 1630 cm^{-1} and 1600 cm^{-1}. In addition, bands were observed at 3400, 2990 and 1410 cm^{-1} in copper complex spectrum assigned to ν(OH), ν(CH) and ν(COO) respectively. These bands arise from ethanoic acid, probably in the crystal lattice of the copper(II) complex. Data from the u.v.-visible spectra recorded in different solvents are shown in Table 3.2.

The visible spectrum of $[Cu(L^5H_{-2})]$ in aqueous solution shows a band at 677 nm which is close to the value reported for the $[Cu(NH_3)_5]^{2+}$ ion (678 nm) and indicates that all five N atoms of L^5 are coordinated.[132] Attempts to prepare Cd^{II} and Zn^{II} complexes of L^5 following the same procedure described for Ni^{II} and Cu^{II} were unsuccessful. The ^{13}C n.m.r. of the white solid recovered from both reactions show no significant difference in chemical shifts compared with the chemical shifts arising from the free ligand in the same solvent. In addition two extra resonances were observed, one of them located upfield and arising from the methyl group of acetate

ion. This observation is similar to that reported by Kimura, *et al.*:[133] "The most successful metal ion in promoting the deprotonation was Cu^{II}. With Zn^{II}, Cd^{II}, or Pb^{II} the dioxo-ligands underwent no deprotonation at pH < 7. At pH > 7 precipitation of hydrolysed metal ions occurred."

SECTION 3.2 SYNTHESES OF METAL COMPLEXES OF L^6 AND L^7

These were obtained in good yields from the 1:1 reactions of the appropriate ligand and the dimethyl sulphoxide (DMSO) solvates of Cu^{II}, Ni^{II} and Zn^{II} perchlorate, and Cd^{II}, Pb^{II} nitrate in ethanol solution. Analytical data (Table 3.1) indicate the formation of either six coordinate mono-solvent complexes of formula $[M(L)(DMSO)](ClO_4)_2$ (L = L^6 and L^7, M = Ni^{II}; L = L^6, M = Zn^{II}), or five-coordinate complexes of formula $[M(L)](ClO_4)_2$ (L = L^6 and L^7, M = Cu^{II}; L = L^7, M = Zn^{II}). The Cd^{II} and Pb^{II} complexes of L^6 are five coordinate of formula $[M(L)](NO_3)_2$ (L = L^6, M = Cd^{II}, Pb^{II}); whereas the data for the lead(II) complex of L^7 reveals that the complex has a formula close to $[(PbL^7)_2(H_2O)_4(NO_3)_2][Pb(NO_3)_4]$. No further attempt was made to confirm this formulation. The visible spectra and magnetic moments of the Ni^{2+} and Cu^{2+} complexes (Table 3.2) are consistent with the formulations given above. The fast atom bombardment (f.a.b.) mass spectra of the complexes (Table 3.3) gave clusters of peaks as expected for the ions $[M(L)ClO_4]^+$ or $[M(L)NO_3]^+$ and $[M(L-H)]^+$ (L = L^6, L^7; M = Ni, Cu, Zn, Cd and Pb). This behaviour is as expected from our earlier studies.[113] The f.a.b. spectrum of $[Zn(L^7)](ClO_4)_2$ also showed a strong peak assigned to $[H_2L^7(ClO_4)]^+$. This unexpected behaviour may indicate that the zinc(II) complex is the less stable of the five.

The proton decoupled ^{13}C n.m.r. spectrum of $[Zn(L^6)(DMSO)]^{2+}$ ion in the CD_3NO_2 solution is shown in Figure 3.2, It reveals the presence of a coordinated (DMSO) molecule as a broad resonance at δ 40.0 p.p.m., broadening presumably being due to chemical exchange. The existence of a *ca.* 2:1 mixture of two isomers, one symmetric and the other asymmetric, is evident from the number of resonances in the spectrum; the assignments for the two isomers are in Table 3.4. The presence of two isomers is also apparent in the ^{13}C n.m.r. spectrum of the $[Cd(L^6)]^{2+}$ ion, and of the $[Zn(L^7)]^{2+}$ ion, although only *ca.* 10% of the symmetric isomer is present in the Cd^{II} complex of L^6, whereas *ca.* 90% of symmetric isomer is present in the ^{13}C n.m.r. spectrum of $[Zn(L^7)]^{2+}$ ion (Table 3.4). The ^{13}C n.m.r. spectrum of $[Pb(L^7)]^{2+}$ ion in CD_3NO_2 solution is shown in Figure 3.3, and reveals the presence of single asymmetric species. It is interesting to note that in the case of large metal ions such as Cd^{II} or Pb^{II} the coordinated macrocyclic ligands L^6 and L^7 adopt an asymmetric coordination mode, whereas with smaller metal ions such as Zn^{II} the symmetric species is the predominant one. This may be due to the size of the cavities of these macrocycles which are not large enough to fit large metal ions such as Cd^{II} and Pb^{II}, so distortion of the symmetry occurs in those cases.

Previous studies of pyridyl-containing pentaazamacrocycles have revealed three modes of coordination (I-III) shown schematically in Figure 3.4. With saturated macrocyclic rings, seven-coordinate pentagonal bipyramidal complexes (II) are formed by Mn^{2+} and Fe^{3+} and six coordinate pseudooctahedral complexes (II) are formed by Co^{3+}, Ni^{2+}, Ni^{3+} and Cu^{2+} ions in which unidentate anions

FIGURE 3.2 ^{1}H decoupled ^{13}C n.m.r. specrum of $[Zn(L^{6})(DMSO)](ClO_4)_2$ in CD_3NO_2 solution.

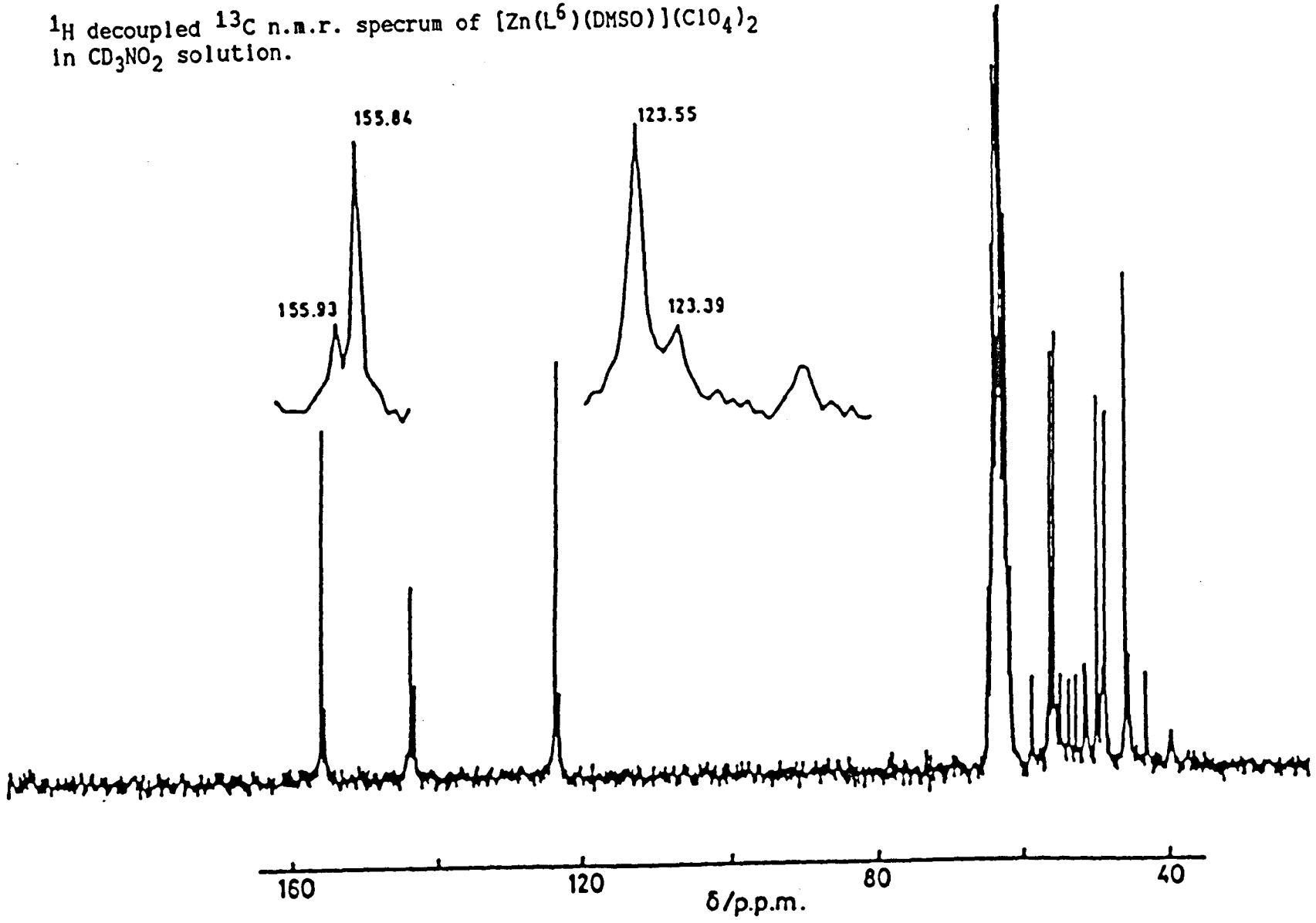

FIGURE 3.3 ^{1}H Decoupled ^{13}C n.m.r. spectrum of $[Pb(L^{7})](NO_3)_2$ in CD_3NO_2 solution

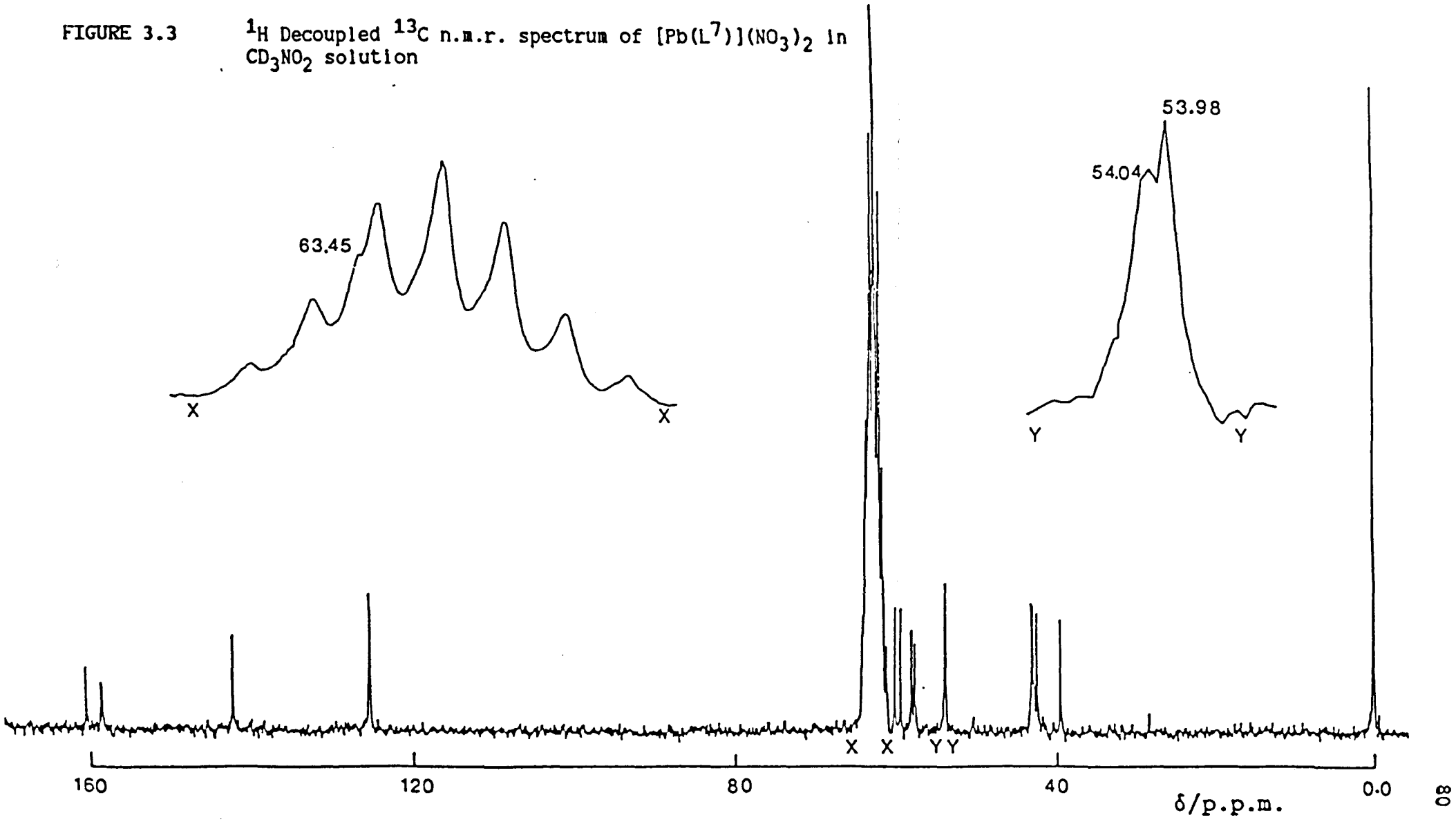

or solvent molecules occupy the remaining coordination sites.[129,130,131]

A structure of type (II) is reported for the Co^{3+} complexes of 1,4,7,10,13-pentaazacyclohexadecane.[134] Pentagonal bipyramidal Schiff base complexes are also well known, including a complex of Zn^{2+}.[60] A structure in which one of the N-atoms is uncoordinated in a *trans*-octahedral arrangement of type (III) is also postulated for a low-spin Schiff base macrocyclic complex of Fe^{2+} with cyanide ions occupying the axial positions.[135] Five co-ordinate structures can also be envisaged for these pentaazamacrocycles, in which the macrocycle either occupies the corners of a square-pyramid (analogous to structure(II) but with no axial unidentate ligand), or a trigonal bipyramidal mode as shown in structure (IV). In both modes of five-coordination the expected planarity of the metal ion with the pyridine N-atom and the two flanking N-atoms is maintained. There are, of course many isomers of these structures possible depending on the different chiralities of the N-H and $N-CH_3$ groups. A symmetric structure observed in the ^{13}C n.m.r. spectra of the Zn^{2+} complexes is possible for structure (IV) with the N-substituents arranged as shown. In this structure there is a C_2 rotation axis passing through the metal and pyridine N-atoms and bisecting the macrocyclic C-C bond furthest removed from the pyridine ring. The asymmetric species observed in the ^{13}C n.m.r. spectra could have either a square pyramidal structure or a non-symmetric structure (IV) with one of the chiral N-atoms inverted.

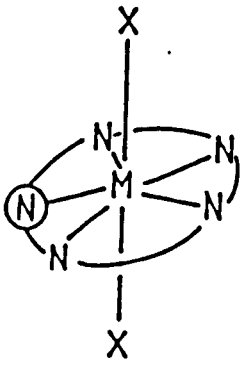

(I)

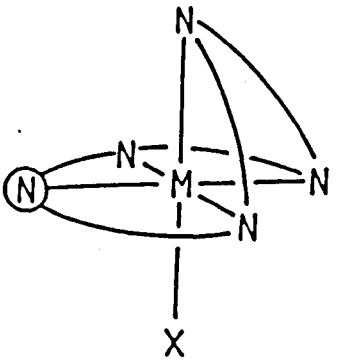

(II)

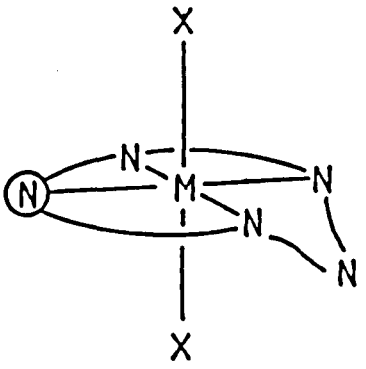

(III)

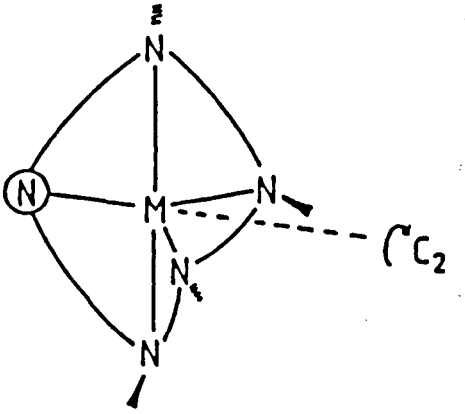

(IV)

FIGURE 3.4

Schematic representation of the different modes of coordination found in metal complexes of L^5-L^9 (X = unidentate ligand, M = metal ion). The pyridine N-atom is circled.

SECTION 3.3 CRYSTAL STRUCTURE

To gain further insight into the structure of the Zn^{2+} complexes, the crystal structure of $[Zn(L^7)](ClO_4)_2$ was determined. The cation geometry is shown in Figure 3.5. This can be equated to structure (IV), with a non-crystallographic C_2 rotation axis passing through the Zn, N(1) and C(3) atoms. Such a symmetric isomer gives a satisfactory explanation for the major component identified in the ^{13}C n.m.r. spectrum of a nitromethane solution. The Me-N groups at positions 3 and 9 [N(2) and N(4)] are on the opposite side of the macrocycle to those at positions 6 and 12 [N(3) and N(5); Figure 3.5]. Major distortions from the idealised trigonal bipyramidal geometry depicted in structure (IV) are apparent from the bond lengths and angles in Table 3.6. The 'axial' N(2)-Zn-N(5) angle is only 155.9°(2), and the other N-Zn-N bond angles involving N(2) and N(5) are in the range of 78.1°(2) to 114.0°(2). The 'in-plane' N-Zn-N bond angles involving N(1), N(3) and N(4) are 137.5°(2) and 134.3°(2) to the pyridine N-atom [N(1)], and only 88.2°(2) for N(3)-Zn-N(4). However, the 'axial' Zn-N bond lengths (2.24 and 2.25 Å) are significantly longer than the 'equatorial' bond lengths (*ca.* 2.0-2.1 Å) as expected for a trigonal bipyramid. A very similar five-coordinate structure is reported for the $[Cu(L^8)]^{2+}$ ion although in the copper(II) complex further distortions are apparent, attributable to the Jahn-Teller effect, which results in a structure between that of a square-pyramid and a trigonal bipyramid.[136] For $[Zn(L^7)]^{2+}$ the structure is closer to that of a trigonal bipyramid than a square pyramid; for compounds showing square pyramidal geometry, the N-metal-N bond angles are observed to have a characteristic pattern of four nearly equal and large values

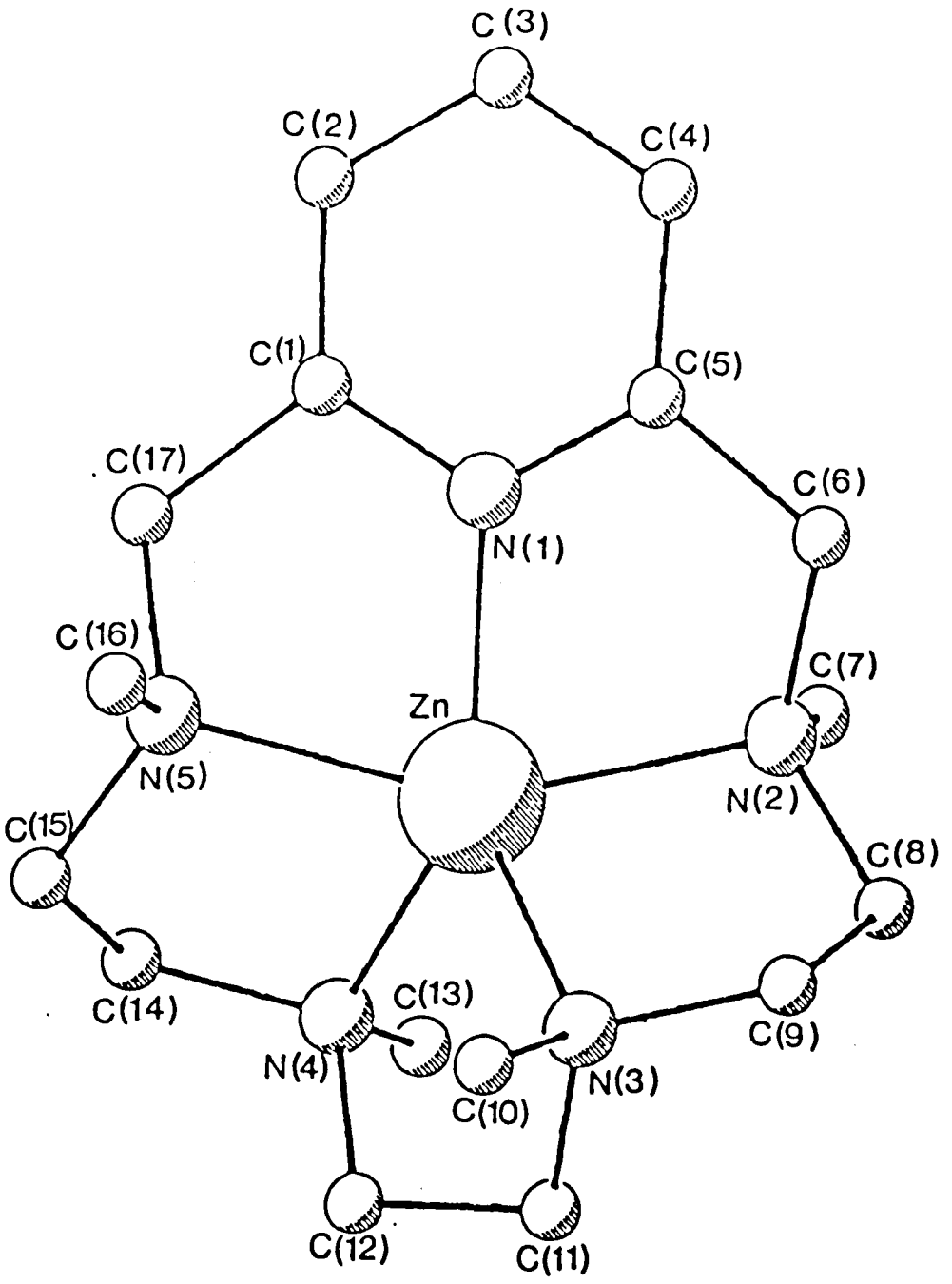

FIGURE 3.5

View of the symmetric isomer of $[Zn(L^7)]^{2+}$ ion, showing the atomic numbering. H-atoms are omitted for clarity.

(usually *ca.* 135°), rather than having one angle much larger than the others, and the bond lengths are more nearly equal.[136]

TABLE 3.1

METAL COMPLEXES OF L^5, L^6 AND L^7 AND THEIR ELEMENTAL ANALYSES[a]

Complex[b]	Colour	Recrystal. from CH_3NO_2: EtOH: Et_2O	Yield (%)	Formula	C	H	N
$[Ni(L^5H_{-2})]$	Pale Green		80	$C_{15}H_{21}N_5O_2Ni$	49.8(49.7)	7.0(5.8)	19.0(19.3)
$[Cu(L^5H_{-2})].2CH_3COOH$	Blue		90	$C_{19}H_{29}N_5O_6Cu$	46.5(46.9)	5.7(5.9)	14.5(14.4)
$[Ni(L^6)(DMSO)](ClO_4)_2$	Green	1:1:2	60	$C_{17}H_{33}Cl_2N_5NiO_9S$	33.8(33.3)	5.2(5.4)	11.8(11.4)
$[Cu(L^6)](ClO_4)_2$	Blue Green	1:2:1	69	$C_{15}H_{27}Cl_2CuN_5O_8$	33.1(33.4)	5.0(5.0)	12.8(13.0)
$[Zn(L^6)(DMSO)](ClO_4)_2$	White		48	$C_{17}H_{33}Cl_2N_5O_9SZn$	32.9(32.9)	5.1(5.4)	11.6(11.3)
$[Cd(L^6)](NO_3)_2$	White		60	$C_{15}H_{27}N_7CdO_6$	35.1(35.1)	5.2(5.3)	19.0(19.1)
$[Pb(L^6)](NO_3)_2$	White		73	$C_{15}H_{27}N_7PbO_6$	29.5(29.6)	4.2(4.4)	16.0(16.1)
$[Ni(L^7)(DMSO)](ClO_4)_2.H_2O$	Green		53	$C_{19}H_{39}Cl_2N_5NiO_{10}S$	34.9(34.6)	5.9(6.0)	10.8(10.6)
$[Cu(L^7)](ClO_4)_2$	Blue	1:1:2	59	$C_{17}H_{31}Cl_2CuN_5O_8$	35.8(36.0)	5.6(5.5)	12.2(12.3)
$[Zn(L^7)](ClO_4)_2$	White		64	$C_{17}H_{31}Cl_2N_5O_8Zn$	36.4(35.8)	5.7(5.5)	11.9(12.3)
$[Cd(L^7)](NO_3)_2.5H_2O$	White		50	$C_{17}H_{41}N_7O_{11}Cd$	32.0(32.3)	4.9(6.5)	15.8(15.5)
$[(PbL^7)_2(H_2O)_4(NO_3)_2][Pb(NO_3)_4]$	White		60	$C_{34}H_{70}N_{16}O_{22}Pb_3$	24.6(24.3)	4.2(4.2)	13.4(13.3)

[a]%Calculated values in parentheses, [b]DMSO = dimethyl sulphoxide

TABLE 3.2

U.V.-VISIBLE SPECTRA [λ/nm (ϵ/dm^3 mol^{-1} cm^{-1})] OF THE COMPLEXES OF Ni^{2+} AND Cu^{2+} WITH L^5, L^6 AND L^7, AND THEIR MAGNETIC MOMENTS IN THE SOLID PHASE AT 293 K

Complex	Colour	$\lambda_{max}(\epsilon)$		μ_{eff} B.M.
		In Nitromethane Solvent	In Dimethyl Sulphoxide Solvent	
$[Ni(L^5H_{-2})]$	Pale Green	580(sh), 875(18), 1170(6)	430(sh), 864(8), 1000(sh)[a]	3.10
		430(sh), 890(23), 1100(sh)[b]	368(sh), 590(27), 790(sh), 910(25)[c] 1210(10)	
$[Cu(L^5H_{-2})]$	Blue	540(sh), 690(180)	530(sh), 680(209)	1.83
		530(sh), 685(207)[b]	677(166), 830(sh)[c]	
$[Ni(L^6)(DMSO)](ClO_4)_2$	Green	500(sh), 830(sh), 895(32)	550(13), 660(13), 825(sh), 893(36)	3.10
$[Cu(L^6)](ClO_4)_2$	Blue	612(239), 908(120)	612(208), 910(85)	1.93
$[Ni(L^7)(DMSO)](ClO_4)_2.H_2O$	Green	555(16), 620(sh), 930(28)	602(14), 680(14), 830(sh), 975(31)	3.05
$[Cu(L^7)](ClO_4)_2$	Blue	626(287), 894(132)	640(227), 925(95)	1.93

[a]sh = shoulder, [b]In $CHCl_3$ solvent, [c]In H_2O solvent

TABLE 3.3*

COMPARISON OF PARTS OF THE F.A.B. MASS SPECTRA OF METAL COMPLEXES OF L^5, L^6 AND L^7 WITH VALUES CALCULATED FOR THE FRAGMENT IONS $[M(L^5H_{-2})]^+$, (M = Cu OR Ni) AND $[M(L)ClO_4]^+$ $[M(L-H)]^+$ (M = Ni, Cu, Zn, Cd, Pb; L = L^6 and L^7)

	$[Ni(L^5H_{-2})]^+ + 1$							$[Cu(L^5H_{-2})]^+ + 1$				
Observed m/z	362	363	364	365	366	367	368	367	368	369	370	371
Relative Height	100	32	41	12	7	2	1	100	42	51	15	3
Calculated m/z	362	363	364	365	366	367	368	367	368	369	370	371
Relative Height	100	19	41	9	7	1	2	100	19	47	9	1

	$[Ni(L^6)ClO_4]^+$				$[Ni(L^6-H)]^+$				$[Cu(L^6)ClO_4]^+$			$[Cu(L^6-H)]^+$			
Observed m/z	434	435	436	437	334	335	336	337	439	440	441	339	340	341	342
Relative height	100	24	62	18	100	72	44	29	100	46	85	100	99	54	32
Calculated m/z	434	435	436	437	334	335	336	337	439	440	441	339	340	341	342
Relative height	100	19	73	16	100	19	40	9	100	8	79	100	19	46	9

	$[Zn(L^6)ClO_4]^+$			$[Zn(L^6-H)]^+$			$[Cd(L^6)NO_3]^+$					$[Cd(L^6-H)]^+$				
Observed m/z	440	442	444	340	341	342	453	452	451	450	449	390	389	388	387	386
Relative height	100	55	21	100	36	86	100	73	96	58	43	100	79	85	77	46
Calculated m/z	440	442	444	340	341	342	453	452	451	450	449	390	389	388	387	386
Relative height	100	55	23	100	19	58	100	54	84	48	39	100	55	84	47	39

	$[Pb(L^6)NO_3]^+$			$[Pb(L^6-H)]^+$			$[Ni(L^7)ClO_4]^+$				$[Ni(L^7-H)]^+$			
Observed m/z	547	546	545	484	483	482	462	463	464	465	362	363	364	365
Relative height	100	60	51	100	56	53	100	30	72	27	100	32	40	39
Calculated m/z	547	546	545	484	483	482	462	463	464	465	362	363	364	365
Relative height	100	48	41	100	48	41	100	22	74	17	100	21	41	10

	$[Cu(L^7)ClO_4]^+$					$[Cu(L^7-H)]^+$				$[Zn(L^7)ClO_4]^+$					$[Zn(L^7-H)]^+$		
Observed m/z	467	468	469	470	471	367	368	369	370	468	469	470	471	472	368	369	372
Relative height	100	23	45	24	31	100	11	23	50	100	17	91	26	51	100	62	65
Calculated m/z	467	468	469	470	471	367	368	369	370	468	469	470	471	472	368	369	372
Relative height	100	22	80	17	17	100	21	47	10	100	13	91	28	61	100	21	41
	$[Cd(L^7)NO_3]^+$					$[Cd(L^7-H)]^+$				$[Pb(L^7)NO_3]^+$					$[Pb(L^7-H)]^+$		
Observed m/z	481	480	479	478	477	418	417	416		575	574	573			512	511	510
Relative height	100	67	93	55	44	100	81	90		100	50	44			100	75	39
Calculated m/z	481	480	479	478	477	418	417	416		575	574	573			512	511	510
Relative height	100	56	84	48	38	100	55	85		100	48	41			100	48	41

*A mixture of *erythro*-1,4-dimercapto-2,3-butanediol and *threo*-1,4-dimercapto-2,3-butanediol in ratio 1:5 matrix, 8 KeV, xenon plasma was used.

TABLE 3.4

^{13}C N.M.R. CHEMICAL SHIFTS (δ/P.P.M. REFERENCE $SiMe_4$) AT 298 K IN CD_3NO_2 SOLUTION UNLESS SPECIFIED OTHERWISE (RELATIVE POPULATIONS IN PARENTHESES)

Compound	Isomer	O ‖ -C-	Pyridine C			Py-CH_2-N	N-CH_2-C			N-CH_3	
			Ortho	Para	Meta						
L^5[a]		163.17(2)	148.54(2)	138.94(1)	123.72(2)		57.40(2)	56.78(2)	36.36(2)	38.73(2)	
L^6			158.89(2)	138.12(1)	121.41(2)	58.29(2)	56.15(2)	54.15(2)	47.74(2)	42.58(2)	
$[Zn(L^6)(DMSO)](ClO_4)_2$[b]	Symmetric		155.84(2)	143.64(1)	123.55(2)	56.38(2)	55.73(2)	50.01(2)	48.89(2)	46.19(2)	
	Asymmetric		155.93(1)	142.98(1)	123.39(1)	58.75	53.79(1)	52.77(1)	51.58(1)	45.70(1)	
			155.11(1)		122.93(1)	54.87(1)	51.39(1)	49.9(1)	49.18(1)	43.76(1)	
$[Cd(L^6)](NO_3)_2$	Symmetric		156.82(2)	141.01(1)	122.99(2)	61.38(2)	61.15(2)	58.62(2)	51.91(2)	41.75(2)	
	Asymmetric		156.56(1)		124.64(1)	60.89(1)	57.63(1)	52.44(1)	47.41(1)	45.80(1)	
			156.33(1)		123.62(1)	58.75(1)	53.16(1)	51.22(1)	46.09(1)	40.37(1)	
$[Pb(L^6)](NO_3)_2$	Asymmetric		161.00(1)	141.67(1)	124.77(1)	59.61(1)	55.04(1)	51.49(1)	44.94(1)	40.41(1)	
			160.27(1)		123.75(1)	58.09(1)	52.57(1)	50.53(1)	43.40(1)	40.24(1)	
L^7			158.80(2)	137.72(1)	123.78(2)	63.52(2)	54.58(2)	53.82(2)	53.36(2)	44.09(2)	43.96(2)
$[Zn(L^7)](ClO_4)_2$	Symmetric		155.70(2)[c]	144.53(1)[c]	125.00(2)	59.51(2)	56.02(2)	53.72(2)	53.10(2)	46.98(2)	46.39(2)
	Asymmetric		155.70(2)[c]	144.53(1)[c]	125.98(1)	59.05(1)	58.26(1)	57.93(1)	57.24(1)	46.39(1)	44.98(1)
					126.21(1)	55.79(1)	55.79(1)	55.53(1)	50.01(1)	44.29(1)	43.59(1)
$[Cd(L^7)](NO_3)_2$	Asymmetric		156.56(1)	142.36(1)	125.19(1)	63.78(1)	58.59(1)	56.42(1)	54.31(1)	46.22(1)	43.33(1)
			155.51(1)		124.87(1)	62.21(1)	57.93(1)	56.29(1)	52.93(1)	44.45(1)	40.77(1)
$[Pb(L^7)](NO_3)_2$	Asymmetric		161.00(1)	142.59(1)	125.46(1)	63.45(2)[c]	60.26(1)	58.22(1)	54.04(1)	43.27(1)	42.64(1)
			159.09(1)		125.36(1)		59.61(1)	57.80(1)	53.98(1)	43.04(1)	39.75(1)

[a] In $CDCl_3$;

[b] At 253K; coordinated dimethyl sulphoxide (DMSO) at δ = 40.0 p.p.m.

[c] Overlapping resonances, tentative assignment.

SECTION 4 EXPERIMENTAL

MATERIALS

Dry toluene was obtained by refluxing over CaH_2 for 20 h followed by distillation under dry dinitrogen. Pyridine-2,6-dicarboxylic acid dichloride was prepared from pyridine-2,6-dicarboxylic acid (20 g; Aldrich) by refluxing overnight under dry dinitrogen with excess thionyl chloride (100 g). Most of the excess thionyl chloride was removed by rotary evaporation, but to remove the last traces the residue was dissolved in dry toluene (20 cm^3) and the solvent removed by rotary evaporation. This procedure was repeated four more times, and the solid residue then transferred to a dry-box where it was stirred with dry light petroleum (50 cm^3) b.p. 40-60°C, for 15 min., filtered, and washed with more light petroleum (3 x 10 cm^3) to give the product (21.2 g, 87%). The compound purity was confirmed by ^1H n.m.r. spectroscopy.

All other chemicals were reagent grade commercial materials which were used without further purification.

SECTION 5 LIGAND PREPARATIONS

The synthetic routes are outlined in the Scheme 3.1 overleaf.

(i) Preparation of $[CNCH_2N(Me)CH_2-]_2$ (1): Sodium metabisulphite (46 g, 242 mmol) was dissolved in water (100 cm^3) and 37% aqueous formaldehyde (34 cm^3) added. The solution was boiled for 10 min., then cooled to room temperature, and N,N'-di-methyl-1,2-diaminoethane (20 g, 227 mmol) added with vigorous stirring. After 4 h, a solution of sodium cyanide (25 g, 510 mmol) in water (50 cm^3) was added. The mixture was left to stir overnight, whereupon a solid formed which was extracted with dichloromethane (4 x 100 cm^3). The combined extracts were dried with anhydrous $MgSO_4$, filtered, and the solvent removed with a rotary evaporator to leave a pale yellow solid. This was stirred with diethyl ether (200 cm^3), filtered and washed with more ether (3 x 20 cm^3) to leave a white solid, 1,6-dicyano-2,5-dimethyl-2,5-diazahexane, (1) (30 g, 181 mmol, 80% yield). M.p. 79-80°C; ^1H n.m.r. ($CDCl_3$): δ, 2.40 (6H, s), 2.63 (4H, s), and 3.64 p.p.m. (4H, s). ^{13}C n.m.r. ($CDCl_3$): 42.25 (2C, $N-CH_2-CH_2$), 45.24 (2C, N-Me), 52.90 (2C, CH_2-CN) and 114.64 p.p.m. (2C, CN). Electron impact mass spectrum: found, m/z 166; calc. for M^+ 166.

(ii) Preparation of $[NH_2CH_2CH_2N(Me)CH_2-]$ (2): A slurry of (1) (25 g, 151 mmol) in ethanol (300 cm^3) was stirred under dinitrogen at room temperature during the addition of small pieces of sodium metal (25 g, 1.09 mmol) over a period of 2 h. The slurry dissolved after *ca.* half the sodium had been added. The mixture was heated at 70°C for 4 h, and after cooling to room temperature water (300 cm^3)

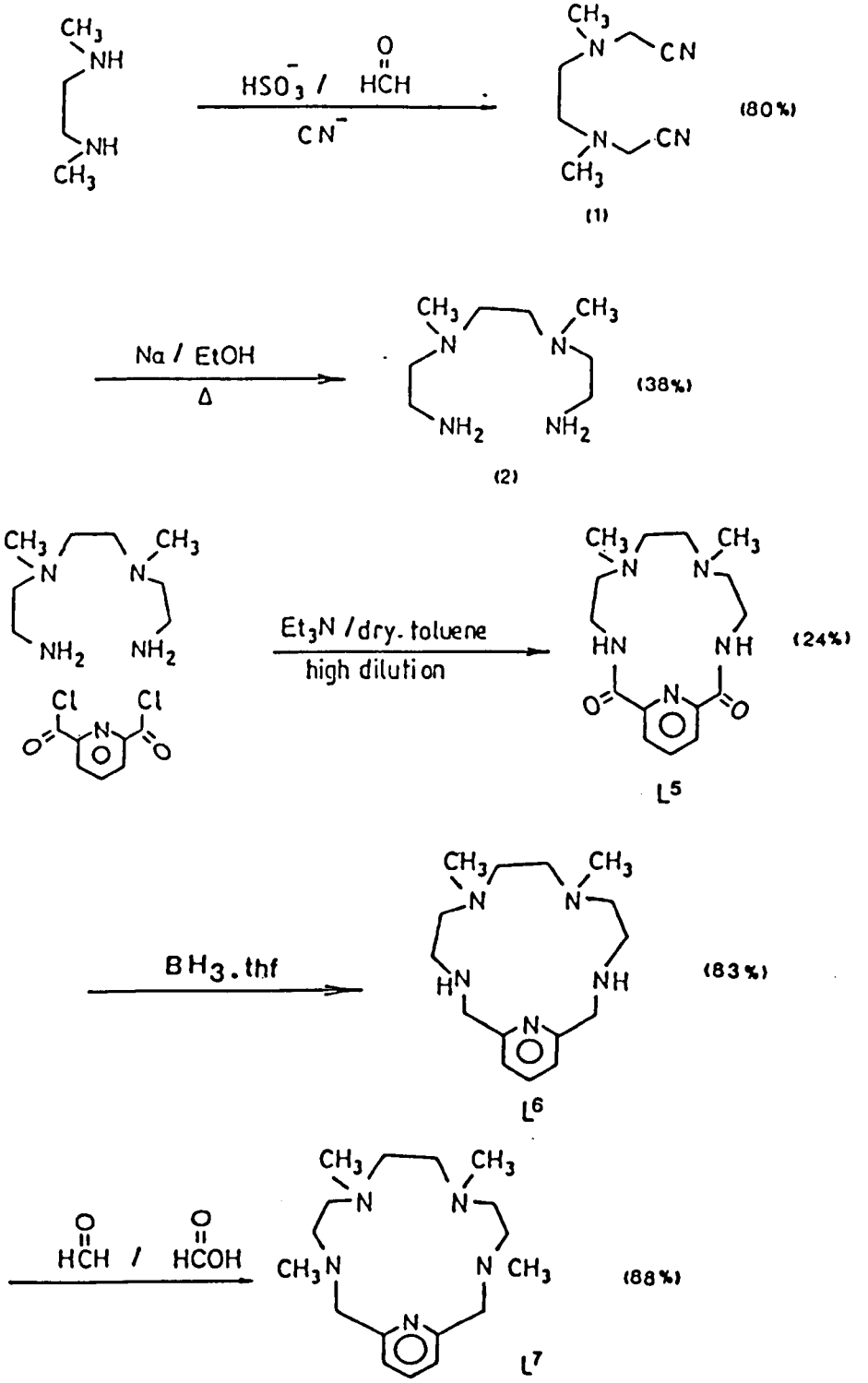
HSO3- / HCH=O
CN-
(80%)
(1)
Na / EtOH
Δ
(38%)
(2)
Et3N / dry. toluene
high dilution
(24%)
L5
BH3.thf
(83%)
L6
HCH=O / HCOH
(88%)
L7

SCHEME 3.1

was added. The product was extracted with dichloromethane (4 x 200 cm^3), the extracts dried with anhydrous $MgSO_4$, and the solvent removed with a rotary evaporator to leave a pale yellow oil. The product was distilled *in vacuo* (b.p. 94-96°C, 0.7 mm Hg) to give a colourless oil (10 g, 57.5 mmol, 38%).

^1H n.m.r. ($CDCl_3$, $Si(CH_3)_4$, 0.00): δ, 1.40 (4H, broad), 2.26 (6H, s), 2.45 (4H, t), 2.52 (4H, s), and 2.78 p.p.m. (4H, t). Electron impact mass spectrum: found m/z 174; calc. for M^+ 174.

(iii) Preparation of 2,13-dioxo-6,9-di-methyl-3,6,9,12,18-pentaaza-bicyclo[12.3.1]octadeca-1(18),14,16-triene, L^5: The high dilution technique was used to condense $[NH_2CH_2CH_2N(Me)CH_2-]_2$ with pyridine-2,6-dicarboxylic acid dichloride. A dry 5 dm^3 three-necked flask was evacuated and filled with dry dinitrogen (3 times) and then dry toluene (2 dm^3) and triethylamine (10 g, 99 mmol) were added. Two 50 cm^3 syringes were connected to the flask *via* long stainless steel needles passing through a rubber suba-seal plug in one neck of the flask. The syringes were connected to a motor driven syringe pump (Sage instrument model 355) to allow controlled slow addition of the two reagents. The flask was connected to a magnetic stirrer, and cooled with an ice bath to 0°C. The two syringes were charged separately with solution of (2) (8.5 g, 48.9 mmol) and pyridine-2,6-dicarboxylic acid dichloride (9.97 g, 48.9 mmol), each dissolved in dry toluene (50 cm^3). The reagents were pumped into the flask dropwise, with vigorous stirring, at a flow rate of 0.0774 cm^3 min^{-1}. After complete addition (*ca.* 11 h), stirring was continued for a further 11 h. The triethylamine hydrochloride which precipitated was removed by filtration, and the solution evaporated with a rotary evaporator. The remaining paste

was dissolved in dichloromethane (50 cm^3), and the solution passed through a column of neutral alumina (20 cm long, 2 cm diameter) and eluted with more dichloromethane (100 cm^3). After removal of the solvent with a rotary evaporator, the product was obtained as a white solid (3.59 g, 11.8 mmol; 24% yield). M.p. 155-156°C.

^1H n.m.r. ($CDCl_3$): 2.20 (6H, s), 2.60 (4H, s), 2.73 (4H, t), 3.54 (4H, p), 8.05 (1H, t), 8.30 (2H, d), and 9.14 p.p.m. (2H broad). Electron impact mass spectrum: found m/z 305; calc. for M^+ 305. The ^1H-decoupled ^{13}C n.m.r. chemical shifts are given in Table 3.4.

(iv) Preparation of 6,9-dimethyl-3,6,9,12,18-penta-azabicyclo-[12.3.1]octadeca-1(18),14,16-triene, L^6: L^5 (1.1 g, 3.6 mmol) was dissolved in dry tetrahydrofuran (thf; 100 cm^3) in a 250 cm^3 round bottomed flask. The flask was flushed with dry nitrogen, and a solution of BH_3.thf (45 cm^3 of a 1.0 mol dm^{-3} solution) added. The solution was refluxed under dinitrogen for 3 h. Excess BH_3.thf was then destroyed by the dropwise addition of methanol, and the solvent removed with a rotary evaporator to give the borane salt of L^6 as a white solid. This salt was dissolved in a mixture of water (50 cm^3) and methanol (50 cm^3), and concentrated. HCl (30 cm^3) was added. The solution was refluxed overnight and the pH then adjusted to *ca.* 12 by adding sodium hydroxide. The product was extracted with dichloromethane (4 x 100 cm^3), the extracts dried with anhydrous $MgSO_4$, filtered and evaporated to leave L^6 as a pale yellow oil. This oil was purified by passage through a neutral alumina column as described for L^5, using dichloromethane as eluent. The final yield was 83%, ^1H n.m.r. ($CDCl_3$): δ, 2.20 (6H, s), 2.48 (4H, s), 2.60 (4H, t), 2.72 (4H, t), 3.92 (4H, s), 4.40 (2H, broad), 7.05 (2H, d) and 7.58 p.p.m. (1H, t). Electron impact mass spectrum, found: m/z

277; calc. for M^+ 277. The ^1H-decoupled ^{13}C n.m.r. chemical shifts are given in Table 3.4.

(v) Preparation of 3,6,9,12-tetramethyl-3,6,9,12,18-pentaazabicyclo[12.3.1]octadeca-1(18),14,16-triene, L^7: L^6 (0.9 g, 3.25 mmol) was added to 37% aqueous formaldehyde (10 cm^3) followed by formic acid (10 cm^3). The mixture was refluxed overnight at 90°C, cooled to room temperature, basified with 20% aqueous NaOH to pH 12, and extracted with dichloromethane (5 x 100 cm^3). Work-up was as described for L^6, using dichloromethane methanol (4:1, 200 cm^3) to elute from the neutral alumina column. The product was obtained as a pale yellow oil (0.87 g, 2.85 mmol, 88% yield).

^1H n.m.r. ($CDCl_3$): δ, 2.25 (12H, s), 2.45 (12H, m), 3.71 (4H, s), 7.20 (2H, d) and 7.61 p.p.m. (1H, t). Electron impact mass spectrum, found: m/z 305; calc. for M^+ 305. The ^1H-decoupled ^{13}C n.m.r. chemical shifts are given in Table 3.4.

SECTION 5.2 PREPARATION OF METAL COMPLEXES

Metal complexes of L^5 were prepared by overnight refluxing of solution of L^5 (0.3 mmol) in dry methanol with an equimolar amount of the nickel(II) or copper(II) acetate. The solvent was removed and the residue was stirred in dry diethyl ether (10 cm^3) to give a solid which filtered under di-nitrogen and washed with (5 x 10 cm^3) diethyl ether. The metal complexes of L^6 and L^7 were obtained in *ca.* 50-70% yields by adding a solution of each ligand (0.5 mmol) in ethanol (5 cm^3) to an equimolar amount of the appropriate metal dimethyl sulphoxide (DMSO) solvates of formula $[M(DMSO)_n](ClO_4)_2$ (M = Ni or Cu, n = 6, M = Zn, n = 4; prepared as described)[121] in ethanol (10 cm^3). The mixtures were stirred for 1 h, whereupon the solid products separated. These were collected by

filtration and in some cases recrystallised from mixtures of nitromethane, ethanol and diethyl ether using the solvent ratios indicated in Table 3.1. The products were finally washed with ethanol (2 x 5 cm^3) and diethyl ether (3 x 5 cm^3). The Pb^{2+} and Cd^{2+} metal complexes of L^6 and L^7 were prepared by mixing (0.4 mmol) of each ligand in ethanol (5 cm^3) with $[Cd(H_2O)_4][NO_3]_2$, and $Pb(NO_3)_2$ in ethanol (10 cm^3) and the reaction mixture stirred for ½ h. The product precipitated as white solid by addition of dry diethyl ether (25 cm^3). These were filtered under dinitrogen and washed with dry diethyl ether (3 x 10 cm^3). The yields and elemental analyses are collected in Table 3.1. Proton-decoupled ^{13}C n.m.r. chemical shifts of the diamagnetic Zn^{2+}, Cd^{2+} and Pb^{2+} complexes are compared with those of the free ligands in Table 3.4, and details of the visible spectra and magnetic moments of the Ni^{2+} and Cu^{2+} complexes are in Table 3.2. Parts of the fast atom bombardment (f.a.b.) mass spectra of the complexes of L^5, L^6 and L^7 compared with calculated values in Table 3.3.

SECTION 6 CRYSTAL STRUCTURE ANALYSIS FOR $[Zn(L^7)](CLO_4)_2$

Crystals of $C_{17}H_{31}Cl_2N_5O_8Zn$ suitable for crystallography were obtained as white plates from nitromethane solution. A crystal with dimensions 0.30 x 0.12 x 0.13 mm was chosen. Systematic absences *h0l*, $h + l = 2n$, and *0k0*, $k = 2n$ indicated the monoclinic space group $p2_1/c$; M = 569.74, a = 9.935 (3), b = 15.603 (4), c = 15.202(3) Å, β = 94.30(2)°, U = 2349.9(1.0) Å^3, Z = 4, D_c = 1.61 g cm^{-3}, *Mo-*K_α radiation, λ = 0.71069 Å, μ(Mo-K_α) = 13.48 cm^{-1}, T = 290 K, F(000) = 1183.76. Data were collected with a maximum 2θ of 45° scan range ± 0.9° (2θ) around $K_{\alpha1}$-$K_{\alpha2}$ and with a minimum scan speed of 2.5 min^{-1}, depending on the intensity of a 2 S pre-scan. Backgrounds were measured at each end of the scan for 0.25 of the scan time. Three standard reflections were monitored every 200 reflections, and showed slight changes during data collection; the data were rescaled to correct for this. Unit cell dimensions and standard deviations were obtained by a least-squares fit to 15 reflections with 18 < 2θ < 20°.

Reflections were processed using profile analysis to give 3380 unique reflections; 1816 with [I/σ(I) ⩾ 3.0] were used in refinement, and corrected for Lorentz, polarisation and absorption effects, the last by the Gaussian method. Heavy atoms were located by the Patterson interpretation section of SHELXTL[123], and light atoms found by successive Fourier syntheses. Anisotropic thermal parameters were used for all of the non-hydrogen atoms. Hydrogen atoms were given fixed isotropic thermal parameters, U = 0.07 Å^2, inserted at calculated positions, and not refined. Methyl groups were treated as rigid CH_3-units, with their initial orientation taken from the strongest H-atom peaks on a difference Fourier

synthesis. Final refinement was on F by cascaded least-squares methods, refining 310 parameters. Largest positive and negative peaks on a final difference Fourier synthesis were of height +0.3 and $-0.2e\text{Å}^{-3}$. A weighting scheme of the form $W = 1/[\delta(F)^2 + gF^2]$ with $g = 0.00015$ was used, and shown to be satisfactory by a weight analysis. The final R value was 0.0394 ($R_w = 0.361$). In the final cycle, the maximum shift/error was 0.03. Scattering factors in the analytical form and anomalous dispersion factors were taken from International Tables (1974).[124] Final atomic coordinates are given in Table 3.5, and selected bond lengths and angles in Table 3.6.

TABLE 3.5
ATOMIC COORDINATES (x 10^4) IN $[Zn(L^7)](CLO_4)_2$

Atom	X	Y	Z
Zn	2308.3(7)	6966.5(4)	6067.7(4)
Cl(1)	2725.3(17)	8822.7(11)	8455.6(10)
Cl(2)	2427.3(19)	5263.7(11)	1704.7(12)
O(1)	2434(6)	8728(4)	7559(3)
O(2)	3305(6)	9632(3)	8653(4)
O(3)	3652(6)	8165(3)	8735(4)
O(4)	1553(7)	8735(4)	8880(5)
O(5)	3494(5)	5110(3)	1146(3)
O(6)	2826(8)	5894(4)	2320(4)
O(7)	1296(6)	5522(4)	1176(4)
O(8)	2171(6)	4494(4)	2139(4)
N(1)	2246(5)	6550(3)	7307(3)
N(2)	104(4)	7067(3)	6271(3)
N(3)	1985(5)	8099(3)	5387(3)
N(4)	2723(5)	6387(3)	4874(3)
N(5)	4495(5)	6677(3)	6449(3)
C(1)	3291(6)	6139(4)	7698(4)
C(2)	3279(7)	5850(4)	8551(4)
C(3)	2155(7)	5996(4)	8995(4)
C(4)	1056(7)	6409(4)	8568(4)
C(5)	1132(6)	6697(4)	7729(4)
C(6)	74(6)	7235(4)	7233(4)
C(7)	-680(7)	6286(4)	6047(4)
C(8)	-390(6)	7808(4)	5728(4)
C(9)	707(6)	8486(4)	5667(4)
C(10)	3079(7)	8748(4)	5503(4)
C(11)	1840(7)	7807(4)	4439(4)
C(12)	2880(7)	7136(4)	4282(4)
C(13)	1693(7)	5789(4)	4472(4)
C(14)	4014(6)	5904(4)	5033(4)
C(15)	5066(6)	6384(4)	5638(4)
C(16)	5319(7)	7377(4)	6877(5)
C(17)	4400(6)	5968(4)	7098(4)

TABLE 3.6
SELECTED BOND LENGTHS (Å) AND ANGLES (°) IN
$[Zn(L^7)](ClO_4)_2$

Zn-N(1)	1.999(4)	Zn-N(2)	2.240(5)
Zn-N(3)	2.061(5)	Zn-N(4)	2.095(5)
Zn-N(5)	2.252(5)	Cl(1)-O(1)	1.379(5)
Cl(1)-O(2)	1.411(5)	Cl(1)-O(3)	1.423(6)
Cl(1)-O(4)	1.380(7)	Cl(2)-O(5)	1.428(5)
Cl(2)-O(6)	1.394(6)	Cl(2)-O(7)	1.392(6)
Cl(2)-O(8)	1.403(6)	N(1)-C(1)	1.322(7)
N(1)-C(5)	1.340(8)	N(2)-C(6)	1.489(7)
N(2)-C(7)	1.473(8)	N(2)-C(8)	1.481(7)
N(3)-C(9)	1.496(8)	N(3)-C(10)	1.485(8)
N(3)-C(11)	1.508(7)	N(4)-C(12)	1.490(7)
N(4)-C(13)	1.483(8)	N(4)-C(14)	1.492(8)
N(5)-C(15)	1.468(8)	N(5)-C(16)	1.485(8)
N(5)-C(17)	1.489(8)	C(1)-C(2)	1.375(8)
C(1)-C(17)	1.506(9)	C(2)-C(3)	1.366(10)
C(3)-C(4)	1.386(9)	C(4)-C(5)	1.360(8)
C(5)-C(6)	1.504(8)	C(8)-C(9)	1.527(8)
C(11)-C(12)	1.502(9)	C(14)-C(15)	1.535(9)

N(1)-Zn-N(2)	78.1(2)	N(1)-Zn-N(3)	137.5(2)
N(2)-Zn-N(3)	83.8(2)	N(1)-Zn-N(4)	134.3(2)
N(2)-Zn-N(4)	114.0(2)	N(3)-Zn-N(4)	88.2(2)
N(1)-Zn-N(5)	77.8(2)	N(2)-Zn-N(5)	155.9(2)
N(3)-Zn-N(5)	114.4(2)	N(4)-Zn-N(5)	83.6(2)

SECTION 1 INTRODUCTION

The growing interest in recent years in the synthesis and study of binucleating ligands has been stimulated in part by studies of ferro- and anti-ferromagnetic exchange coupling, as well as interest in the binding and activation of small substrate molecules between two metal centres, and an examination of multi-electron redox reactions. The binucleating ligands may also serve as small molecule models for bimetallic metalloenzyme systems. The area has been very well documented.[60,138-144] The synthesis and study of an octaazamacrocycle, and its bimetallic nickel(II), copper(II) and zinc(II) complexes are reported in this Chapter.

SECTION 2 RESULTS AND DISCUSSION

SECTION 2.1 LIGAND SYNTHESIS

The disodium salt of the ditosylated derivative of the readily available amine, N,N'-bis(3-aminopropyl)piperazine, was reacted with the ditosylated dialcohol (1,3-propane diol) using the Richman & Atkins procedure (Scheme 4.1, page 120) in the hope to obtain the 1 + 1 addition product and the 15-membered macrocycle shown in Figure 4.1.

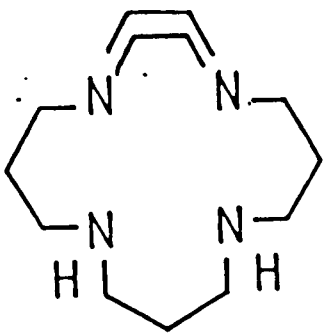

FIGURE 4.1

Such a macrocycle is interesting because of the rigidity imposed by piperazine ring, and the availability of two secondary amine groups which are accessible for further derivatisation (e.g. enabling the addition of two pendent arms and the formation of sexidentate macrocycles). However, when the reaction was carried out as described in Section 5.1 (page 119), and the macrocycle isolated and characterised by ^{1}H and ^{13}C n.m.r. (Figure 4.2), although these n.m.r. spectra were consistent with structure 4.1, the mass spectrum showed that the coupling reaction involved 2 + 2 addition to give the dimer shown in Figure 4.3 (molecular mass m/z 480).

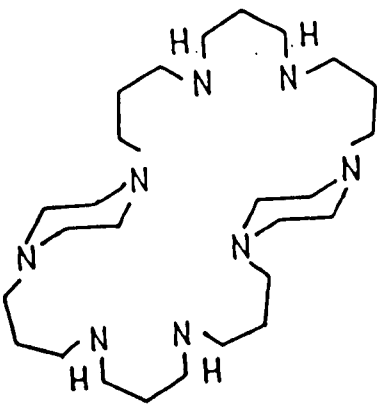

FIGURE 4.3

This is not surprising considering that the piperazine ring is more stable in the chair form.[145,146] Molecular models of the open chain precursor show that the amine ends are far apart and this geometry precludes 1 + 1 addition making 2 + 2 addition more feasible (Figure 4.4).

FIGURE 4.2

Proton decoupled ^{13}C n.m.r. of L^{10} in $CDCl_3$ solvent

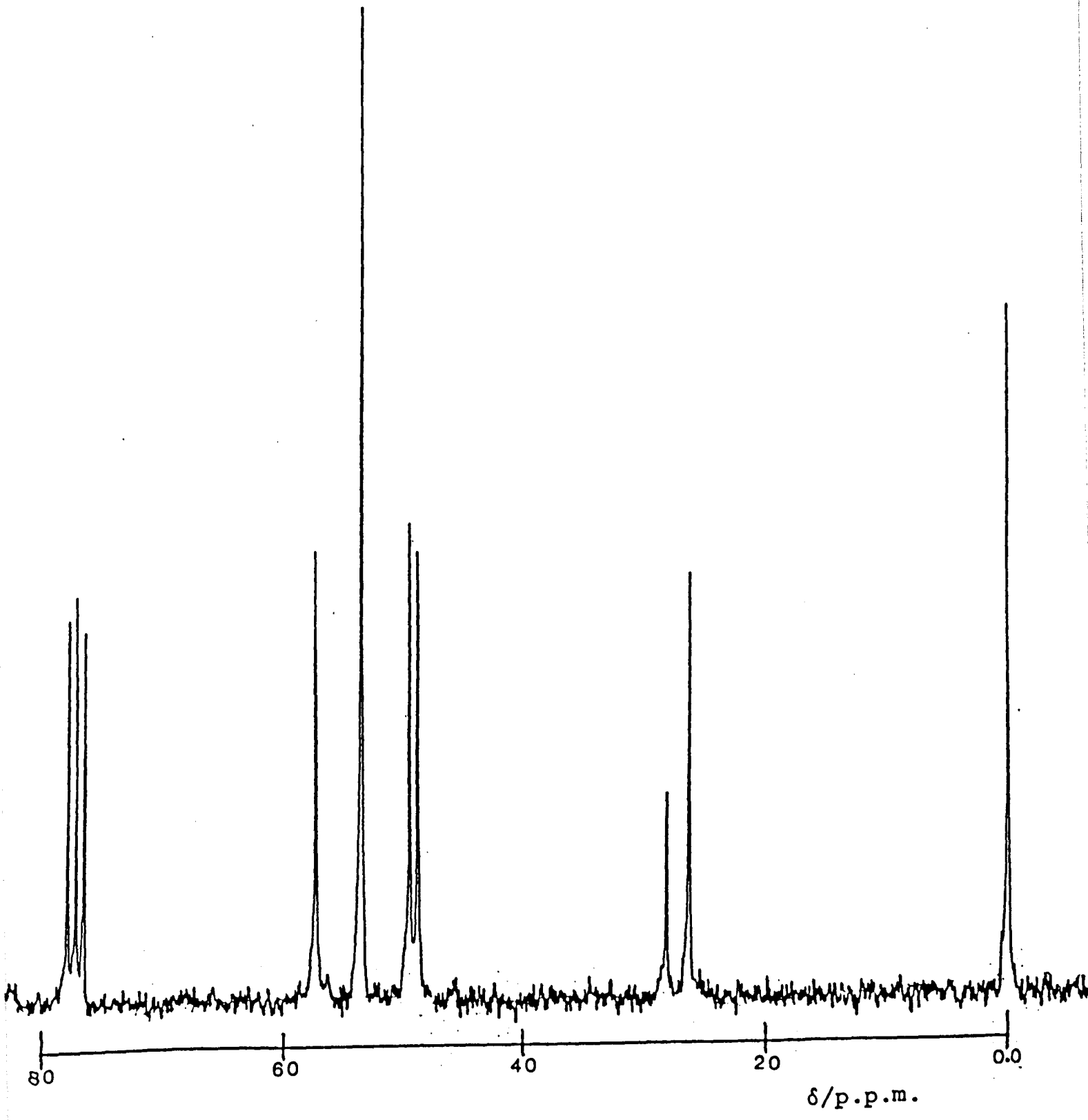

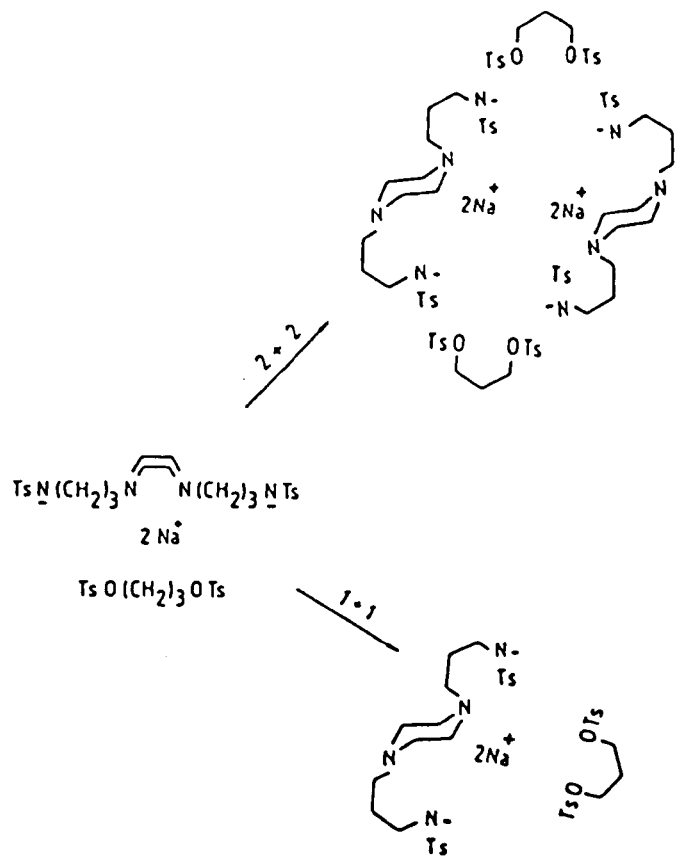

FIGURE 4.4

The macrocycle L^{10} was extracted from basic aqueous solution with dichloromethane as described in Section 5.1 (p. 119). To improve the yield a continuous extraction procedure was employed to the remaining aqueous layer for 48 h. The white solid recovered from this continuous extraction has a ^{13}C n.m.r. spectrum (Figure 4.5) characteristically different from the spectrum obtained in the same solvent for the first fraction. On the basis of the number of ^{13}C resonances and their chemical shifts (all are methylene carbons), together with the mass spectrum of this molecule which shows a parent ion peak at m/z 504, it is evident that in the presence of dichloromethane at high pH, and with a long extraction time, two of the secondary amine groups in macrocycle L^{10} react with

FIGURE 4.5
PROTON DECOUPLED ^{13}C N.M.R. OF L^{11} IN $CDCl_3$ SOLVENT

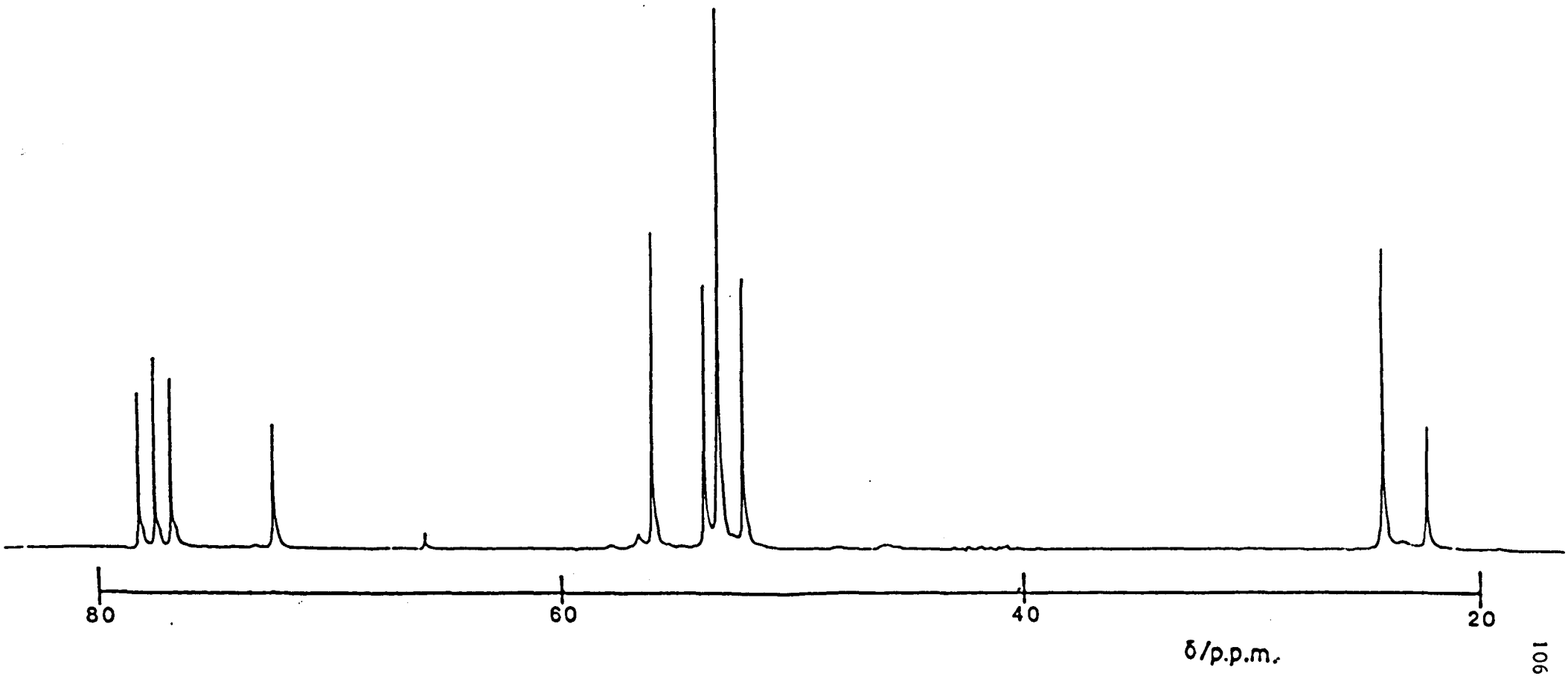

the dichloromethane solvent to form a bridge-head methylene group between each of the two secondary amine groups giving the new ligand L^{11} (Figure 4.6).

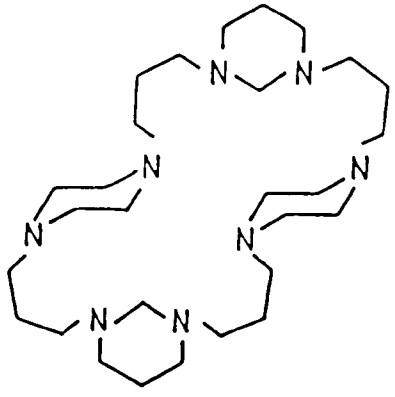

FIGURE 4.6

SECTION 2.2 SYNTHESIS OF BINUCLEAR COPPER(II), NICKEL(II) AND ZINC(II) COMPLEXES OF L^{10}

The binuclear metal complexes of L^{10} were prepared by mixing ethanolic solutions of the dimethyl sulphoxide solvates in case of the Ni^{2+} and Cu^{2+} complexes or aquo-solvates in the Zn^{2+} complex. In each metal (2 moles equivalents) were mixed with L^{10} (1 mole equivalent) as described in detail in Section 5.2. The complexes were isolated in good yield and found to have formulae $[M_2(L^{10})(DMSO)_m](ClO_4)_4.nDMSO$ (M = Cu, m = 0, n = 1; M = Ni, m = 1, n = 0; and M = Zn, n = m = 0). The visible spectra of $[Cu_2(L^{10})]^{4+}$, and $[Ni_2(L^{10})(DMSO)]^{4+}$ in H_2O, DMSO, DMF, CH_3CN and CH_3NO_2 solvents are given in Table 4.1. The visible spectrum of an aqueous solution of $[Cu_2(L^{10})](ClO_4)_4.DMSO$ shows a single strong band at 590 nm. A similar spectrum is reported for $[Cu(NH_3)_4]^{2+}$, indicating that the copper(II) complex of L^{10} is four-coordinate.[147] Although

chemical analyses (including sulphur analysis) confirm the presence of DMSO in the Cu^{2+} complex of L^{10}, the infrared spectrum of the complex shows no S=O stretching frequency in the 900-1000 cm^{-1} region as expected for a co-ordinated DMSO molecule. Uncoordinated DMSO is obscured by the broad band from ClO_4^- ion in the 1000-1100 cm^{-1} region. The magnetic moment of $[Cu_2(L^{10})]^{4+}$ ion at room temperature is 1.34 B.M. per copper(II) ion. This unusually low value could indicate some magnetic interaction between the two copper(II) ions. No other evidence for such an interaction was found and the question was not pursued further. The diffuse reflectance spectrum of $[Ni_2(L^{10})(DMSO)](ClO_4)_4$ shown in Figure 4.7 is clearly complicated; it differs from any of the spectra found for octahedral and square planar nickel(II) complexes.[148] Since it is evident from infrared spectral data that DMSO coordinates to the nickel(II) ion [ν(S=O), 965 cm^{-1}],[149] a five-coordinate geometry is assigned to one of the Ni^{2+} ions in the complex. Recently a comprehensive spectroscopic investigation of five-coordinate nickel(II) complexes has been reported, and it is now well known that most low-spin square planar nickel(II) complexes have d-d bands in the region 400-560 nm.[148] On the other hand, high-spin tetragonal-pyramidal nickel(II) complexes show d-d bands in the region 370-1500 nm.[150] Considering these facts, at least one of the two nickel(II) ions in the $[Ni_2(L^{10})(DMSO)](ClO_4)_4$ complex appears to have a high-spin five-coordinate geometry possibly with the structure shown in Figure 4.8.

FIGURE 4.7

Diffuse reflectance spectrum of $[Ni_2(L^{10})(DMSO)](ClO_4)_4$

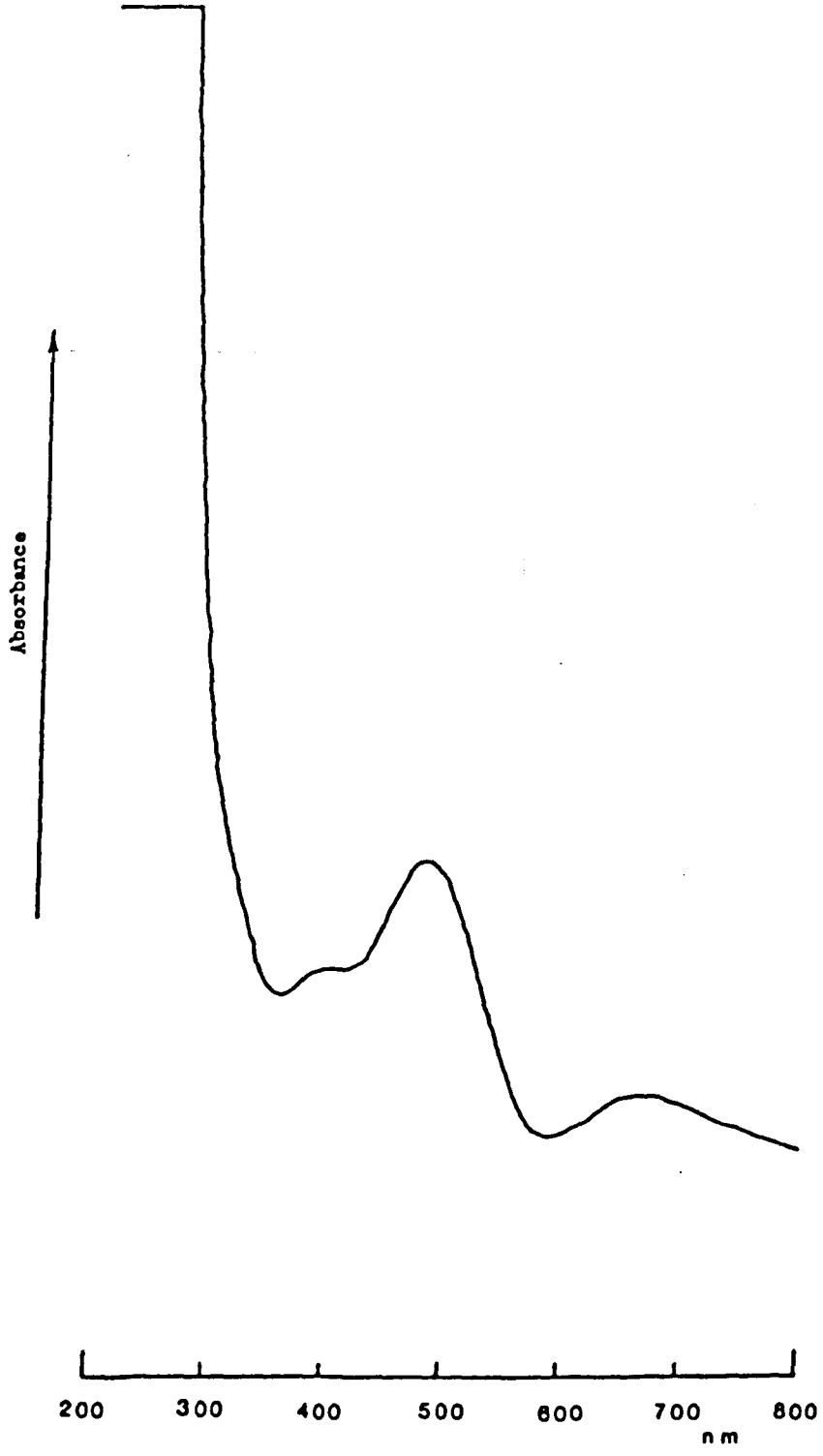

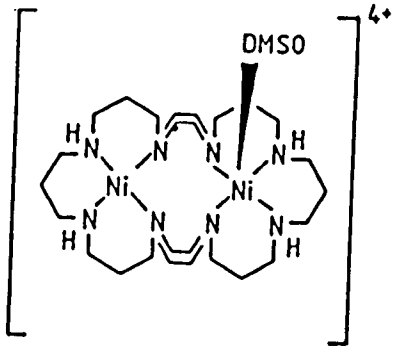

FIGURE 4.8

In fact the magnetic moment of the dinickel(II) complex at room temperature is 2.10 B.M. per nickel(II) ion. The relatively low magnetic moment of the complex can be explained on the basis of either (i) an antiferromagnetic exchange interaction between a pair of paramagnetic nickel(II) ions or (ii) a binuclear system having one of paramagnetic and one diamagnetic nickel(II) ion. To clarify this point a variable temperature magnetic susceptibility study of this complex is required, but the equipment for such a study was not available to us. There are only a few reports of complexes containing mixed high and low spin nickel(II) ions.[151-154]

The diffuse reflectance spectrum given in Figure 4.7 for $[Ni_2(L^{10})DMSO]^{4+}$ as well as the nitromethane solution spectrum of this complex, can be explained as the superposition of the spectra of low-spin planar and high-spin square pyramidal five-coordinate nickel(II) ions. A crystal structure determination of solid $[Ni_2(L^{10})DMSO]^{4+}$ ion is required to confirm the proposed structure shown in Figure 4.8.

The visible spectra of $[Ni_2(L^{10})(DMSO)](ClO_4)_4$ in coordinating solvents (DMSO, DMF, CH_3CN and H_2O) are given in Table 4.1, and are typical of octahedral nickel(II) complexes. The f.a.b. (fast atom bombardment) mass spectra of the binuclear

copper(II), nickel(II) and zinc(II) complexes of L^{10} show a cluster of peaks centred at m/z 905, 895, and 907 respectively attributable to the $[M_2(L^{10})(ClO_4)_3]^+$ ions (M = Cu, or Ni or Zn), and show sequential loss of 3 moles of perchloric acid (m/z 100) in each complex. This behaviour is similar to our earlier studies (see Chapters 2 and 3). In addition, strong peaks centred at m/z 781, 681 and 581, attributed to protonated ligand were observed in the zinc(II), and nickel(II) spectra, but not in copper(II) spectrum, indicating that the copper(II) complex of L^{10} is the most stable of the three. The proton decoupled ^{13}C n.m.r. spectrum of $[Zn_2(L^{10})](ClO_4)_4$ (chemical shifts compared with those for the free macrocycle in Table 4.2) reveals the presence of a single symmetric species. The number of resonances expected for such a species is six, with two upfield resonances arising from the $C-CH_2-C$ carbon atoms, one of them at δ 23.61 p.p.m. (relative area 2), and the other at δ 20.78 (relative area 4) (these resonances appear at δ 25.41 and 25.32 p.p.m. respectively in the free macrocycle).

Attempts to prepare bimetallic complexes of L^{11} using a similar procedure to that described for L^{10} were unsuccessful. The products recovered from these reactions were oils, and these oils did not solidify upon repeated treatment with dry diethyl ether.

SECTION 3 ATTEMPTS TO PREPARE A HETEROBIMETALLIC COPPER(II) AND NICKEL(II) COMPLEX OF L^{10}

Synthesis of heterobimetallic Ni^{2+} and Cu^{2+} macrocyclic complexes have been achieved either by reacting an aqueous solution of a suitable macrocyclic ligand (L) [L = bis-cyclam (C-C bridging); cyclam = 1,4,8,11-tetraazacyclotetradecane] with one equivalent of Ni^{2+} followed by one equivalent of Cu^{2+}, and the heterobimetallic complex separated by column chromatography as reported by Kaden and Fabbrizzi,[61] or by refluxing a methanolic solution of mono-copper(II) complex of a 30-N_6O_4-dipyridyl containing macrocycle with a four-fold excess of Ni^{2+} for 5 h as described by Nelson's group.[155] In this study the method of Kaden and Fabbrizzi was used to generate $[CuNi(L^{10})]^{4+}$ ion, and the mixture was separated by column chromatography on Sephadex C-25 at 0°C. Elution with 0.4 mol dm^{-3}aqueous NaCl gave three distinct bands. A blue band (λ_{max} = 628 nm) was eluted first and which was found to be the dicopper(II) complex. Then a green-blue second band (λ_{max} 640 nm) was obtained which analysed for the mixed-metal species $[NiCu(L^{10})]^{4+}$ ion. Finally a green band of $[Ni_2(L^{10})]^{4+}$ (λ_{max} = 415, 640, and 1180 nm) was eluted with 1.0 mol dm^{-3} NaCl. These results are analogous to those found by Kaden's group. The original solution contains 25% of the dicopper(II) complex, 50% of the mixed nickel(II)-copper(II) complex and 25% of the dinickel(II) complex, and they should separate in the observed sequence. The metal analysis of the three bands using atomic absorption spectroscopy showed the first band contained 10 μg per cm^3 of Cu^{2+} and no Ni^{2+}, the second band contained 33 μg per cm^3 of Cu^{2+} and 24 μg per cm^3 of Ni^{2+}, and the

third band contained 20 μg per cm^3 of Ni^{2+} and no Cu^{2+} ion. The low metal content in all bands is due to dilution by the eluant and the Cu^{2+} content in the second band is higher than Ni^{2+} due to contamination of this band with a little dicopper complex of L^{10} (from the first band).

The middle band was collected, concentrated under vacuum over silica gel overnight and treated with ethanol several times (to precipitate NaCl first) to give a green-blue solid. In order to eliminate the sodium chloride in the product an equivalent amount of $AgClO_4$ was added to an aqueous solution of the complex, filtered, concentrated as previously, and treated again with ethanol to give green-blue crystals. The visible spectrum of this solid in 0.4 mol dm^{-3} aqueous NaCl solution was found to be the same as the dicopper(II) complex, and the metal analyses showed very low nickel content (< 0.01%) and acceptable copper analyses for $[Cu_2(L^{10})](ClO_4)_4$ (found for Cu, 13.0%; Calc., 12.8%). The difference in the visible spectrum of the second band immediately after being eluted from the column and the spectrum of the solid recovered from this band after crystallisation in the same solvent, indicate that disproportionation has occurred.

$$2[CuNi(L^{10})]^{4+} \rightleftharpoons [Cu_2(L^{10})]^{4+} + [Ni_2(L^{10})]^{4+} \qquad (1)$$

The driving force for this disproportionation is presumably the greater stability of the dicopper(II) complex.

Further evidence for this disproportionation came from a visible spectral study at 52°C over a period of 2 h, which showed changes in absorbance with time as expected for equilibrium (1) (Figure 4.9). A plausible mechanism is as follows:

FIGURE 4.9

Visible spectra for equilibrium

$$2[CuNi(L^{10})]^{4+} \rightleftarrows [Cu_2(L^{10})]^{4+} + [Ni_2(L^{10})]^{4+}$$

recorded at 5 min. time intervals. Absorbance increases with time (A to B) following an initial induction period.

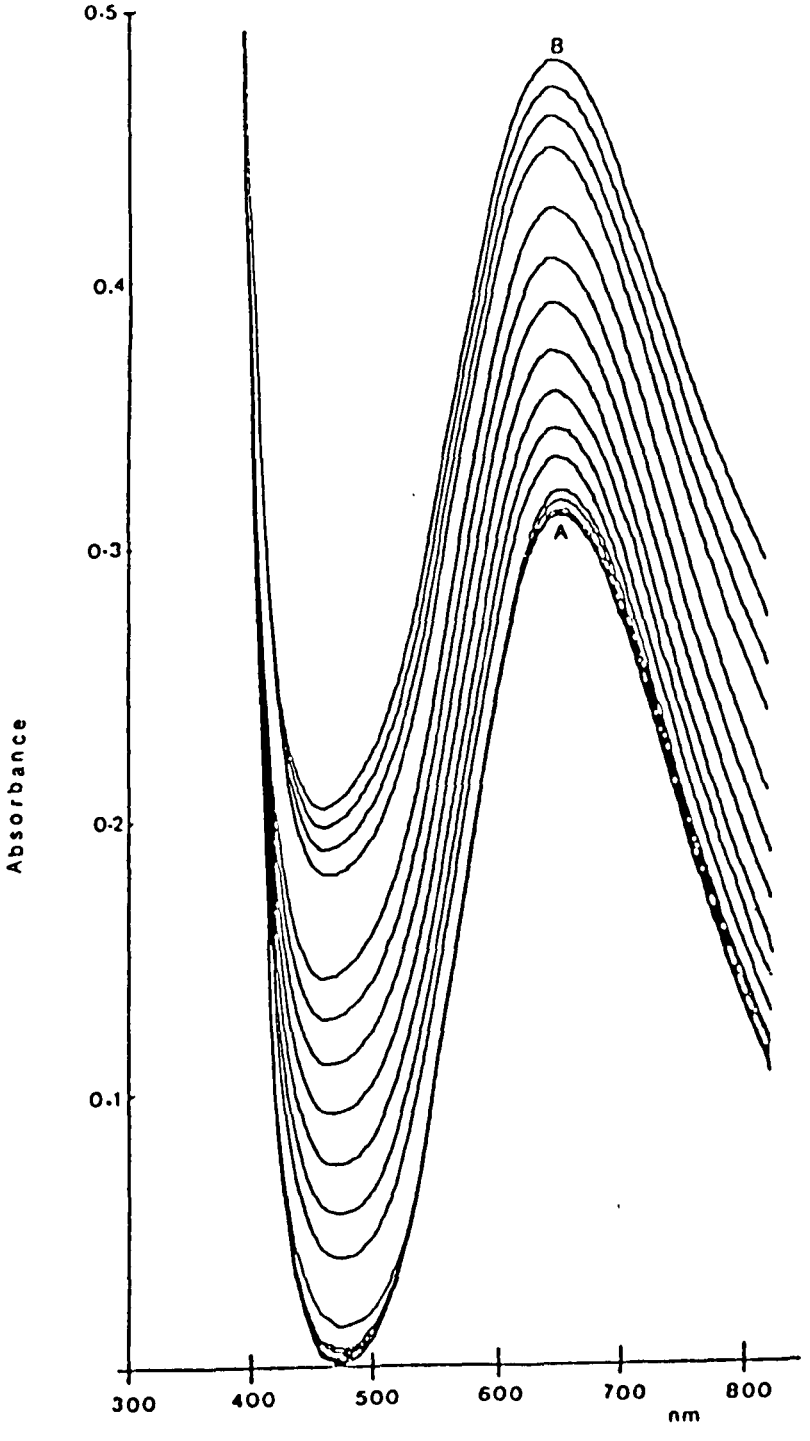

$$[CuNiL]^{4+} \underset{k_{-1}}{\overset{k_1}{\rightleftharpoons}} [CuL]^{2+} + Ni^{2+}$$

$$[CuNiL]^{4+} \underset{k_{-2}}{\overset{k_2}{\rightleftharpoons}} [NiL]^{2+} + Cu^{2+}$$

$$[CuL]^{2+} + Cu^{2+} \underset{k_{-3}}{\overset{k_3}{\rightleftharpoons}} [Cu_2L]^{4+}$$

$$[NiL]^{2+} + Ni^{2+} \underset{k_{-4}}{\overset{k_4}{\rightleftharpoons}} [Ni_2L]^{4+}$$

The spectral changes are complex (e.g. an induction period is evident), and obviously more than one kinetic step is involved. Conformational changes within the mononuclear complex could also contribute to the overall dynamic process, complicating this simplified scheme further.

TABLE 4.1
ELECTRONIC SPECTRAL DATA AND MAGNETIC MOMENTS FOR BINUCLEAR NICKEL(II) AND COPPER(II) COMPLEXES OF L^{10}

Complex	Colour	μ_{eff} B.M.	$\lambda_{max}(\epsilon)$		Reference
$[Ni_2(L^{10})(DMSO)](CLO_4)_4$	Pink	2.10[f]	1250(8), 755(7), 680(10), 398(sh)	a	This work
			1015(12), 655(26), 480(sh)	b	This work
			930(25), 580(36), 375(sh)	c	This work
			1130(13), 662(19), 385(68)	d	This work
			1240(15), 1040(19), 540(30), 375(sh)	e	This work
$[Cu_2(L^{10})](ClO_4)_4.DMSO$	Blue	1.34[f,g]	608(394)	a	This work
			575(368)	b	This work
			588(416)	c	This work
			602(392)	d	This work
			590(203)	e	This work
			590	e	147

a = In dimethyl sulphoxide.
b = In nitromethane.
c = In acetonitrile.
d = In N,N-dimethyl formamide.
e = In water.
f: This magnetic moment is per metal ion.
g: This unusually low value per copper(II) ion may indicate some magnetic interaction between the two copper(II) ions.

TABLE 4.2

^{13}C N.M.R. DATA (δ P.P.M.) FOR LIGANDS L^{10} AND L^{11} AND $[Zn_2(L^{10})](ClO_4)_4$ AT 298 K
(REFERENCE $SiMe_4$ AT δ 0.00; FIGURES IN PARENTHESES REPRESENT THE RELATIVE AREAS OF THE RESONANCES)

Compound	Solvent	N-CH_2-N	C-CH_2-N	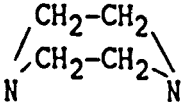	N-CH_2-C	C-CH_2-N	C-CH_2-C	C-CH_2-C
L^{10}	$CDCl_3$		57.37(4)	53.47(8)	49.44(4)	48.92(4)	29.46(2)	27.00(4)
L^{11}	$CDCl_3$	72.28(2)	55.89(4)	52.99(8)	53.61(4)	51.91(4)	22.40(2)	24.35(4)
L^{10}	DMSO-d_6		55.86(4)	52.77(8)	47.74(4)	46.65(4)	25.41(2)	25.32(4)
$[Zn_2(L^{10})](ClO_4)_4$	DMSO-d_6		56.91(4)	52.01(8)	53.13(4)	50.24(2)	23.61(2)	20.78(4)

SECTION 4 EXPERIMENTAL

The experimental techniques and instrumentation are discussed in detail in Chapter VII.

CHEMICALS AND SOLVENTS

(i) See Chapter II, Section 5.

(ii) 1,3-Propananediol and N,N'-bis(3-aminopropyl) piperazine were obtained from Aldrich and used without further purification.

(iii) 4-Methyl benzene sulphonyl chloride was purified by recrystallisation from diethyl ether.

SECTION 5.1 PREPARATION OF 1,5,9,13,16,20,24,28-OCTAAZATRICYCLO-[26.2.2.$2^{13,16}$]-TETRATRIACONTANE (L^{10})

The ligand L^{10} was prepared following the synthetic routes outlined in Scheme 4.1 overleaf.

(i) Preparation of 1,3-propanediol bis-(4-methyl-benzene sulphonate)

To a mixture of 1,3-propanediol (10 g, 0.131 mol) and triethyl amine (26.6 g, 0.263 mol) in (300 cm^3) CH_2Cl_2 was added dropwise a solution of *p*-toluene sulphonyl chloride (50.11 g, 0.263 mol) in CH_2Cl_2 (200 cm^3) at room temperature with good stirring over a period of 1½ h. The reaction mixture was left to stir for 2 more hours and then 500 cm^3 of light petrol (b.p. 40-60°) was added to precipitate the product as white solid. This was filtered and washed with diethyl ether (3 x 50 cm^3) and water (4 x 100 cm^3). The product was kept in a dessicator over silica gel for a week to dry. The yield was (28.26 g, 73.6 mmol; 56%); m.p. 94°C (reported 94°C)[156] ^1H n.m.r. ($CDCl_3$); δ 2.00 (2H, pentet), 2.46 (6H, s), 4.08 (4H, t), 7.33 (4H, d), 7.73 (4H, d) p.p.m.

(ii) Preparation of N,N'-bis(4-methyl-benzene sulphonate)-N,N'-bis(3-aminopropyl)piperazine

The amine N,N'-bis(3-aminopropyl)piperazine (30 g, 150 mmol) was dissolved in CH_2Cl_2 (200 cm^3) and triethyl amine (30 g, 299 mmol) was added. The reaction mixture was stirred at room temperature during the dropwise addition of 4-methyl benzene sulphonyl chloride (57.1 g, 300 mmol) in CH_2Cl_2 (200 cm^3) over a period of 1 h. The reaction mixture was left to stir for 2 h, and then poured into diethyl ether (200 cm^3) to give white solid. This

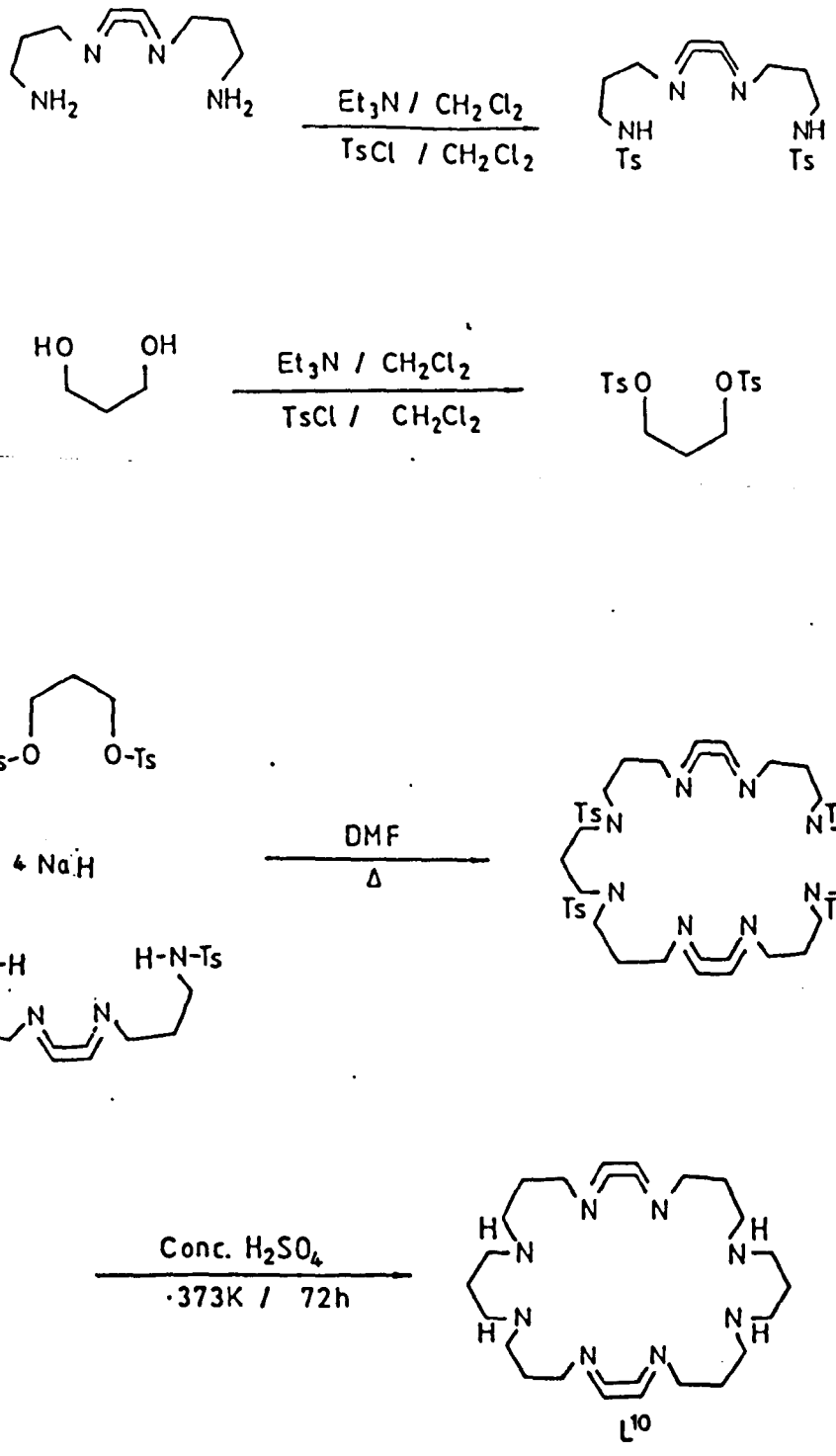
NH2
NH2
Et3N / CH2Cl2
TsCl / CH2Cl2
NH Ts
NH Ts
HO
OH
Et3N / CH2Cl2
TsCl / CH2Cl2
TsO
OTs
2
Ts-O
O-Ts
4 NaH
DMF
Δ
2
Ts-N-H
H-N-Ts
Conc. H2SO4
·373K / 72h
L10

SCHEME 4.1

was filtered, washed with water (5 x 100 cm^3), and dried in a dessicator over silica gel (1 week). The yield was (66.72 g, 131 mmol; 88%). M.p. 200 dec.; ^1H n.m.r. ($CDCl_3$) δ 1.63 (4H, pentet), 2.45 (18H, m), 3.07 (4H, t), 7.15 (2H, broad), 7.30 (4H, d), 7.72 (4H, d), p.p.m.

(iii) Preparation of the tosylated macrocycle

N,N'-di(4-methyl benzene sulphonate)-N,N'-bis(3-amino propyl) piperazine (20 g, 39.37 mmol) was dissolved in dry N,N'-dimethyl formamide (300 cm^3) and NaH (2.77 g, 115 mmol; 20% excess) was added in small portions, whilst the reaction mixture was stirring under dinitrogen. Effervescence occurred. When gas evolution ceased, the solution was heated to 100°C and a solution of 1,3-propanediol-bis(4-methyl benzene sulphonate) (15.085 g, 39.3 mmol) was added dropwise over a period of 3 h. The resulting pale brown solution was heated at 110°C overnight, and then allowed to cool to room temperature. An equal volume of water was added, and the whole solvent was then removed by evaporation under reduced pressure to leave a viscous brown oil, which was re-dissolved in water and extracted with CH_2Cl_2 (4 x 100 cm^3). The dichloromethane extracts were dried over $MgSO_4$, filtered and the solvent removed to give a very viscous brown oil, which was kept under high vacuum at 65°C overnight to remove the last trace of DMF. The product was used in the next stage without further purification.

(iv) Preparation of ligand (L^{10})

The tosylated L^{10} (product of the reaction described above) (12 g, 10.9 mmol) was dissolved in concentrated H_2SO_4 (80 cm^3) and heated at 100°C for 72 h. After cooling in an ice bath, the solution was poured into cold ethanol (200 cm^3), followed by the

addition of diethyl ether (500 cm^3). The resulting pale brown precipitate was filtered and dissolved in water (50 cm^3). The pH of the solution was adjusted to 11 with 15% aqueous NaOH followed by extraction with CH_2Cl_2 (7 x 100 cm^3). The combined extracts were dried over $MgSO_4$, filtered, and the solvent removed with a rotary evaporator to give a pale yellow solid. This was passed through an alumina column using CH_2Cl_2 as eluant. Upon removal of the solvent from the first fraction L^{10} (1.5 g, 3.125 mmol) was obtained in 29% yield. ^1H n.m.r. ($CDCl_3$) 1.74 (12H, pentet), 2.32-2.70 (40H, m), 3.2 (4H, broad). The electron impact spectrum showed m/z at 480; calc. for parent ion, 480. ^{13}C n.m.r. chemical shifts are given in Table 4.2, and the spectrum is shown in Figure 4.2.

SECTION 5.2 PREPARATION OF METAL COMPLEXES OF L^{10}

(1) $[Ni_2(L^{10})(DMSO)](ClO_4)_4$

$[Ni(DMSO)_6](ClO_4)_2$ (605 mg, 0.833 mmol) was dissolved in ethanol (10 cm^3) and a solution of L^{10} (200 mg, 0.417 mmol) in ethanol (5 cm^3) was added dropwise (½ h). The resulting pink precipitate was filtered and washed with ethanol (3 x 5 cm^3), then diethyl ether (3 x 5 cm^3) and dried in vacuum to give the product (250 mg, 0.233 mol) in 56% yield. Microanalysis; found: C, 31.6; H, 5.8; N, 9.9; S, 3.6. Calc. for $C_{28}H_{62}Cl_4N_8Ni_2O_{17}S$: C, 31.3; H, 5.8; N, 10.4; S, 3.0%.

(11) $[Cu_2(L^{10})](ClO_4)_4.DMSO$

L^{10} (100 mg, 0.208 mmol) in ethanol (5 cm^3) was added to $[Cu(DMSO)_6](ClO_4)_2$ (304 mg, 417 mmol) in ethanol (10 cm^3) in the similar method as described for nickel(II) complex. The resulting blue precipitate was filtered, washed with ethanol and dried in

vacuum to give $[Cu_2(L^{10})](ClO_4)_4.DMSO$, (180 mg, 0.179 mmol) in 80% yield. Microanalysis; found: C, 31.3; H, 5.8; N, 9.8 and S, 3.2. Calc. for $C_{28}H_{62}Cl_4Cu_2N_8O_{17}S$: C, 31.0; H, 5.8; N, 10.3; and S, 3.0%.

(iii) $[Zn_2(L^{10})](ClO_4)_4$

$Zn(ClO_4)_2.6H_2O$ (466 mg, 1.25 mmol) was dissolved in EtOH (10 cm^3) and added to a solution of L^{10} (300 mg, 0.625 mmol) in EtOH (10 cm^3) under dry dinitrogen. The product was precipitated by the addition of dry diethyl ether (30 cm^3). Filtration under dinitrogen and drying in vacuum gave $[Zn_2(L^{10})](ClO_4)_4$, (360 mg, 0.358 mmol) in 57% yield. Microanalysis; found: C, 31.1; H, 6.0; N, 10.80. Calc. for $C_{26}H_{56}Cl_4N_8O_{16}Zn_2$: C, 30.9; H, 5.6; N, 11.1%.

SECTION 6 ATTEMPTS TO PREPARE A HETEROBIMETALLIC COPPER(II) AND NICKEL(II) COMPLEX OF L^{10}

To a stirred solution of L^{10} (233 mg, 0.485 mmol) in water (20 cm^3) at 35°C, was added $Ni(NO_3)_2.6H_2O$ (141 mg, 0.485 mmol) in water (10 cm^3) to give a green solution. After ½ h a solution of $Cu(NO_3)_2.3H_2O$ (117 mg, 0.485 mmol) in water (10 cm^3) was added. The solution colour was changed to blue-green. The reaction mixture was left to stir for ½ h more, cooled in ice bath, carefully transferred to a jacket-column (400 x 20 mm) packed with Sephadex C-25 resin (16 g), which had been swelled in distilled water, and the column cooled with ice at 0°C. Elution with 0.4 mol dm^{-3} aqueous NaCl gave three distinct bands as described in Section 3. The third band which is the dinickel complex of L^{10} is eluted with 1.0 mol dm^{-3} aqueous NaCl.

CHAPTER V

SYNTHESIS OF PENDENT-ARM MACROCYCLES AND THEIR COPPER(II) AND NICKEL(II) COMPLEXES

SECTION 1 INTRODUCTION

There is considerable current interest in the synthesis and investigation of functionalised macrocyclic ligands and their metal complexes especially those with pendent coordinating arms.[9] An interesting ligand is the mono-substituted derivative (L^{12}) which was reported by Kaden.[157]

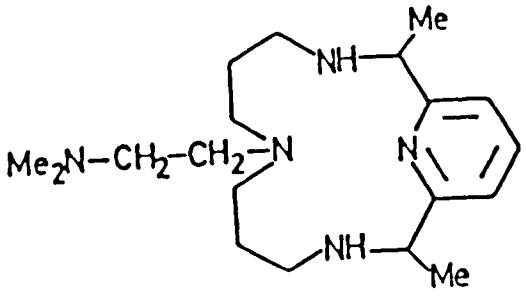

L^{12}

Synthesis of such ligands using one equivalent of an alkylating agent in the direct alkylation of a tetraazamacrocycle such as 1,4,8,11-tetraazacyclotetradecane (cyclam) has proved unsatisfactory due to the formation of a mixture of di-, tri- and tetra-substituted macrocycles, which can be difficult to separate. Two main routes have been found for the satisfactory synthesis of these monosubstituted macrocycles.[9] The first route devised by Kaden[158] involved the use of a template reaction, in which one of the compounds already had the required side-chain attached to it. Generally, the side-chain used has a hydroxide or chloride functional group, so conversion to other derivatives is possible. The second main method of synthesis involves the use of protecting

groups. Tosyl or mesyl groups are normally used to protect the nitrogens, and these are removed later by acid hydrolysis.[159] In this method a variety of attacking species may be used for attachment of a pendent group. So far macrocycles with pendent co-ordinating amino[51,52,160-163], amido[164-166], pyridyl[160,167,168], hydroxo[169,170], phenolato[171,172], phosphino[173,174] and carboxylato[175-177] arms have been investigated. Many of these new macrocycles are able to impose unusual coordination numbers and geometries on a metal ion.

In this Chapter synthesis of macrocycles with pyrrolidinyl, cyano, amido and acetato pendent-arms and their copper(II), and nickel(II) complexes are reported.

SECTION 2 RESULTS AND DISCUSSION

SECTION 2.1 SYNTHESIS OF 7-[2'-(1"-PYRROLIDINYL)ETHYL]-3,7,11,17-TETRAAZABICYCLO[11.3.1]HEPTADECA-1(17),13,15-TRIENE (L^{13})

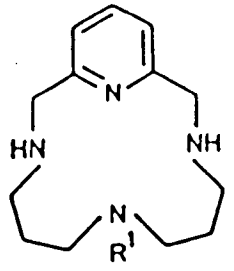

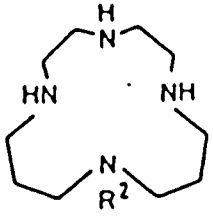

L^{13}; R^1 = 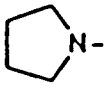 $N-CH_2CH_2-$ L^{16}; R^2 = $Me_2NCH_2CH_2-$

L^{14}; R^1 = $Me_2NCH_2CH_2-$

L^{15}; R^1 = $Me_2NCH_2CH_2CH_2-$

FIGURE 5.1

The synthesis is outlined in Scheme 5.1 (p. 146). The Michael addition of excess acrylonitrile to 1-(2-aminoethyl) pyrrolidine proceeds smoothly in the presence of ethanoic acid as catalyst. The addition of this catalyst gives cleaner products, and the reaction time is significantly shortened. The two nitrile groups of (1) are readily reduced to the corresponding amino groups (2) using sodium in ethanol. Formation of the di-imine macrocyclic takes 6-8 h starting with amine (2) and pyridine-2,6-dicarbaldehyde in the presence of Ni^{2+}. The sluggish nature of this reaction may be due to the formation of an 'umbrella-like' complex by (2), which is well known for the analogous ligand

tren (2,2',2"-triaminotriethylamine). In an 'umbrella like' structure the primary amino groups are not favourably disposed for the di-imine formation, which requires a planar geometry. Sodium tetrahydroborate was used to reduce the two imine groups, and the free ligand (L^{13}) was liberated by treatment of the reaction mixture with excess sodium cyanide.

The new pendent arm macrocycle L^{13} (Figure 5.1) was designed with an arm able to produce a five-membered chelate ring, and was obtained for comparison with the related ligands containing pendent $\{CH_2\}_nNMe_2$ arms (n = 2 or 3) which have been reported previously.[113,161] It was expected that the bulkier pyrrolidinyl groups would hinder folding of the macrocycles, and be more likely to produce complexes in which the metal ion is six-coordinate, with axial unidentate ligand (X) occupying a *trans* position to the pendent arm, structure type (I), Figure 5.2, rather than the folded macrocyclic trigonal bipyramidal structures, type (II), found previously.[161]

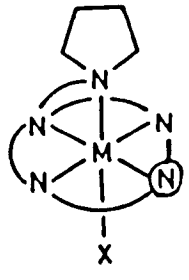

(I)

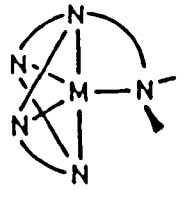

(II)

FIGURE 5.2

SECTION 2.2 SYNTHESIS OF NICKEL(II) AND COPPER(II) COMPLEXES OF L^{13}

Reaction of L^{13} with $[M(DMSO)_6](ClO_4)_2$ (M = Ni or Cu) in ethanolic solution rapidly gives complexes of formula $[M(L^{13})OClO_3]ClO_4$ which precipitate soon after mixing and can be recrystallised from nitromethane-ethanol. The blue nickel(II) complex is paramagnetic (μ_{eff} = 2.8 B.M.) and six-coordinate as shown by the crystal structure (Figure 5.3, p. 132). Bonding is of type (I) (Figure 5.2) in which the pendent arm is coordinated at the apex of a square pyramid, with a perchlorate ion coordinated in a *trans* position to the pendent arm, and with the macrocyclic ring occupying the equatorial plane. The complex remains six-coordinate in nitromethane solution as shown by the visible spectrum (Table 5.1, p. 143). The copper(II) and nickel(II) complexes of L^{13} are isomorphous, and both may be protonated to give four-coordinate complexes of formula $[M(HL^{13})](ClO_4)_3$ (M = Ni or Cu) in which the pendent arm is protonated and non-coordinating. The yellow protonated nickel(II) complex is diamagnetic and in nitromethane solution the sharp ^{13}C n.m.r. spectrum (chemical shifts are in Table 5.2, p. 144) and the visible spectrum (Table 5.1, p. 143) confirm the expected square planar geometry. The n.m.r. data show that only a single symmetric isomer is present. Three isomers are possible as shown schematically in Figure 5.4; of the two possible symmetric isomers, (A) is believed to be the more likely structure for $[Ni(HL^{13})](ClO_4)_3$; based on previous studies and the crystal structure in Section 2.3.

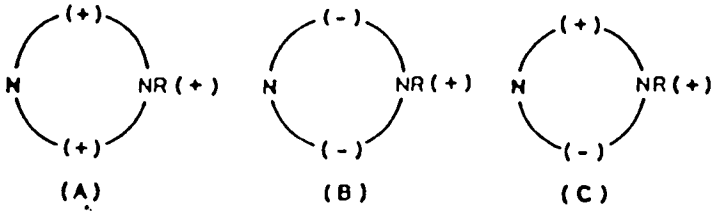

FIGURE 5.4

Schematic representation of the three possible isomers of square-planar $[Ni(HL)]^{3+}$ ions (L = L^{13}); (+) and (-) represent the positions of either macrocyclic NH groups or N pendent arm (R), either above (+) or below (-) the macrocyclic ligand plane. The pyridine-N atom is in bold type. (C) is enantiomeric.

The visible spectrum of $[Cu(HL^{13})](ClO_4)_3$ indicates that this is also four-coordinate.

The protonation-deprotonation equilibria are reversible (Figure 5.5), careful adjustment of the pH to *ca.* 6-7 with a suitable base immediately regenerating the complexes with pendent arm coordinated.

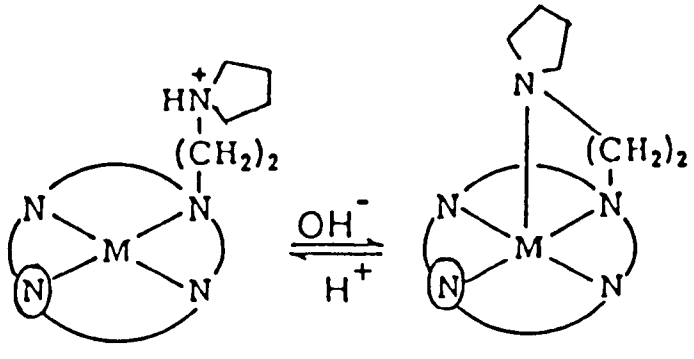

FIGURE 5.5

SECTION 2.3 X-RAY CRYSTAL STRUCTURE OF $[Ni(L^{13})OClO_3]ClO_4$

The molecular structure of $[Ni(L^{13})OClO_3]ClO_4$, is given in Figure 5.3, and shows that the macrocycle coordinates in a square-pyramidal fashion, bonding mode (I) (Figure 5.2, p. 128), in contrast to the trigonal-bipyramidal geometry [bonding mode (II)], found for the Ni^{2+} complex of pendent arm macrocycle L^{16} (Figure 5.1, p. 127).[161] The pyridine group of L^{13} probably aids the formation of the square-pyramidal mode of co-ordination, and the bulkier pendent pyrrolidine group will also assist such a geometry for steric reasons. The overall geometry of the complex shown in Figure 5.3 is close to octahedral as shown by the bond angles at Ni^{2+} which are in the range 81-104°. The Ni-N bond lengths are all close to 2.1 Å except that to the pyridine-N-atom which is significantly shorter (1.96 Å). This behaviour has been observed in several related structures. The Ni-O bond length is somewhat longer at 2.39 Å, as expected.

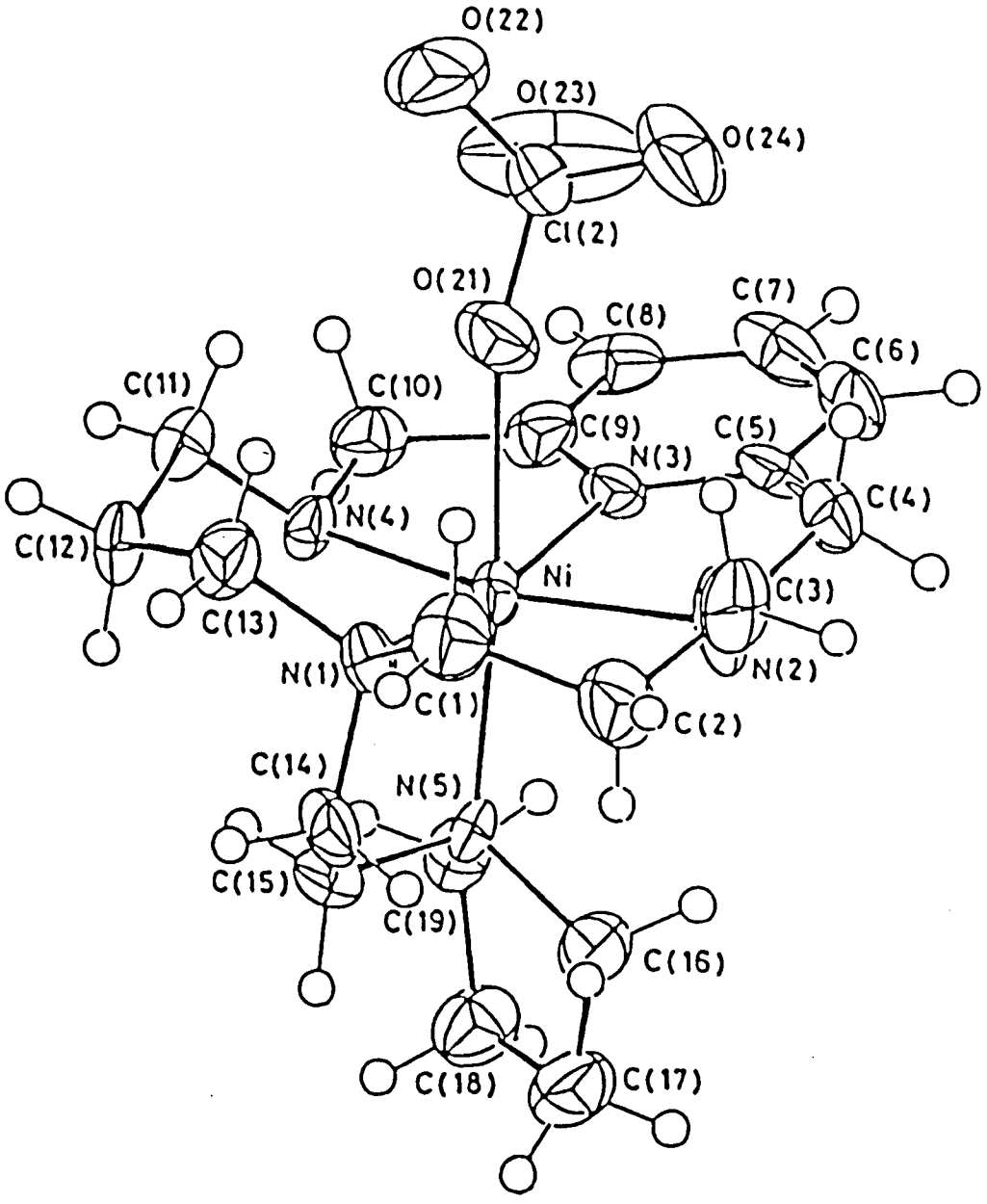

FIGURE 5.3

X-ray structure of $[Ni(L^{13})(OClO_3)]ClO_4$ showing the atomic numbering scheme

SECTION 3.1 SYNTHESIS OF 3,11-DI(CYANOMETHYL)-7-METHYL-3,7,11,17-TETRAAZABICYCLO[11.3.1]HEPTADECA-1(17),13,15-TRIENE L^{17}

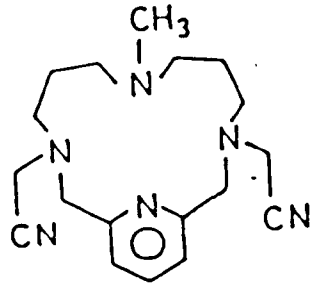

L^{17}

FIGURE 5.6

The drawback of the synthetic routes previously used to give pendent-arm azamacrocycles is the low yield. These routes involve coupling reaction between two components one of which already has the attached pendent-arm.

One way of avoiding this difficulty is to prepare an azamacrocycle with only one or two NH-groups accessible for alkylation. An example of such a ligand is L^2 (previously prepared as described in Chapter 2 and reference 113). Starting from L^2 a range of possible sexidentate macrocycles can be synthesised. Thus, L^2 was reacted with formaldehyde in the presence of cyanide ion, to add two cyanomethyl groups at the secondary amine groups of L^2, thereby giving the sexidentate ligand L^{17} in excellent yield. The purity of the ligand was confirmed by ^1H and ^{13}C n.m.r.; its ^1H decoupled ^{13}C n.m.r. spectrum is shown in Figure 5.7.

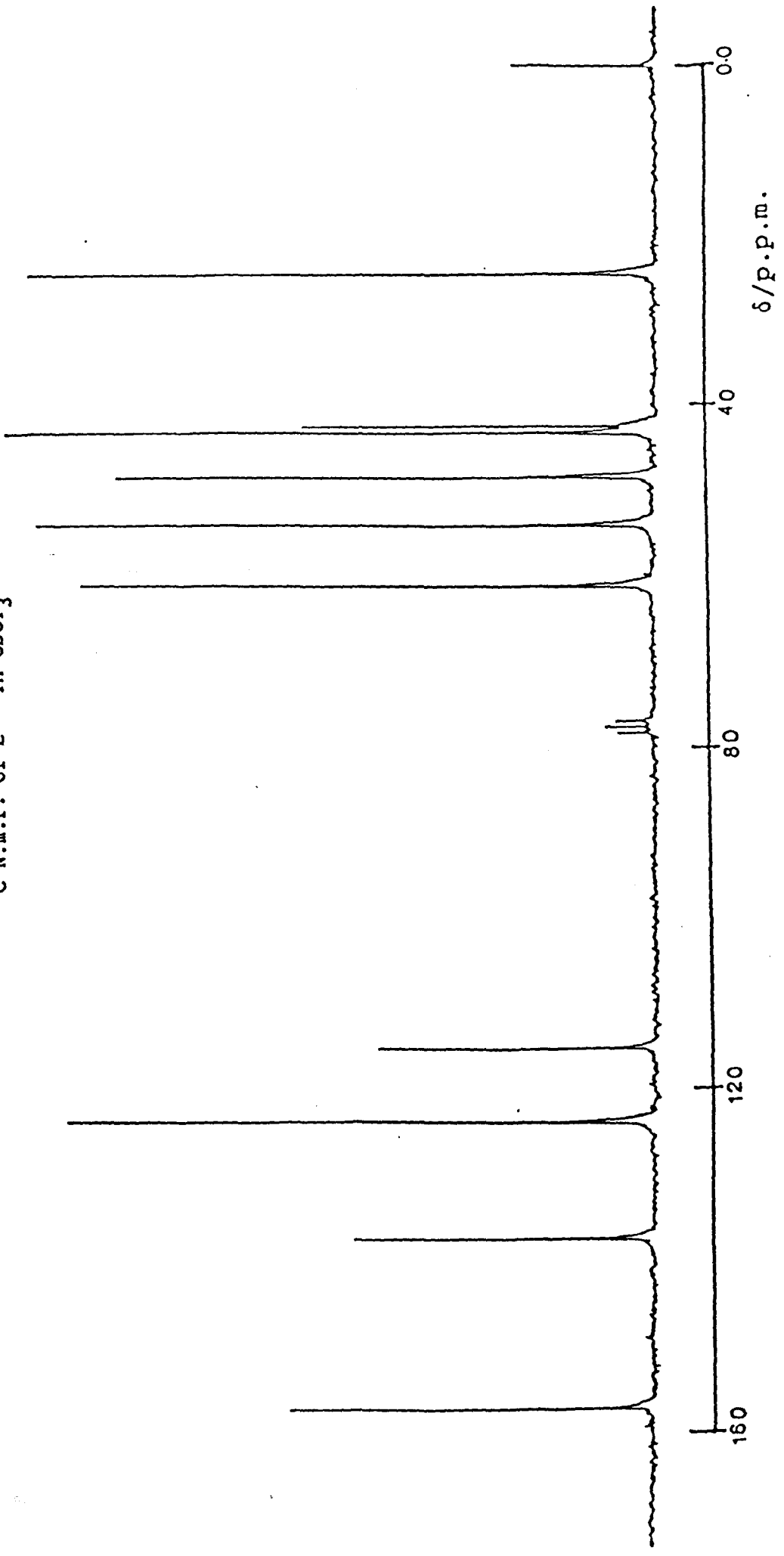

FIGURE 5.7

^{13}C N.m.r. of L^{17} in $CDCl_3$

SECTION 3.2 ATTEMPTS TO PREPARE METAL COMPLEXES OF L^{17}

Reaction of L^{17} with equal amounts of DMSO solvates of either copper(II), nickel(II) or zinc(II) perchlorate salts in ethanolic solution gives blue, pale-blue and white solids respectively. The parent peaks m/z shown in f.a.b. mass spectra of the copper(II) complex (506 and 488) and the nickel(II) complex (501 and 483), and also their i.r. spectra [showing bands at 1624 cm^{-1} and 1610 cm^{-1} for υ (C=O) of an amide arm, for Cu^{2+} and Ni^{2+} complexes respectively] confirmed that the products were a mixture of hydrolysed and unhydrolysed species. The ^{13}C n.m.r. spectrum of the zinc(II) complex of L^{17} in nitromethane solution also shows that this complex is partially hydrolysed. It has been reported that the nitrile group of a copper(II) complex of a cyanomethyl-substituted tetraazamacrocycle undergoes hydrolysis to give a corresponding amide due to reaction of the metal complex with water in aqueous solution.[178]

It is not surprising therefore, that the metal complexes of L^{17} behave similarly; reaction occurring with traces of water in ethanol.

Attempts at separation of the unhydrolysed and hydrolysed products on Sephadex proved difficult due to continuing reaction of the cyano-groups with water during the separation. However, these metal complexes were used in the next preparation without any further purification.

SECTION 3.3 HYDROLYSIS OF ONE NITRILE GROUP OF L^{17} USING THE COPPER(II) AND NICKEL(II) COMPLEXES

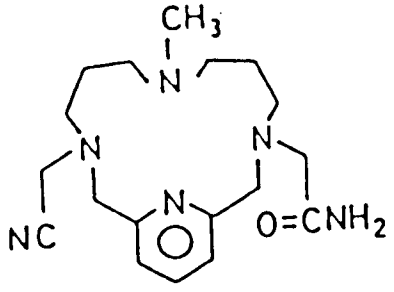

L^{18}

FIGURE 5.7

Upon refluxing an aqueous solution of the copper(II) or nickel(II) complexes of L^{17} overnight, one of the nitrile groups is hydrolysed to an amide group. The f.a.b. mass spectra of the complexes shows cluster of parent ion peaks centred at 506, and 501 for the copper(II) and nickel(II) complexes respectively, confirming the previous deduction. Analytical data and visible spectra (Table 5.1) of these complexes indicate the formation of five coordinate complexes of formula $[Cu(L^{18})](ClO_4)_2.H_2O$ and $[Ni(L^{18}-H)](ClO_4).2\frac{1}{2}H_2O$ in which the fifth position is occupied by an amide oxygen in the case of copper(II) complex, and by a deprotonated amide nitrogen in the case of the nickel complex. The visible absorption maximum of the Cu^{2+} complex shift to longer wavelength (from 590 nm to 650 nm) when pH of the solution is increased to 12, whereas the spectrum of the Ni^{2+} complex does not show any pH dependence; this indicates that the pendent amide group

is coordinated through oxygen in the Cu^{2+} complex at neutral or low pH and through amide nitrogen at high pH. In the Ni^{2+} complex, however, the absence of a pH dependence indicates that the nitrogen is deprotonated and coordinated at all pH values (6-11). This behaviour has been reported previously for a similar system.[159]

Attempts were made to hydrolyse the zinc(II) complex of L^{17} by refluxing in aqueous solution, and to hydrolyse the free ligand in 6 mol dm^{-3} HCl. The ^{13}C n.m.r. spectra showed loss of the pendent-arms under these conditions, to give mixtures of products with none, one and two arms. ^{13}C N.m.r. of the free ligand after refluxing in HCl is shown in Figure 5.8.

FIGURE 5.8

^{13}C N.m.r. in D_2O of hydrolysed products of L^{17} obtained by refluxing the ligand in 6 mol dm^{-3} HCl overnight at 85°C. The spectrum is complicated and the aromatic region consistent with monoamide arm macrocycle (unsymmetric species), none and two amide arms macrocycles (both symmetric species). There are no resonances in the region of 110–120 p.p.m. indicating all cyano groups were hydrolysed.

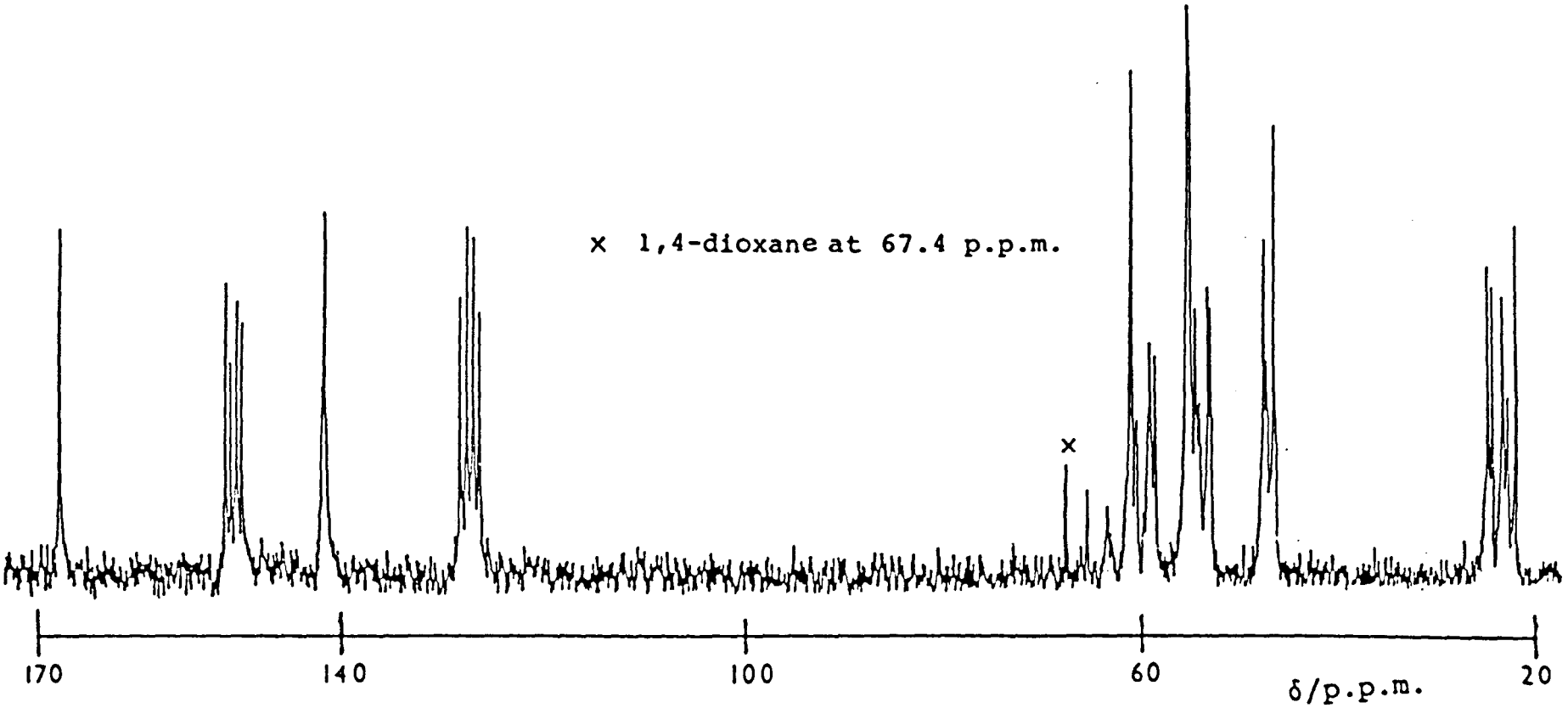

SECTION 4.1 SYNTHESIS OF 3,11-DIACETATO-7-METHYL-3,7,11,17-TETRAAZABICYCLO[11.3.1]HEPTADECA-1(17),13,15-TRIENE (L^{19}) AND ITS COPPER(II) COMPLEX

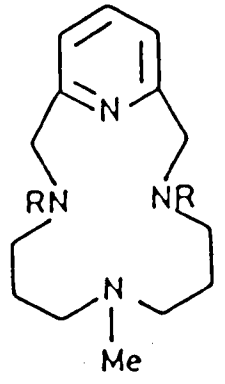

L^{19}; R = $CH_2CO_2^-$
L^{2}; R = H

FIGURE 5.9

Reaction of L^2 with two moles of 2-bromoethanoic acid in the presence of base (using a published method)[175] gave L^{19} (Scheme 5.2, p. 156), and the ligand was isolated as the tetrahydrochloride salt in reasonable yield. $L^{19}.4HCl$ was reacted with an equimolar amount of $CuSO_4.4H_2O$ in water to give green crystals of $[Cu(L^{19}H_2)Cl]Cl.4H_2O$. The visible spectrum of the complex in water showed a band at 624 nm which is close to the value reported for the $[Cu(NH_3)_3(H_2O)_3]^{2+}$ ion (λ_{max} 625 nm), and indicated that not all four N atoms of L^{19} were coordinated.[147] The f.a.b. mass spectrum of the complex showed a cluster of parent ion peaks centred at m/z 462 as expected for $[Cu(L^{19}H)Cl]^+$.

SECTION 4.2 CRYSTAL STRUCTURE OF $[Cu(L^{19}H_2)Cl]Cl$

As outlined in Chapter 2, there is considerable current interest in the isomerisation reactions of metal complexes of tetraazamacrocyclic ligands.[116] These isomerisation reactions involve nitrogen-inversions, and it has been postulated that intermediates must be formed in which one or more of the metal-nitrogen bonds are broken to allow nitrogen inversion to occur. Until recently no evidence has been found for the existence of such an intermediate in which one of the nitrogen atoms is uncoordinated, and only the endo-mode of co-ordination had been found for potentially quadridentate tetraazamacrocycle of the type shown in structure (A) [X = NR; R = Me or H] (Figure 5.10).

In contrast, for tetrathiamacrocycles (X = S) the *exo*-structures (B)[179] and (C)[180] have been found as possible modes of co-ordination. The ability of these tetrathiamacrocycles to give *exo*-structures is believed to be due to the larger size of the sulphur-donor atoms which reduces the macrocycle cavity size and produces greater repulsions between the sulphur lone-pairs.

Recently, an example of a structure of type (B) was reported for binuclear copper(II) complex of a functionalised azamacrocycle.[181]

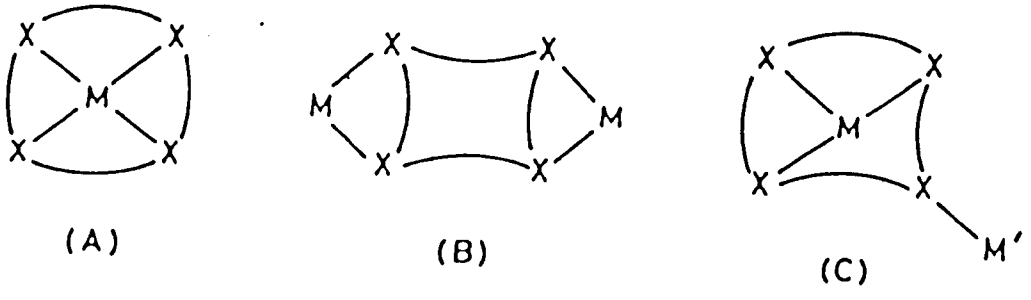

FIGURE 5.10

The copper(II) complex of L^{19} was found to have coordination mode (C) ($M = Cu^{II}$; $M' = H^+$; $X = NR$). This is the first example reported for a tetra-azamacrocycle with such a coordination mode; the only previous example of mode (C) is in a polymeric copper(I) complex of a tetrathiamacrocycle ($M = M' = Cu^I$; $X = S$).[180] The molecular structure of $[Cu(L^{19}H_2)Cl]^+$ is shown in Figure 5.11. The Me-N group, and one of the two acetate-arms of L^{19} are clearly protonated and non-coordinating. The copper(II) complex is approximately trigonal bipyramidal, with apical co-ordination to Cl and the N(pyridine) atom, and with equatorial coordination to the other two nitrogen atoms and one acetate arm of L^{19}. The bond lengths and angles are shown in Table 5.6, p. 159. As is common for tetraazamacrocycles which contain a pyridine moiety, the Cu-N (pyridine) bond length (1.949 Å) is significantly shorter than the other two Cu-N bond lengths (average 2.124 Å). The Cl-Cu-N (pyridine) bond angle (178.6°) is close to the ideal for a trigonal bipyramidal structure, and the other three donor atoms and the copper(II) are approximately coplanar. However, the pendent-arm chelate ring forms an acute angle of only 69° at copper(II), and this significantly distorts the trigonal bipyramidal structure. The non-coordinating acetate-arm is on the same side of the azamacrocyclic plane as the coordinating acetate-arm, which prevents ready coordination in an idealised *trans*-six-coordinate structure. The significant feature of the structure is the non-coordination of the Me-N group, giving rise to bonding mode (C) ($M' = H^+$), which has not been reported previously for a tetraazamacrocycle. The conclusion one can draw is that it is reasonable to postulate the presence of similar intermediates in the isomerisation reactions of tetraazamacrocyclic complexes.[116]

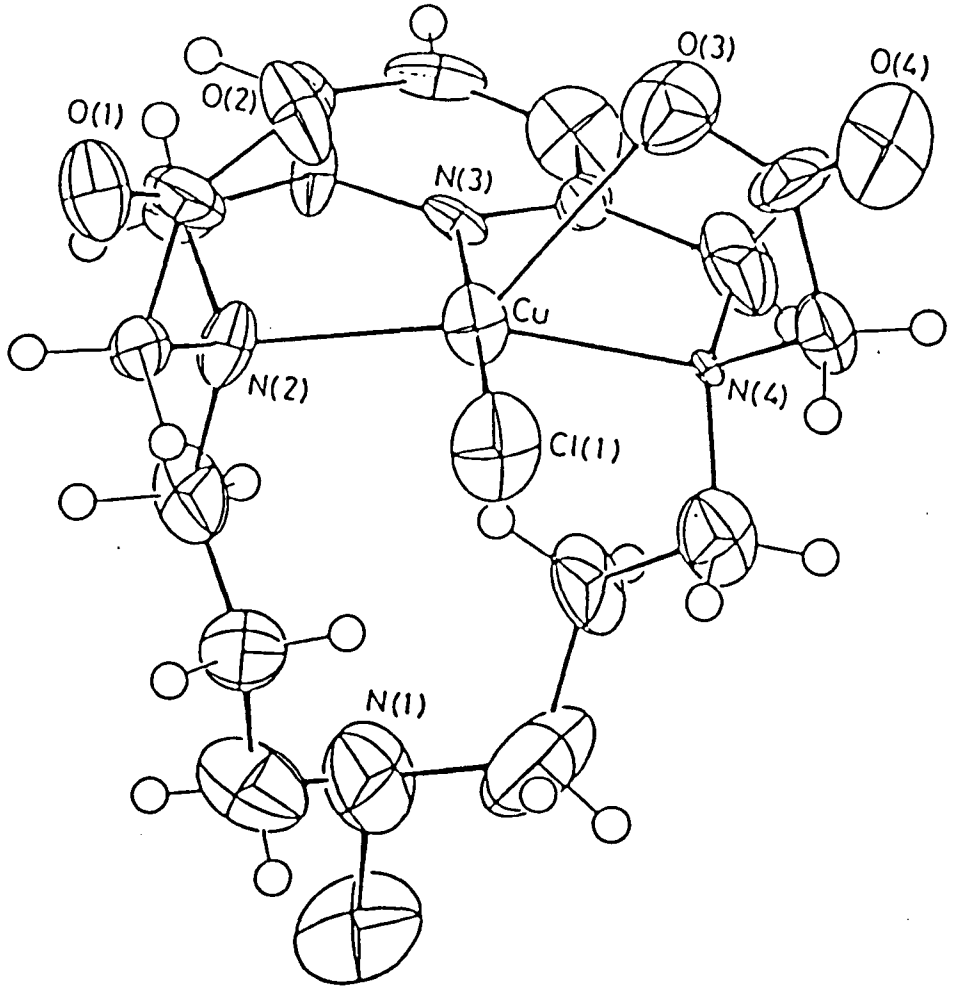

FIGURE 5.11

Molecular Structure of $[Cu(L^{19}H_2)Cl]Cl.4H_2O$

TABLE 5.1

U.v. Visible Spectra [λ_{max}/nm (ϵ/$dm^3mol^{-1}cm^{-1}$)] and Magnetic Moments (μ_{eff}/B.M.) at Room Temperature

Complex	Colour		$\lambda_{max}(\epsilon)$	μ_{eff}
$[Ni(L^{13})(OClO_3)]ClO_4$	Blue	a	572(45), 772(15), 1368(17)	2.8[d]
$[Ni(HL^{13})](ClO_4)_3$	Yellow	a	468(148)	
$[Cu(L^{13})(OClO_3)]ClO_4$	Blue	a	600(187), 848(37)	1.7[d]
$[Cu(HL^{13})](ClO_4)_3$	Purple	a	554(122)	
$[Ni(L^{18}-H)]ClO_4.2½H_2O$	Mauve	a	554(55), 850(40), 1030(sh)	2.85[e]
$[Ni(L^{18}-H)]ClO_4.2½H_2O$	Mauve	b	350(sh), 556(25), 860(19), 1210(6)	
$[Ni(L^{18}-H)]ClO_4.2½H_2O$	Mauve	c	355(111), 570(20), 895(17)	
$[Cu(L^{18})](ClO_4)_2.H_2O$	Blue	a	584(137)	1.8[e]
$[Cu(L^{18})](ClO_4)_2.H_2O$	Blue	b	590(343)	
$[Cu(L^{18})](ClO_4)_2.H_2O$	Blue	c	600(233)	
$[Cu(L^{19}H_2)Cl]Cl.4H_2O$	Green	a	644	
$[Cu(L^{19}H_2)]Cl.4H_2O$	Blue	b	624(60)	
$[Cu(L^{19}H_2)Cl]Cl.4H_2O$	Blue	c	692(71)	

a: In nitromethane;
b: In water;
c: In dimethyl sulphoxide;
d: In nitromethane solution using Evans method (reference 120);
e: In solid state.

TABLE 5.2

^1H Decoupled ^{13}C n.m.r. Chemical Shifts of L^{13} and L^{17} and some of their Nickel(II) and Zinc(II) Complexes and of $[Zn(L^{18})]^{2+}$ (δ/p.p.m. Reference $SiMe_4$) at 298K. Relative Intensities in Parentheses

Compound	Solvent	O ‖ /C\	Pyridine			-CN	N-CH_2-C				N-$\underline{C}H_3$	C-$\underline{C}H_2$-C	
			Ortho	*Para*	*Meta*								
L^{13}	CD_3NO_2		161.2(2)	137.8(1)	121.1(2)		55.3(2)	55.1(3)[a]	54.3(2)	53.6(2)	47.0(1)	28.8(2)	24.4(2)
$[Ni(HL^{13})](ClO_4)_3$	CD_3NO_2		159.8(2)	144.3(1)	123.5(2)		61.9(2)	58.7(2)	56.8(2)	50.5(3)	49.0(1)	25.8(2)	25.4(2)
L^{17}	$CDCl_3$		156.9(2)	137.1(1)	123.3(2)	114.9(2)	61.2(2)	54.1(2)	48.4(2)	43.2(2)	42.4(1)		24.7(2)
L^{17}	CD_3NO_2		158.4(2)	138.2(1)	124.3(2)	116.6(2)	61.9(2)	55.3(2)	49.9(2)	44.0(2)	42.7(1)		25.8(2)
$[Zn(L^{17})DMSO](ClO_4)_2$[b]	CD_3NO_2		157.7(2)	139.3(1)	124.2(2)	116.8(2)	60.6(2)	56.8(2)	52.8(2)	43.9(2)	40.3(1)		21.5(2)
$[Zn(L^{18})](ClO_4)_2$	CD_3NO_2	177.7	154.4 153.2	144.0	125.4 125.3	115.1	58.3 58.1	56.8 56.5	55.7 55.1	44.3 43.8	41.6		22.9 22.3

a = Two overlapping resonances

b = Coordinated DMSO at δ 40.0 p.p.m.

c = Partial hydrolysis of the zinc complex of L^{17}, identified from the original spectrum of $[Zn(L^{17})(DMSO)](ClO_4)_2$ which is also present in solution

SECTION 5 EXPERIMENTAL

SECTION 6.1 PREPARATION OF L^{13}

The synthetic routes are outlined in Scheme 5.1.

(i) Preparation of Compound (1): 1-(2-Aminoethyl)pyrrolidine (24 g, 0.21 mol) was dissolved in acrylonitrile (300 cm^3, 4.56 mol) and glacial ethanoic acid (25.2 g, 0.42 mol) was added. The solution was heatd under reflux for 24 h, and excess acrylonitrile was then removed with a rotary evaporator. The residue was extracted with dichloromethane (3 x 100 cm^3), and the combined extracts shaken with 0.88 ammonia solution (150 cm^3). The organic phase was separated, washed with water, dried with anhydrous $MgSO_4$, filtered and then evaporated to give a thick yellow oil. Fractional distillation of the crude product gave a colourless oil (36 g, 0.16 mol, 77%), b.p. 160°C (0.07 mm Hg). ^1H n.m.r. ($CDCl_3$): 1.77 (4H, m) 2.60 (12 H, m), and 2.92 p.p.m. (4H, t). I.r. (thin film): 2342 cm^{-1} (CN).

(ii) Preparation of Compound (2): Compound (1) (28.6 g, 0.13 mol) was dissolved in dry ethanol (400 cm^3) and stirred under dinitrogen during the slow stepwise addition of sodium metal (50 g, 2.17 mol). The resulting solution was heated under reflux for 8 h, and then poured into an equal volume of distilled water. Extraction with dichloromethane (5 x 200 cm^3) followed by drying of the extracts with anhydrous $MgSO_4$, filtration and evaporation (rotary evaporator) gave a crude oil (25 g). Careful fractional distillation gave compound (2) (21 g, 0.092 mol; 70%), b.p. 105°C (0.05 mmHg). ^1H N.m.r. ($CDCl_3$): 1.30 (4H, s), 1.59 (4H, t), 1.75 (4H, m), 2.55

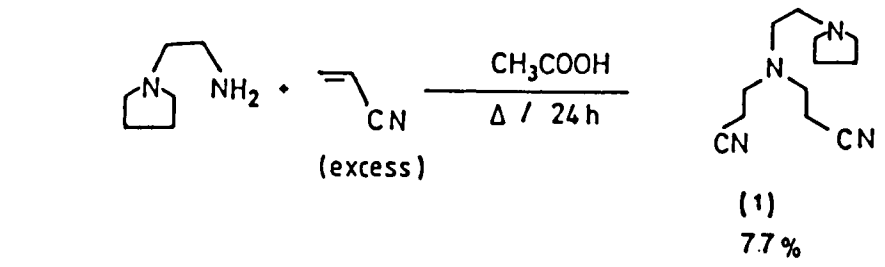

(1)
77%

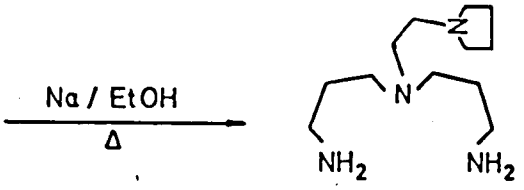

(2)
70%

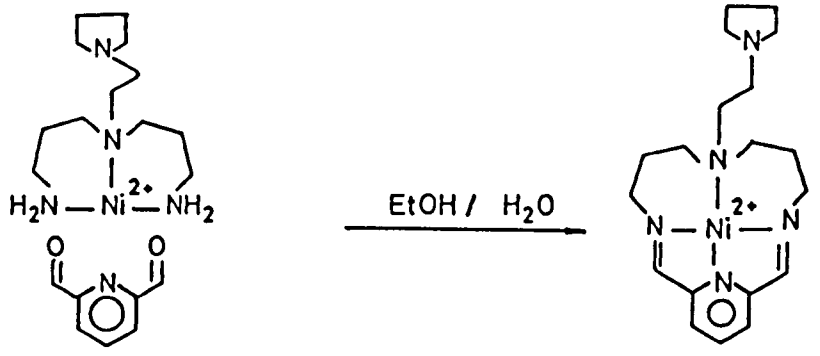

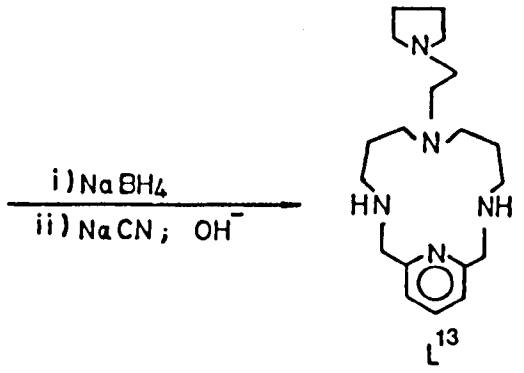

L^{13}

SCHEME 5.1

(12H, m), and 2.70 p.p.m. (4H, t); ^{13}C n.m.r. ($CDCl_3$): 54.49(1), 54.41(2), 53.15(1), 52.30(2), 40.61(2), 31.10(2) and 23.38 p.p.m. (2). I.r. (thin film): 3350 cm^{-1} (NH).

(iii) Preparation of L^{13}: $NiCl_2.6H_2O$ (2.35 g, 9.9 mmol) was dissolved in ethanol-water (1:1, 30 cm^3) and compound (2) (2.26 g, 9.9 mmol) added to give a blue solution. Pyridine-2,6-dicarbaldehyde (1.34 g, 9.9 mmol) was then added, followed by ethanoic acid (0.8 cm^3); the resulting brown solution was stirred for 2 h, then heated at 80°C for 6 h. The solution was then cooled with ice, and sodium tetrahydroborate (1.5 g, 39.7 mmol) was added slowly over a period of 30 min. The mixture was stirred at room temperature until effervescence ceased, and then heated at 80°C for 2 h. The ethanol was then removed with a rotary evaporator, and sodium cyanide (4g, 81.6 mmol) was added. After heating at 80°C for 1 h, the reaction mixture was cooled and basified with 15% aqueous NaOH to pH 12. The solution was extracted with dichloromethane (8 x 50 cm^3) and the combined extracts were dried with anhydrous $MgSO_4$. Filtration, evaporation, and distillation with a Kugelrohr apparatus gave L^{13} (1.26 g, 38 mmol; 38%) as a pale yellow liquid, b.p. 130-132°C (0.1 mmHg). ^1H N.m.r. ($CDCl_3$): 1.71 (8H, m), 2.50 (16H, m), 3.89 (4H, s), 7.00 (2H, d), and 7.55 p.p.m. (1H, t). ^1H Decoupled ^{13}C n.m.r. chemical shifts are shown in Table 5.2.

SECTION 6.2 PREPARATION OF METAL COMPLEXES OF L^{13}

(i) Preparation of $[Ni(L^{13})OClO_3](ClO_4)$: A solution of L^{13} (0.166 g, 0.5 mmol) in ethanol (10 cm^3) was added to a solution of $[Ni(DMSO)_6](ClO_4)_2$ (0.364 g, 0.5 mmol) in ethanol (10 cm^3). The

resulting purple precipitate was filtered off, washed with cold ethanol, then diethyl ether, and dried *in vacuo* to give $[Ni(L^{13})(OClO_3)](ClO_4)$ (0.204 g, 0.4 mmol; 81%). Microanalysis, found: C, 38.3; H, 5.8; N, 11.7%. Calc. for $C_{19}H_{33}Cl_2N_5NiO_8$: C, 38.7; H, 5.7; N, 11.9%. The highest mass peaks in the f.a.b. mass spectrum were at m/z 488 and 490 as calculated for the $[Ni(L^{13})ClO_4]^+$ ion.

(ii) Preparation of $[Ni(HL^{13})](ClO_4)_3$: $[Ni(L^{13})(OClO_3]ClO_4$ (0.118, 0.2 mmol) was stirred in ethanol (10 cm^3), and 4 or 5 drops of 70% perchloric acid (CARE! danger of explosion) added slowly causing a complete and rapid colour change from purple to orange-red. The precipitate was filtered, washed with cold ethanol, then diethyl ether, and dried *in vacuo* to give $[Ni(HL^{13})](ClO_4)_3$ (0.128 g, 0.18 mmol, 92%). Peaks were found in the f.a.b. mass spectrum at m/z 590 and 588 as calculated for the $[Ni(HL^{13})(ClO_4)_2]^+$ ion. Microanalysis, found: C, 32.6; H, 5.2; N, 10.1%. Calc. for $C_{19}H_{34}Cl_3N_5NiO_{12}$: C, 33.1; H, 5.0 and N, 10.2%.

(iii) Preparation of $[Cu(L^{13})(OClO_3)]ClO_4$ and $[Cu(HL^{13})](ClO_4)_3$: These were obtained in 88 and 93% yields as blue and purple solids respectively, using the same methods described for the nickel(II) analogues. Microanalysis for the two complexes were respectively as follows; found for the blue product: C, 37.0; H, 5.5; N, 11.6%. Calc. for $C_{19}H_{35}Cl_2CuN_5O_9$: C, 37.3; H, 5.8; N, 11.4%; found for the purple product: C, 32.8; H, 5.1; N, 10.3%. Calc. for $C_{19}H_{34}Cl_3CuN_5O_{12}$: C, 32.9; H, 4.9 and N, 10.1%.

SECTION 6.3 CRYSTAL DATA FOR $[Ni(L^{13})(OClO_3)](ClO_4)$

The crystals (pink prisms and plates) of formula $C_{19}H_{33}Cl_2N_5NiO_8$, M = 589.12, are monoclinic, space group $P2_1/c$, with a = 15.583(3), b = 9.656(3), c = 16.835(3) Å, β = 104.95(2), U = 2447.4(10), Å^3, Z = 4, D_c = 1.50 g cm^{-3}, Mo-K_α radiation, λ = 0.71069 Å, μ(Mo-K_α) = 10.68 cm^{-1}, F(000) = 1232.

Data were collected with a Syntex $P2_1$ four-circle diffractometer. Maximum 2 θ was 45°, with scan range ± 1.2° (2θ) around $K_{\alpha1}$-$K_{\alpha2}$ angles, scan speed 2-29° min^{-1}, depending on the intensity of a 2-s pre-scan; backgrounds were measured at each end of the scan for 0.25 of the scan time. The crystal was held at ambient temperature. Three standard reflections were monitored every 200 reflections, and showed slight changes during data collection; the data were rescaled to correct for this. Unit-cell dimensions and standard deviations were obtained by a least-squares fit to 15 high-angle reflections. 1394 Observed reflections with $I/\sigma(I) > 3.0$ were used in refinement, and corrected for Lorentz, polarisation, and absorption effects, the last by Gaussian integration; maximum and minimum transmission factors were 0.83 and 0.89. The crystal dimensions were 0.17 x 0.33 x 0.24 mm. Systematic absences h0l, l ≠ 2n; 0k0, k = 2n, indicated space group $P2_1/c$. The heavy atom was located by Patterson techcniques, and the light atoms were then found on successive Fourier syntheses. Hydrogen atoms were given fixed isotropic thermal parameters, U = 0.07 Å^2, as defined by the molecular geometry, and not refined. Final refinement was by cascaded least-squares methods, with anisotropic thermal parameters for all atoms other than hydrogen. The largest peak on a final

difference Fourier synthesis was of height 0.8 e $\mathring{A}^{-3}$ (in the vicinity of the ClO_4^- ion). A weighting scheme of the form $w = 1/[\sigma^2(F) + gF^2]$ with $g = 0.0009$ was used. This was shown to be satisfactory by a weight analysis. The final R value was 0.059. Computing was with the SHELXTL system[123] on a Data General DG30 computer. Scattering factors were in the analytical form, and anomalous dispersion factors were taken from ref. 124. Final atomic co-ordinates are given in Table 5.3, and selected bond lengths and angles in Table 5.4.

TABLE 5.3

Atomic Coordinantes (x 10^4) for $[Ni(L^{13})(OClO_3)](ClO_4)$

Atom	X	Y	Z
Ni	2328(1)	6871(1)	6789(1)
Cl(1)	3674(2)	1849(4)	5789(2)
Cl(2)	13(2)	7250(3)	6790(2)
O(11)	2904(7)	2568(10)	5496(9)
O(12)	4434(7)	2671(12)	5857(8)
O(13)	3697(9)	1428(15)	6610(8)
O(14)	3686(11)	659(12)	5349(8)
O(21)	944(5)	7022(8)	7150(5)
O(22)	-501(6)	6488(12)	7188(7)
O(23)	-194(7)	6999(17)	5955(7)
O(24)	-162(7)	8617(10)	6883(9)
N(1)	2828(6)	6224(9)	7967(6)
N(2)	2422(7)	9036(9)	6980(6)
N(3)	1634(6)	7462(10)	5697(5)
N(4)	1981(6)	4887(9)	6242(5)
N(5)	3656(6)	6611(8)	6643(6)
C(1)	2748(9)	7286(12)	8608(8)
C(2)	3049(9)	8754(13)	8455(9)
C(3)	2398(10)	9526(12)	7788(8)
C(4)	1748(8)	9730(11)	6283(7)
C(5)	1456(8)	8851(14)	5546(9)
C(6)	975(8)	9235(13)	4788(8)
C(7)	658(8)	8307(14)	4173(7)
C(8)	806(7)	6881(15)	4353(7)
C(9)	1294(8)	6521(12)	5131(7)
C(10)	1408(8)	5065(11)	5426(7)
C(11)	1613(8)	3955(12)	6775(7)
C(12)	2250(9)	3739(11)	7605(8)
C(13)	2364(9)	4987(11)	8200(8)
C(14)	3802(8)	5916(12)	8068(7)
C(15)	4008(8)	5546(12)	7284(7)
C(16)	4277(8)	7807(12)	6765(8)
C(17)	5028(8)	7431(13)	6379(9)
C(18)	4661(8)	6263(13)	5777(8)
C(19)	3712(8)	6106(13)	5815(8)

TABLE 5.4

Selected Bond Lengths (Å) and Angles (°) in $[Ni(L^{13})(OClO_3)](ClO_4)$

Ni-N(1)	2.034(9)	Ni-N(4)	2.134(9)
Ni-N(2)	2.114(9)	Ni-N(5)	2.159(10)
Ni-N(3)	1.961(8)	Ni-O(21)	2.393(8)
N(1)-Ni-N(2)	99.3(4)	N(1)-Ni-N(3)	169.5(4)
N(2)-Ni-N(3)	81.7(4)	N(1)-Ni-N(4)	97.8(3)
N(2)-Ni-N(4)	162.4(3)	N(3)-Ni-N(4)	80.8(4)
N(1)-Ni-N(5)	86.4(4)	N(4)-Ni-N(5)	89.4(3)
N(2)-Ni-N(5)	95.8(4)	N(3)-Ni-N(5)	103.9(4)
O(21)-Ni-N(1)	85.1(3)	O(21)-Ni-N(2)	86.2(4)
O(21)-Ni-N(3)	84.5(3)	O(21)-Ni-N(4)	91.1(3)
O(21)-Ni-N(5)	171.5(3)		

SECTION 7.1 PREPARATION OF L^{17}

Sodium metabisulphite (2.3 g, 12.1 mmol) was dissolved in water (10 cm^3) and added to 2.5 cm^3 of 37% aqueous formaldehyde. The solution was boiled for 1 h, then cooled to room temperature, and the macrocycle L^2 (1.5 g, 6.04 mmol) added with vigorous stirring. After 4 h, a solution of sodium cyanide (3.3 g, 67.3 mmol) in water (20 cm^3) was added. The mixture was left to stir overnight, whereupon a solid formed which was extracted with dichloromethane (5 x 50 cm^3). The combined extracts were dried with anhydrous $MgSO_4$, filtered and the solvent removed with a rotary evaporator to leave a viscous oil. This was kept under high vacuum to leave a white solid (1.92 g, 5.89 mmol) in 97% yield. M.p. 138-140°C; ^1H n.m.r. ($CDCl_3$): δ 1.50 (4H, pentet), 1.96 (3H, s), 2.25 (4H, t), 2.47 (4H, t), 3.80 (4H, s), 3.87 (4H, s), 7.20 (2H, d), 7.69 (1H, t), p.p.m. ^{13}C n.m.r. chemical shifts are given in Table 5.2 (p. 144). Electron impact mass spectrum: found, m/z 326, calc. for M^+ 326.

SECTION 7.2 ATTEMPTS AT THE PREPARATION OF METAL COMPLEXES OF L^{17}

(i) **Nickel(II) Complex:** A solution of $[Ni(DMSO)_6](ClO_4)_2$ (0.725 g, 1 mmol) in ethanol (20 cm^3) was added to L^{17} (0.326 g, 1 mmol) in ethanol 10 cm^3. A pale-blue precipitate formed immediately after the addition. The mixture was stirred at room temperature for 1 h, then filtered and washed with ethanol (3 x 10 cm^3) and diethyl ether (3 x 10 cm^3) to give the product (0.45 g).

(ii) Copper(II) Complex: This was prepared with the same method described for preparation of nickel(II) complex of L^{17}, using $[Cu(DMSO)_6](ClO_4)_2$ to give a blue precipitate of the copper(II) complex of L^{17} (0.57 g).

(iii) Zinc(II) Complex: A solution of $[Zn(DMSO)_4](ClO_4)_2$ (0.264 g, 0.46 mmol) in ethanol (10 cm^3) was added to a solution of L^{17} (0.15 g, 0.46 mmol) in ethanol (10 cm^3) under dinitrogen. The resulting solution was stirred at room temperature for 1 h, then dry diethyl ether (10 cm^3) was added dropwise to cause precipitation. The white solid which formed was then filtered under dinitrogen and washed with dry diethyl ether (3 x 20 cm^3) to give the product (0.271 g).

All complexes of L^{17} found to be a mixture of hydrolysed and unhydrolysed product.

SECTION 7.3 CONVERSION OF ONE CYANO GROUP TO AN AMIDO GROUP IN THE NICKEL(II) AND COPPER(II) COMPLEXES OF L^{17}

0.25 g of each complex was dissolved in H_2O (50 cm^3) and heated under reflux for 24 h. The solution of both complexes were concentrated to *ca.* 10 cm^3 with a rotary evaporator, and ethanol 15 cm^3 was added to cause precipitation. A blue copper(II) solid (0.2 g) and a mauve nickel(II) complex (0.15 g) formed and were isolated. In both complexes only one cyano group found to be hydrolysed. Microanalyses found for the Ni^{2+} complex: C, 39.3; H, 5.4; N, 15.1%. Calc. for $C_{18}H_{33}ClN_6NiO_8$: C, 39.5; H, 6.0; N, 15.4; found for Cu^{2+} complex: C, 34.2; H, 4.3; N, 13.1%. Calc. for $C_{18}H_{31}Cl_2CuN_6O_{10}$: C, 34.1; H, 4.9 and N, 13.2%.

SECTION 8.1 PREPARATION OF L^{19}

To bromo-ethanoic acid (1.12 g, 8.06 mmol) in H_2O (10 cm^3), NaOH (0.32 g, 8.06 mmol) in cold water (5 cm^3) was added in such a way that the temperature remained below 5°C. Then L^2 (1.0 g, 4.03 mmol) in EtOH (5 cm^3) was added. The mixture was stirred and the temperature was maintained at 65°C for 20 h. The reaction mixture was then cooled and filtered. The filtrate was concentrated to *ca.* 10 cm^3 and acidified to pH 3.7 with concentrated hydrochloric acid. The solution was left in a refrigerator overnight. A white solid formed. This was filtered and washed with cold ethanol (3 x 5 cm^3) to give the product (1.1 g, 53%).

SECTION 8.2 PREPARATION OF A COPPER(II) COMPLEX OF L^{19}

$L^{19}.4HCl$ (0.255 g) in water (75 cm^3) was treated with $CuSO_4.5H_2O$ (1.0 g) in water (75 cm^3). The mixture was warmed to 60°C for 1 h, filtered whilst hot, and the solution allowed to evaporate slowly for several days. During this time deep green crystals deposited, which were filtered and air dried, to give the product (0.11 g, 33% yield).

SECTION 8.3 CRYSTAL STUDY OF $[Cu(L^{19}H_2)Cl]Cl$

The copper(II) complex of L^{19} with formula of $C_{18}H_{28}Cl_2CuN_4O_4.4H_2O$, M = 570.9 crystallises as small green plates which are monoclinic, space group $P2_1/n$, with a = 14.695(9), b = 12.955(6), c = 13.831(6) Å, β = 91.84(4)°, U = 2632 $Å^3$, Z = 4, D_c = 1.44 g cm^{-3}, λ (Mo-K_α) = 0.71069 Å, μ = 11.0 cm^{-1} (no absorption correction). The crystals were poorly diffracting, and showed some

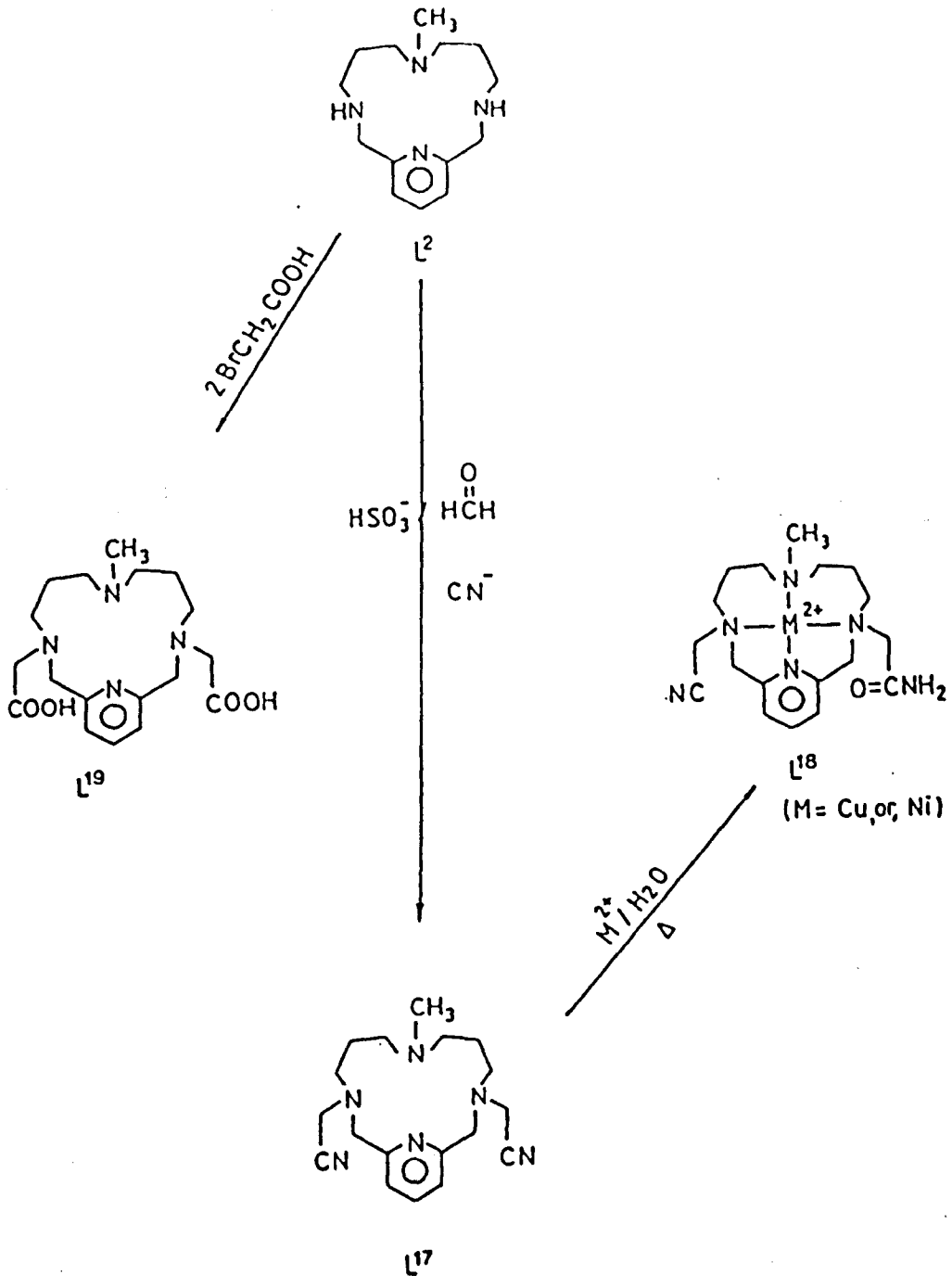
CH3
HN
NH
L2
2BrCH2COOH
HSO3-
O
HCH
CN-
COOH
COOH
L19
NC
O=CNH2
L18
(M= Cu, or, Ni)
M2+/H2O
Δ
CN
CN
L17

SCHEME 5.2

decay under x-ray irradiation. 3796 Reflections were collected with a Syntex $P2_1$ diffractometer [1102 with $I/\sigma(I) \geq 3.0$], and the structure solved by the heavy-atom method and refined to a final R value of 0.091 (anisotropic temperature factors were used for all non-hydrogen atoms apart from four solvent water molecules). The results of the structure analysis are shown in Figure 5.11 (p. 142). Final atomic co-ordinates are given in Table 5.5, and selected bond lengths and angles in Table 5.6.

TABLE 5.5

Atomic Coordinates (x 10^4) for
$[Cu(L^{19}H_2)Cl]Cl$

Atom	X	Y	Z
Cu	1475(2)	5994(2)	7215(3)
Cl(1)	1799(6)	7002(6)	8463(6)
Cl(2)	2369(6)	2621(6)	1272(7)
O(1)	-846(12)	6258(12)	9212(12)
O(2)	-333(14)	6423(14)	771(14)
O(3)	999(13)	7582(15)	6184(15)
O(4)	1654(13)	9123(13)	6202(18)
O(5)	3176(19)	4914(21)	1479(20)
O(6)	3837(21)	5103(24)	3606(22)
O(7)	4413(24)	5852(29)	-61(27)
O(8)	4454(29)	7293(35)	4264(30)
N(1)	3639(19)	3436(18)	8005(22)
N(2)	606(13)	4766(15)	7922(13)
N(3)	1209(13)	5071(14)	6133(13)
N(4)	2556(13)	6490(15)	6343(15)
C(1)	4444(22)	2667(31)	8197(32)
C(2)	3119(23)	3565(25)	6672(24)
C(3)	2300(17)	4266(20)	8661(20)
C(4)	1516(17)	3950(23)	6212(19)
C(5)	196(16)	4261(17)	7192(17)
C(6)	600(16)	4327(17)	6222(17)
C(7)	398(16)	3707(17)	3430(16)
C(8)	873(16)	3835(20)	4603(16)
C(9)	1526(19)	4554(20)	4545(20)
C(10)	1678(16)	5196(17)	5316(20)
C(11)	2375(20)	6064(22)	5328(22)
C(12)	3428(19)	6061(20)	6752(20)
C(13)	3387(21)	4901(19)	6865(22)
C(14)	4027(21)	4495(25)	7691(30)
C(15)	341(16)	5128(20)	8763(17)
C(16)	-350(20)	6010(24)	8476(22)
C(17)	2601(18)	7645(18)	6328(19)
C(18)	1665(17)	8111(22)	6164(21)

TABLE 5.6

Selected Bond Lengths (Å) and Angles (°) in $[Cu(L^{19}H_2)Cl]Cl$

Cu-N(3)	1.95(2)	Cu-N(2)	2.13(2)
Cu-N(4)	2.12(2)	Cu-Cl(1)	2.20(1)
Cu-O(3)	2.59(2)		
Cl(1)-Cu-O(3)	90.5(5)	Cl(1)-Cu-N(2)	100.2(6)
O(3)-Cu-N(2)	136.2(7)	Cl(1)-Cu-N(3)	178.6(6)
O(3)-Cu-N(3)	90.9(7)	N(2)-Cu-N(3)	78.9(8)
Cl(1)-Cu-N(4)	97.0(6)	O(3)-Cu-N(4)	69.2(7)
N(2)-Cu-N(4)	146.6(8)	N(3)-Cu-N(4)	83.3(8)

CHAPTER VI

CONCLUSIONS AND POSSIBLE EXTENSIONS OF THIS RESEARCH

The results reported in previous chapters have led to the following conclusions and suggestions for possible future extensions of this work.

(i) A square-pyramidal geometry is found for the $[Ni(L)X]^{n+}$ complexes (L = L^1 and L^3; X = unidentate ligand) as shown by the crystal structure in Chapter II and two related reports.[115,117]

These paramagnetic square-pyramidal nickel(II) complexes have an uncommon geometry, at which it would be worthwhile studying exchange of the unidentate ligands X by n.m.r., and the equilibrium constants for their formation from square-planar complexes by spectroscopic techniques, in a way similar to those reported previously.[182-184]

(ii) The work reported in Chapter IV revealed how the macrocycle L^{10} can coordinate to two metal ions at the same time in both homo- and heterobimetallic systems. Further work is needed to establish the geometry of the metal complexes reported, preferably by means of an x-ray crystal structure of one of them. This ligand could also be functionalised further by attacking the secondary amine groups to generate octahedral environments around each coordinated metal ion such as in Figure 6.1.

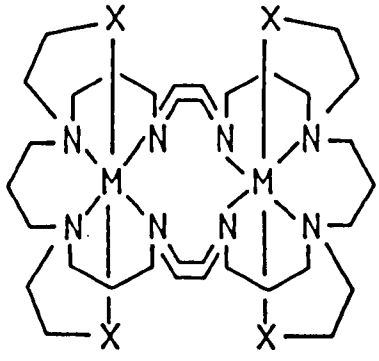

FIGURE 6.1

X = any coordinating group

(iii) The synthetic study of pentaazamacrocycles and their metal complexes reported in Chapter III have shown some interestingly different geometries with several metals. A worthwhile extension to this work would be the further functionalisation of ligand L^6, which has two secondary amine groups available for the addition two pendent co-ordinating arms. This would generate hepta- or hexadentate macrocycles. Possible synthetic routes as shown in Scheme 6.1, including bridge-head macrocycles analogous to those recently reported.[71]

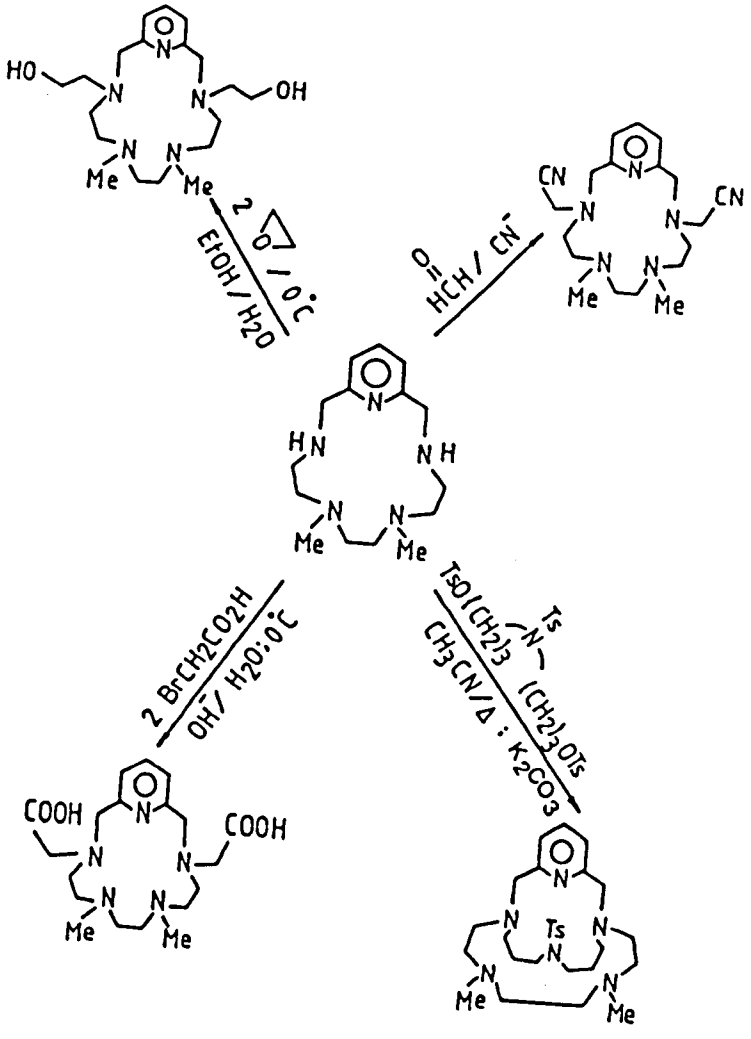

SCHEME 6.1

(iv) The pendent-arm macrocycles in Chapter V have been shown to combine the interesting properties of an inert macrocyclic ring and a labile pendent group. When the pendent-arm terminates in a basic functional group (e.g. an amine) variations in pH can then be used to bring about a rapid transformation of the metal ion geometry and coordination number as shown for the nickel(II) and copper(II) complexes of L^{13}. Extension to Co^{2+}, Mn^{2+} and Fe^{2+} systems will be worthwhile if cases can be found in which activity towards dioxygen occurs. The possibility of synthesising a pH-dependent reversible O_2 carrier exists, viz.:

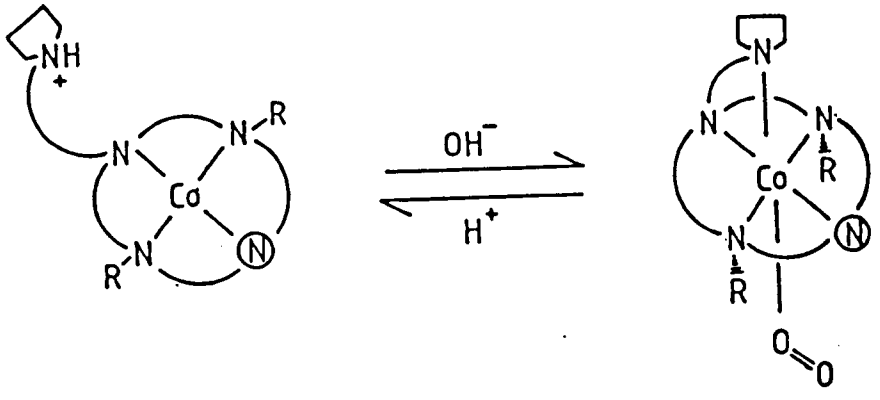

Ⓝ Represents the pyridine nitrogen

Preliminary results indicate that the Co^{2+} complex of L^{13} is O_2 active, but the reaction products have yet to be characterised.

The formation of μ-peroxy-bridged dicobalt(III) dimers is also possible, but could be prevented by adding bulky groups (R) to the pendent-arm macrocycle such that these bulky groups flank the coordinated superoxo-group. Unfortunately, the crystal structure of the $[Ni(L^{13})OClO_3]^+$ ion shows that the N-H groups point towards the coordinated pendent-arm rather than the site occupied by coordinated perchlorate, but this geometry is unlikely if bulky R-groups are added due to steric hindrance from the bulky pendent-arm. Although direct alkylation of the secondary amine groups of L^{13} is difficult using alkyl halides due to quaternisation of the tertiary amine groups, reaction with acid chlorides is possible as shown in the work of J. M. Lehn and coworkers.[185]

CHAPTER VII

EXPERIMENTAL TECHNIQUES

SECTION 1 INSTRUMENTATION AND MEASUREMENTS

^{1}H Decoupled, natural abundance, ^{13}C n.m.r. spectra were obtained either at 45.28 MHz with a Bruker WH180 Fourier transform spectrometer (10 mm diameter n.m.r. tube) or at 100.6 MHz using a Bruker WH400 Fourier transform spectrometer (5 mm diameter n.m.r. tube). 1.5 cm^3 of solution is required for the 10 mm tubes, and 0.5 cm^3 for the 5 mm tubes. A vortex suppression plug made of Teflon was used in the 10 mm tubes. Sample concentrations were generally in the range of 0.1-1.0 mol dm^{-3} in deuterated solvents. Routine ^{1}H n.m.r. spectra of free ligands and diamagnetic complexes were recorded with a Perkin Elmer (Model R34) 220 MHz continuous-wave spectrometer using 0.5 cm^3 of solution in 5 mm diameter sample tubes. Infrared spectra were recorded using a Perkin Elmer (Model 580B) infrared spectrometer, equipped with an internal reference. Nujol mulls, thin liquid films or thin solid films were used with cesium iodide plates. The thin solid films were prepared by making a concentrated solution of the compound in an analytical reagent grade solvent such as $CHCl_3$ and a few drops applied carefully to the cesium iodide plates, and the solvent evaporated under stream of dry dinitrogen. Electronic absorption spectra were recorded with a Schimadzu (Model 365) spectrometer in 1 cm quartz cells. Mass spectra were recorded using a Kratos (MS80) instrument fitted with a fast atom bombardment (f.a.b.) attachment. The latter was used for obtaining mass spectra of metal complexes. Samples for mass spectra were prepared by dissolving a few milligrams of metal complex in a matrix of *erythro*-1,4-dimercapto-2,3-butanediol and *threo*-1,4-dimercapto-2,3-butane diol which was prepared by mixing the two chemicals in ratio of 1:5 respectively at 35°C. Mass spectra were

simulated with a Hewlett Packard 9845B minicomputer.

SECTION 2 MAGNETIC SUSCEPTIBILITY MEASUREMENTS

Magnetic moments of paramagnetic metal complexes were obtained in solution at room temperature by the Evans n.m.r. method[120] or powder samples of the complexes were studied with a Johnson-Matthey (Evans method) magnetic susceptibility torsion balance. In the solution Evans n.m.r. method the chemical shifts of the proton resonances of inert reference molecules caused by the presence of dissolved paramagnetic substances are given by the expression:

$$\frac{\Delta H}{H} = \frac{2\pi}{3} \Delta K$$

ΔK is the change in volume susceptibility. For $^2[H]_3$-nitromethane solutions of complexes discussed in Chapters II and V about 2% of t-butanol was used as the internal reference and 2% of t-butanol solution in $^2[H]_3$-nitromethane was used as an external reference in a capillary (Wilmad) tube placed co-axially inside the 5 mm diameter n.m.r. tube. Two resonances were observed for the methyl protons of the t-butanol because of the difference in volume susceptibilities of the two solutions with the resonance for the paramagnetic solution at the higher frequency. The corrected molar susceptibility of the dissolved substance χ_M' is given by the expression[186]

$$\chi_M' = \frac{3\Delta HM}{2\pi Hm} + \chi_0 M + \frac{M.\chi_0(d_0-d_s)}{m} + DC$$

where

$\frac{\Delta H}{H}$ = shift separation in p.p.m. of the two resonances.

M = molecular weight of the complex

m = mass of complex in 1 cm^3 of solution

χ_0 = mass susceptibility of the solvent (-0.72×10^{-6} for dil. t-butanol)

d_0 = density of the solvent

d_s = density of the solution

DC = diamagnetic correction for the complex (calculated using Pascal's constants reported in reference 187; it was assumed that there was no temperature independent paramagnetism)

The density term (d_0-d_s) is often neglected without serious error. Values of χ'_M calculated from the previous equation may be related to the magnetic moment of the paramagnetic ion μ_{eff} by the equation:

$$\mu_{eff} = 2.828\ (\chi'_M.T)^{1/2} \text{ Bohr Magnetons}$$

where T is the absolute temperature of the measurement. In studies of solid samples (Chapter III and IV) the following equation was used to calculate χ_g.

$$\chi_g = \frac{Cl(R-R_0)}{m\ 10^9}$$

l = length of sample in glass tube in cm (in range 1.5-2.5 cm)

m = mass of sample in grammes (in range 0.1-0.3 g)

c = calibration constant for the instrument

R = reading from balance obtained for tube plus sample

R_0 = empty tube reading

$$\chi_v = \chi_g \times MWt$$

MWt = molecular weight

The χ_v values were corrected by addition of Pascal's constants from reference 187 and μ_{eff} was calculated in a similar way as described for the n.m.r. method.

REFERENCES

1. N. F. Curtis, *J. Chem. Soc.*, 1960, 4409
2. M. C. Thompson and D. H. Busch, *J. Am. Chem. Soc.*, 1964, 86, 3651
3. C. J. Pedersen, *J. Am. Chem. Soc.*, 1967, 89, 2495
4. B. Dietrich, J. M. Lehn, and J. P. Sauvage, *Tetrahedron Lett.*, 1969, 2885, and 2889
5. J. J. Christensen, D. J. Eatough, and R. M. Izatt, *Chem. Rev.*, 1974, 74, 351
6. L. F. Lindoy, *Chem. Soc. Rev.*, 1975, 4, 421
7. G. A. Melson, "Coordination Chemistry of Macrocyclic Compounds", Plenum Press, New York, 1979
8. J. S. Bradshaw, G. E. Maas, R. M. Izatt, and J. J. Christensen, *Chem. Rev.*, 1979, 79, 37
9. T. A. Kaden, *Top. Curr. Chem.*, 1984, 121, 157
10. R. M. Izatt, J. S. Bradshaw, S. A. Nielsen, J. D. Lamb, and J. J. Christensen, *Chem. Rev.*, 1985, 85, 271
11. D. C. Olson and J. Vasilevskis, *Inorg. Chem.*, 1969, 8, 1611
12. D. C. Olson and J. Vasilevskis, *Inorg. Chem.*, 1971, 10, 463
13. A. I. Popov and J. M. Lehn, "Coordination Chemistry of Macrocyclic Compounds", ed. G. A. Melson, Plenum Press,New York, 1979, Ch. 9, p.560
14. C. J. Pedersen, *Org. Synth.*, 1972, 52, 66
15. M. Di Casa, L. Fabbrizzi, A. Perotti, A. Poggi, and P. Tundo, *Inorg. Chem.*, 1985, 24, 1610
16. N. Herron, "Lecture at the Annual Chemical Congress of the Royal Society of Chemistry at Warwick University", April 1986

17. H. K. Frensdorff, *J. Am. Chem. Soc.*, 1971, 93, 600

18. M. A. Bush and M. R. Truter, *J. Chem. Soc., Perkin II*, 1972, 345

19. R. M. Izatt, D.J.Eatough and J. J. Christensen, *Structure and Bonding*, 1973, 16, 161

20. M. R. Truter, *Structure and Bonding*, 1973, 16, 71

21. K. Henrick, P. A. Tasker, and L. F. Lindoy, *Prog. in Inorg. Chem.*, 1985, 33, 1

22. L. Y. Martin, L. J. DeHayes, L. J. Zompa and D. H. Busch, *J. Am. Chem. Soc.*, 1974, 96, 4047

23. V. J. Thöm, C. C. Fox, J. C. A. Boeyens, and R. D. Hancock, *J. Am. Chem. Soc.*, 1984, 106, 5947

24. V. J. Thöm and R. D. Hancock, *J. Chem. Soc., Dalton Trans.*, 1985, 1877

25. V. J. Thöm, G. D. Hosken, and R. D. Hancock, *Inorg. Chem.*, 1985, 24, 3378

26. R. D. Hancock, *Pure & Appl. Chem.*, 1986, 58, 1445

27. K. Henrick, L. F. Lindoy, M. McPartlin, P. A. Tasker, and M. P. Wood, *J. Am. Chem. Soc.*, 1984, 106, 1641

28. R. G. Pearson, *J. Am. Chem. Soc.*, 1963, 85, 3533

29. J. D. Lamb, R. M. Izatt, J. J. Christensen, and D. J. Eatough, "Coordination Chemistry of Macrocyclic Compounds", Ed. G. A. Melson, Plenum Press, New York, 1979, Ch.3, p.158

30. D. K. Cabbiness, D. W. Margerum, *J. Am. Chem. Soc.*, 1969, 91, 6540

31. F. P. Hinz, D. W. Margerum, *Inorg. Chem.*, 1974, 13, 2941

32. G. F. Smith, D. W. Margerum, *J. Chem. Soc., Chem. Commun.*, 1975, 807

33. A. Dei, and R. Gori, *Inorg. Chim. Acta*, 1975, 14, 157

34. M. Kodama and E. Kimura, *J. Chem. Soc., Dalton Trans*, 1976, 116

35. A. Anichini, L. Fabbrizzi, P. Paoletti, and R. M. Clay, *Inorg. Chim. Acta*, 1977, 22, L25-L27

36. L. Fabbrizzi, P. Paoletti, and A. B. P. Lever, *Inorg. Chem.*, 1976, 15, 1502

37. A. Anichini, L. Fabbrizzi, P. Paoletti, and R. M. Clay, *J. Chem. Soc., Dalton Trans.*, 1978, 577

38. R. Barbucci, L. Fabbrizzi, P. Paoletti, and A. Vacca, *J. Chem. Soc., Dalton Trans.*, 1973, 1763

39. M. Kodama and E. Kimura, *J. Chem. Soc., Chem. Commun.*, 1975, 891

40. M. Kodama and E. Kimura, *J. Chem. Soc., Dalton Trans.*, 1977, 1473

41. P. K. Chan and C. K. Poon, *J. Chem. Soc., Dalton Trans*, 1976, 858

42. L. Fabbrizzi, A. Lari, A. Poggi and B. Seghi, *Inorg. Chem.*, 1982, 21, 2083

43. F. V. Lovecchio, E. S. Gore and D. H. Busch, *J. Am. Chem. Soc.*, 1974, 96, 3109

44. K. Nag and A. Chakravorty, *Coord. Chem. Rev.*, 1980, 33, 87

45. R. I. Haines and A. McAuley, *Coord. Chem. Rev.*, 1982, 39, 77

46. L. Fabbrizzi, *Inorg. Chim. Acta*, 1979, 36, L391

47. E. Suet, A. Laouenan, H. Handel and R. Guglielmetti, *Helv. Chim. Acta*, 1984, 67, 441

48. C. O. Dietrich-Buchecker, J. M. Kern, and J. P. Sauvage, *J. Chem. Soc., Chem. Commun.*, 1985, 760

49. G. R. Newkome, J. D. Sauer, J. M. Roper and D. C. Hager, *Chem. Rev.*, 1977, 77, 513

50. J. E. Richman and T. J. Atkins, *J. Am. Chem. Soc.*, 1974, 96, 2268

51. N. W. Alcock, H. A. A. Omar, P. Moore, and C. Pierpoint, *J. Chem. Soc., Dalton Trans.*, 1985, 219

52. N. W. Alcock, E. H. Curzon, P. Moore, H. A. A. Omar, and C. Pierpoint, *J. Chem. Soc., Dalton Trans.*, 1985, 1361

53. P. M. May, R. A. Bulman, *Prog. Med. Chem.*, 1983, 20, 226

54. A. L. Hammond, *Science*, 1971, 171, 788

55. I. Tabushi, H. Okino and Y. Koruda, *Tetrahedron Lett.*, 1976, 4339

56. I. Tabushi, Y. Taniguchi and H. Kato, *Tetrahedron Lett.*, 1977, 1049

57. N. F. Curtis, *Coord. Chem. Rev.*, 1968, 3, 3

58. E. K. Barefield, F. Wagner, A. W. Herlinger and A. R. Dahl, *Inorg. Synthesis*, 1976, 16, 220

59 M. G. B. Drew, A. H. Bin-Othman, S. G. McFall and S. M. Nelson, *J. Chem. Soc., Chem. Commun.*, 1975, 818

60. S. M. Nelson, *Pure & Appl. Chem.*, 1980, 52, 2461

61. L. Fabbrizzi, L. Montagna, A. Paggi, T. A. Kaden, and L. C. Siegfried, *Inorg. Chem.*, 1986, 25, 2671

62. C. J. Pedersen, *J. Am. Chem. Soc.*, 1967, 89, 7017

63. J. M. Lehn, *Acc. Chem. Rec.*, 1978, 11, 49

64. C. R. Paige and M. F. Richardson, *Canad. J. Chem.*, 1984, 62, 332

65. G. W. Gokel and H. D. Durst, *Synthesis*, 1976, 168

66. M. Dobler and R. P. Phizackerley, *Helv. Chim. Acta*, 1974, 57, 664

67. J. M. Lehn, *Structure and Bonding*, 1973, 16, 1

68. G. W. Gokel, D. J. Cram, C. L. Liotta, H. P. Harris and F. L. Cook, *J. Org. Chem.*, 1974, 39, 2445

69. J. M. Lehn and J. P. Sauvage, *J. Chem. Soc., Chem. Commun.*, 1971, 440

70. A. M. Sargeson, *Pure & Appl. Chem.*, 1984, 56, 1603

71. M. Ciampolini, M. Micheloni, F. Vissa, F. Zanobini, S. Chimichi and P. Dapporto, *J. Chem. Soc., Dalton Trans.*, 1986, 505 and

A. Bianchi, E. G. Espana, M. Micheloni, N. Nardi, and F. Vissa, *Inorg. Chem.*, 1986, 25, 4379

72. S. N. Rosenthal and J. H. Fendler, *Adv. Phys. Org. Chem.*, 1976, 13, 279

73. N. W. Alcock, N. Herron and P. Moore, *J. Chem. Soc., Chem. Commun.*, 1976, 886

74. R. E. Desimone and M. D. Glick, *J. Coord. Chem.*, 1976, 5, 181

75. P. H. Davis, L. K. White and R. L. Belford, *Inorg. Chem.*, 1975, 14, 1753

76. P. M. Colman, H. C. Freeman, J. M. Guss, M. Murata, V. A. Norris, J. A. M. Ramshaw and M. P. Venkatappa, *Nature (London)*, 1978, 272, 319

77. U. Sakaguchi and A. W. Addison, *J. Chem. Soc., Dalton Trans.*, 1979, 600

78. D. Sevdic and H. Meider, *J. Inorg. Nucl. Chem.*, 1981, 43, 153

79. R. O. Gould, A. J. Lavery and M. Schröder, *J. Chem. Soc., Chem. Commun.*, 1985, 1492

80. K. Wieghardt, H. J. Küppers, E. Raabe and C. Krüger, *Angew Chem. Int. Ed. Engl.*, 1986, 25, 1101

81. W. N. Setzer, C. A. Ogle, G. S. Wilson, R. S. Glass, *Inorg. Chem.*, 1983, 22, 266

82. D. Sellmann, L. Zapf, *Angew Chem. Int. Ed. Engl.*, 1984, 23, 807

83. D. Sellmann and P. Frank, *Angew Chem. Int. Ed. Engl.*, 1986, 25, 1107

84. E. Weber and F. Vögtle, *Liebigs Ann. Chem.*, 1976, 891

85. D. Parker, J. M. Lehn and J. Rimmer, *J. Chem. Soc., Dalton Trans.*, 1985, 1517

86. C. A. McAuliffe, *Adv. Inorg. Chem., Radio Chem.*, 1975, 17, 165

87. S. G. Murray and F. R. Hartley, *Chem. Rev.*, 1981, 81, 365

88. J. R. Nappier and D. W. Week, *J. Chem. Soc., Chem. Commun.*, 1974, 442

89. M. Ciampolini, P. Dapporto, N. Nardi and F. Zanobini, *Inorg. Chem.*, 1983, 22, 13

90. M. Ciampolini, N. Nardi, P. Dapporto, P. Innocenti, and F. Zanobini, *J. Chem. Soc., Dalton Trans.*, 1984, 575 and 995

91. S. Mangani, P. Orioli, M. Ciampolini, N. Nardi, and F. Zanobini, *Inorg. Chim. Acta*, 1984, 85, 65

92. E. P. Kyba, R. E. Davis, S. T. Liu, K. A. Hassett, and S. B. Larson, *Inorg. Chem.*, 1985, 24, 4629

93. C. W. G. Ansell, M. K. Cooper, K. P. Dancey, P. A. Duckworth, K. Henrick, M. McPartlin, G. Organ and P. A. Tasker, *J. Chem. Soc., Chem. Commun.*, 1985, 437; and 439

94. M. Ciampolini, *Pure & Appl. Chem.*, 1986, 58, 1429

95. D. J. Brauer, F.Gol, S. Hietkamp, H. Peters, H. Sommer, O. Stelzer, and W. S. Sheldrick, *Chem. Ber.*, 1986, 119,349

96. E. P. Kyba, C. W. Hudson, M. J. McPhaul, and A. M. John, *J. Am. Chem. Soc.*, 1977, 99, 8053

97. E. P. Kyba and S. T. Liu, *Inorg. Chem.*, 1985, 24, 1613

98. T. A. DelDonno and W. Rosen, *J. Am. Chem. Soc.*, 1977, 99, 8051

99. J. O. Cabral, M. F. Cabral, M. G. B. Drew, S. M. Nelson, and A. Rodgers, *Inorg. Chim. Acta*, 1977, 25, L77

100. G. A. Barclay and A. K. Barnard, *J. Chem. Soc.*, 1961, 4269

101. D. St. C. Black and A. J. Hartshorn, *Coord. Chem. Rev.*, 1972, 9, 219

102. A. L. Balch, L. A. Fossett, M. M. Olmstead, D. E. Oram, and P. E. Reedy, Jr., *J. Am. Chem. Soc.*, 1985, 107, 5272

103. V. S. Gamayurova, N. V. Shabrukova, R. Z. Musin, I. Kh. Shakirov, and R. R. Shagidullin, *Chem. Abst.*, 1986, 105, 191283p

104. Th. Kauffmann and J. Ennen, *Chem. Ber.*, 1985, 118, 2692, 2703 and 2714

105. L. F. Lindoy and D. H. Busch, *Preparative Inorg. React.*, Ed. W. L. Jolly, Interscience, New York, 1971, Vol.6, p.25

106. J. L. Karn and D. H. Busch, *Nature*, 1966, 211, 160

107. J. L. Karn and D. H. Busch, *Inorg. Chem.*, 1969, 8, 1149

108. R. L. Rich and G. L. Stucky, *Inorg. Nucl. Chem. Lett.*, 1965, 1, 61

109. R. Dewar and E. Fleischer, *Nature*, 1969, 222, 372

110. E. B. Fleischer and S. W. Hawkinson, *Inorg. Chem.*, 1968, 7, 2312

111. E. Ochiai and D. H. Busch, *Inorg. Chem.*, 1969, 8, 1474

112. C.-M. Che, S.-T. Mak, and T. C. W. Mak, *Inorg. Chem.*, 1986, 25, 4705

113. N. W. Alcock, P. Moore, and H. A. A. Omar, *J. Chem. Soc., Dalton Trans.*, 1986, 985; H. A. A. Omar, M.Sc. Thesis, University of Warwick, 1984.

114. H. T. Clarke, H. B. Gillespie and S. Z. Weisshaus, *J. Am. Chem. Soc.*, 1933, 55, 4571

115. K. A. Foster, E. K. Barefield, and D. G. Vanderveer, *J. Chem. Soc., Chem. Commun.*, 1986, 680

116. P. Moore, J. Sachinidis, and G. R. Willey, *J. Chem. Soc., Chem. Commun.*, 1983, 522; S. F. Lincoln, J. H. Coates, D. A. Hadi and D. L. Pisaniello, *Inorg. Chim. Acta*, 1984, 81, L9-L10; T. W. Hambley, *J. Chem. Soc., Chem. Commun.*, 1984, 1228

117. N. W. Alcock, K. P. Balakrishnan, P. Moore, and G. A. Pike, *J. Chem. Soc., Dalton Trans.*, 1987, 889

118. A. R. Davis, F. W. B. Einstein, and A. C. Willis, *Acta Cryst.*, 1982, B38, 443

119. E. K. Barefield, *Inorg. Chem.*, 1980, 19, 3186

120. D. F. Evans, *J. Chem. Soc.*, 1959, 2003

121. J. Selbin, W. E. Bull, and L. H. Holmes, *J. Inorg. Nucl. Chem.*, 1961, 16, 219

122. R. Mozingo, "Organic Syntheses", ed. E. C. Horning, Wiley, New York, 1955, Coll. Vol. 3, p.181

123. G. M. Sheldrick, SHELXTL, User Manual, Nicolet Instruments Co., Madison, Wisconsin, 1983

124. International Tables for X-ray Crystallography, Kynoch Press, Birmingham, 1974, Vol. 4

125. C. Cairns, S. G. McFall, S. M. Nelson and M. G. B. Drew, , *J. Chem. Soc., Dalton Trans.*, 1979, 446

126. S. M. Nelson, S. G. McFall, M. G. B. Drew, A. H. Binothman, and N. B. Mason, *J. Chem. Soc., Chem. Commun.*, 1977, 167

127. M. G. B. Drew, A. H. Binothman, S. G. McFall, P. D. A. McIlroy and S. M. Nelson, *J. Chem. Soc., Dalton Trans.*, 1977, 1173

128. M. G. B. Drew, A. Rodgers, M. McCann, and S. M. Nelson, *J. Chem. Soc., Chem. Commun.*, 1978, 415

129. M. D. Alexander, A. Van Heuvelen, and H. G. Hamilton, *Inorg. Nucl. Chem. Lett.*, 1970, 6, 445

130. M. C. Rakowski, M. Rycheck and D. H. Busch, *Inorg. Chem.*, 1975, 14, 1194

131. E. Kimura, M. Kodama, R. Machida and K. Ishizu, *Inorg. Chem.*, 1982, 21, 595

132. B. J. Hathaway and A. A. G. Tomlinson, *Coord. Chem. Rev.*, 1970, 5, 1

133. M. Kodama and E. Kimura, *J. Chem. Soc., Dalton Trans.*, 1979, 325

134. R. W. Hay, R. Bembi, and B. Jeragh, *Transition Met. Chem.*, 1986, 11, 385

135. S. M. Nelson, P. D. A. McIlroy, C. S. Stevenson, E. Konig, G. Ritter, and J. Waigel, *J. Chem. Soc., Dalton*

Trans., 1986, 991

136. M. G. B. Drew, S. Hollis and P. C. Yates, *J. Chem. Soc., Dalton Trans*, 1985, 1829

137. U. Casellato, P. A. Vigato, and M. Vidali, *Coord. Chem. Rev.*, 1977, 23, 31

138. U. Casellato, P. A. Vigato, D. E. Fenton and M. Vidali, *Chem. Soc. Rev.*, 1979, 8, 199

139. V. A. Kogan, V. V. Zelentsov, O. A. Osipov, and A. S. Burlov, *Russ. Chem. Rev.*, 1979, 48, 645

140. S. M. Nelson, *Inorg. Chim. Acta*, 1982, 62, 39

141. D. E. Fenton, U. Casellato, P. A. Vigato, and M. Vidali, *Inorg. Chim. Acta*, 1982, 62, 57

142. D. E. Fenton, *Pure & Appl. Chem.*, 1986, 58, 1437

143. D. E. Fenton, "Advances in Inorganic and Bio-inorganic Mechanisms", Academic Press, London, 1983, p.187

144. P. Zanello, S. Tamburini, P. A. Vigato and G. A. Mazzocchin, *Co-ord. Chem. Rev.*, 1987, 77, 165

145. M. Hancock, "Conformation Theory; Organic Chemistry a Series of Monographs", ed. A. T. Blomquist, Academic Press, New York and London, 1965, Vol. 3, p.306

146. M. Davis and O. Hassel, *Acta Chem. Scand.*, 1963, 17, 1181

147. J. Bjerrum, C. J. Ballhausen, and C. K. Jørgensen, *Acta. Chem. Scand.*, 1954, 8, 1275

148. A. B. P. Lever, "Inorganic Electronic Spectroscopy", 2nd Edn., Elsevier, Amsterdam, 1984, p. 507

149. K. Nakamoto, "Infrared and Raman Spectra of Inorganic and Coordination Compounds", 3rd Edn., Wiley, New York, 1978, p.345

150. M. Ciampolini, *Structure and Bonding*, 1969, 6, 52

151. H. Okawa, T. Tokii, Y. Muto and S. Kida, *Bull. Chem. Soc. Jpn.*, 1973, 46, 2464

152. M. Mikuriya, S. Kida, and I. Murase, *J. Chem. Soc., Dalton Trans.*, 1987, 1261

153. M. D. Glick, R. L. Lintvedt, T. J. Anderson, and J. L. Mack, *Inorg. Chem.*, 1976, 15, 2258

154. M. Tanaka, M. Kitaoka, H. Okawa, and S. Kida, *Bull. Chem. Soc. Jpn.*, 1976, 49, 2469

155. M. G. B. Drew, M. McCann and S. M. Nelson, *J. Chem. Soc., Dalton Trans.*, 1981, 1868

156. E. R. Nelson, M. Maienthal, L. A. Lane, and A. A. Benderly, *J. Am. Chem. Soc.*, 1957, 79, 3467

157. T. J. Lotz and T. A. Kaden, *J. Chem. Soc., Chem. Commun.*, 1977, 15 and *Helv. Chim. Acta*, 1978, 61, 1376

158. T. A. Kaden, "Proceedings of the 21st International Conference on Co-ordination Chemistry", Calcutta, 1981, p.71

159. M. Hediger and T. A. Kaden, *Helv. Chim. Acta*, 1983, 66, 861

160. D. E. Fenton, and G. Rossi, *Inorg. Chim. Acta*, 1985, 98, L29

161. N. W. Alcock, R. G. Kingston, P. Moore and C. Pierpoint, *J. Chem. Soc., Dalton Trans.*, 1984, 1937

162. N. W. Alcock, P. Moore and C. Pierpoint, *J. Chem. Soc., Dalton Trans.*, 1984, 2371

163. P. S. Pallavicini, A. Perotti, A. Poggi, B. Seghi, and L. Fabbrizzi, *J. Am. Chem. Soc.*, 1987, 109, 5139

164. K. P. Wainwright, *J. Chem. Soc., Dalton Trans.*, 1980, 2117

165. G. M. Freeman, E. K. Barefield, and D. G. Vanderveer, *Inorg. Chem.*, 1984, 23, 3092

166. E. K. Barefield, K. A. Foster, G. M. Freeman, and K. D. Hodges, *Inorg. Chem.*, 1986, 25, 4663

167. N. W. Alcock, K. P. Balakrishnan, P. Moore, *J. Chem. Soc., Chem. Commun.*, 1985, 1731

168. E. Kimura, T. Koike, H. Nada, and Y. Iitaka, *J. Chem. Soc., Chem. Commun.*, 1986, 1322

169. C. M. Madeyski, J. P. Michael, and R. D. Hancock, *Inorg. Chem.*, 1984, 23, 1487

170. R. W. Hay and D. M. S. Clark, *Inorg. Chim. Acta*, 1984, 83, L23

171. E. Kimura, K. Uenishi, T. Koike and Y. Iitaka, *Chem. Letts.*, 1986, 1137

172. R. W. Hay, M. P. Pujari, K. Hideg, and O. H. Hankovszky, *Transition Met. Chem.*, 1985, 10, 188

173. H. Hope, M. Viggiano, B. Moezzi and P. P. Power, *Inorg. Chem.*, 1984, 23, 2550

174. A. Carroy, C. R. Langick, J. M. Lehn, K. E. Matthes, and D. Parker, *Helv. Chim. Acta*, 1986, 69, 580

175. H. Häfliger and T. A. Kaden, *Helv. Chim. Acta.*, 1979, 62, 683

176. X. Ji-De, N. S. Sheng, L. Y. Juan, *Inorg. Chim. Acta*, 1986, 111, 61

177. M. Studer and T. A. Kaden, *Helv. Chim. Acta*, 1986, 69, 2081

178. W. Schibler and T. A. Kaden, *J. Chem. Soc., Chem. Commun.*, 1981, 603

179. N. W. Alcock, N. Herron, and P. Moore, *J. Chem. Soc., Dalton Trans.*, 1978, 394

180. E. R. Dockal, L. L. Diaddario, M. D. Glick, and D. B. Rorabacher, *J. Am. Chem. Soc.*, 1977, 99, 4530

181. I. Murase, M. Mikuriya, H. Sonoda, and S. Kida, *J. Chem. Soc., Chem. Commun.*, 1984, 692

182. P. Moore, J. Sachinidis, and G. R. Willey, *J. Chem. Soc., Dalton Trans.*, 1984, 1323

183. N. Herron and P. Moore, *Inorg. Chim. Acta*, 1979, 36, 89

184. A. E. Merback, P. Moore, and K. E. Newman, *J. Magn. Reson.*, 1980, 41, 30

185. J. M. Lehn, *Pure & Appl. Chem.*, 1980, 52, 2441; P. G. Potvin and J. M. Lehn, "Progress in Macrocyclic Chemistry", Eds. R. M. Izatt and J. J. Christensen, Wiley, Interscience Publication, New York, 1987, Vol.3, p.167

186. W. L. Jolly, "The Synthesis and Characterisation of Inorganic Compounds", Prentice-Hall, London, 1970, p.382

187. J. Lewis and R. G. Wilkins, Ed. "Modern Coordination Chemistry", Interscience, New York, 1960, p.403

APPENDIX

(i) Final Temperature and Structure Factor Tables

Because of their length they have been omitted from this thesis but have been deposited with the published work.

(ii) Deconvolution of Visible Spectra of $[Cu(L^1)]^{2+}$ and $[Cu(L^4)]^{2+}$

In visible spectra, the bands have a Gaussian shape given by an equation of the following type:

$$Y = A\, e^{-c(x-x_0)^2} \qquad (1)$$

Y is the absorbance as a function of wavelength (x), A and c are constants, and x_0 is the wavelength at which the band is centred. For two overlapping bands, an equation of the following type is used:

$$Y = Y_1 + Y_2$$

Y_1 and Y_2 are given by equation (1), resulting in the following equation.

$$Y = A_1 e^{-c_1(x-x_{01})^2} + A_2 e^{-c_2(x-x_{02})^2} + A_3 \qquad (2)$$

The seven parameters in equation (2), x_{01}, x_{02}, c_1, c_2, A_1, A_2 and A_3 are found by non-linear least squares analysis. The two parameters required are x_{01} (λ_1) and x_{02} (λ_2). An iterative computer program (GAUSS2), written for an IBM-PC microcomputer was used to analyse the data.

A typical analysis for $[Cu(L^1)](ClO_4)_2$ is shown below using the data in Table 1.

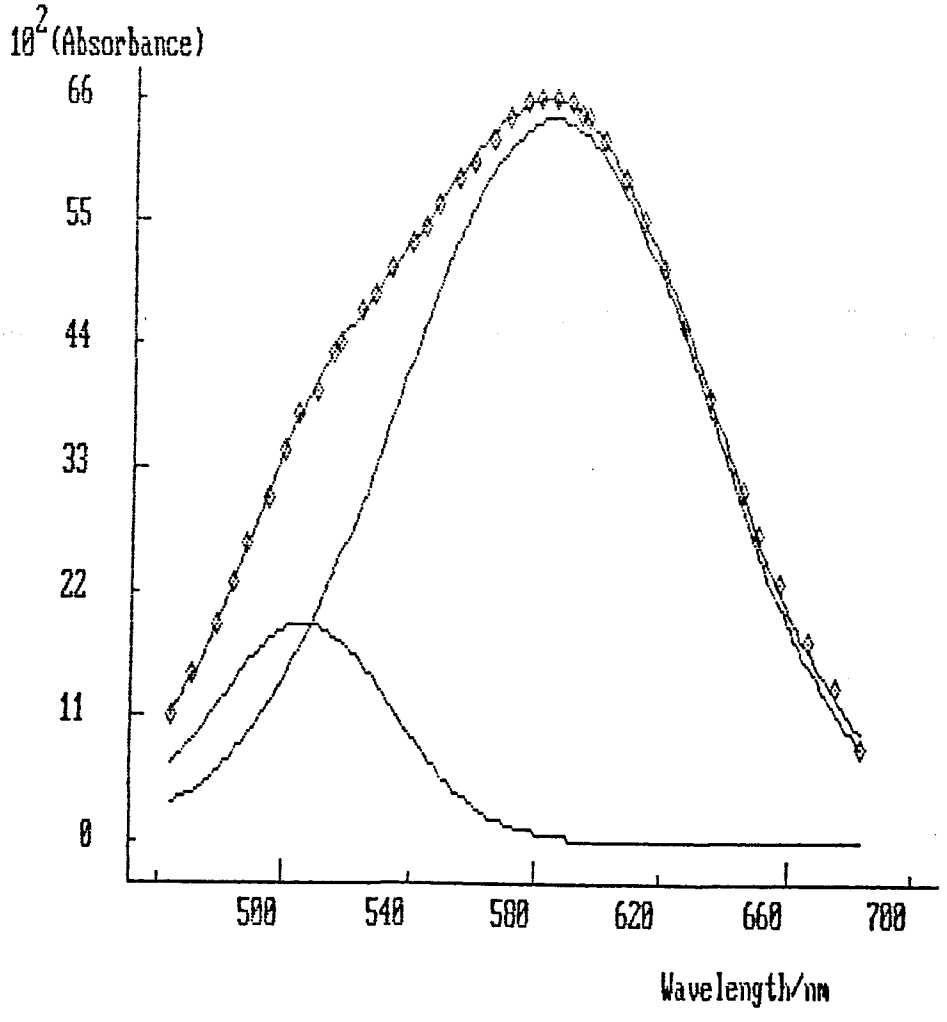

Index	Parameter	Standard Deviation
1	5.058124E+02	1.050871E+00
2	5.843115E+02	6.332439E-01
3	6.183826E-04	3.179951E-05
4	2.069904E-04	6.695812E-06
5	1.921851E-01	7.947898E-03
6	6.419528E-01	7.302914E-03
7	1.177125E-02	6.964693E-03

TABLE I

Number of observations = 39

Index	X	Y(Obs)	Y(calc)	Error
1	6.83800E+02	8.00000E 02	9.45137E 02	1.45137E 02
2	6.75000E+02	1.40000E 01	1.28768E 01	1.12324E 02
3	6.67000E+02	1.75000E 01	1.67675E 01	7.32452E-03
4	6.57300E+02	2.28000E 01	2.24882E 01	3.11799E-03
5	6.50200E+02	2.73000E 01	2.73134E 01	1.34319E-04
6	6.44900E+02	3.10000E 01	3.12036E 01	2.03580E-03
7	6.34300E+02	3.90000E-01	3.94488E 01	-4.48829E-03
8	6.26400E+02	4.53000E-01	4.56692E-01	-3.69233E-03
9	6.19300E+02	5.08000E-01	5.10096E-01	-2.09630E-03
10	6.13100E+02	5.52000E-01	5.52682E 01	-6.81937E-04
11	6.06900E+02	5.90000E-01	5.89728E 01	2.71976E-04
12	6.00800E+02	6.21000E-01	6.19322E-01	1.67841E-03
13	5.95500E+02	6.42000E-01	6.38632E-01	3.36754E-03
14	5.92800E+02	6.48000E-01	6.46005E-01	1.99461E-03
15	5.89300E+02	6.55000E-01	6.53007E-01	1.99300E-03
16	5.84900E+02	6.59000E-01	6.57695E-01	1.30486E-03
17	5.80400E+02	6.58000E-01	6.57855E-01	1.45018E-04
18	5.76000E+02	6.53000E-01	6.53745E-01	-7.44998E-04
19	5.70700E+02	6.43000E-01	6.43794E-01	-7.93755E-04
20	5.64500E+02	6.23000E-01	6.26474E-01	-3.47430E-03
21	5.58300E+02	6.03000E-01	6.04813E-01	-1.81299E-03
22	5.53900E+02	5.87000E-01	5.87871E-01	-8.71181E-04
23	5.47700E+02	5.63000E-01	5.63127E-01	-1.27196E-04
24	5.43300E+02	5.46000E-01	5.45582E-01	4.18186E-04
25	5.38900E+02	5.30000E-01	5.28339E-01	1.66088E-03
26	5.32700E+02	5.06000E-01	5.04543E-01	1.45733E-03
27	5.27400E+02	4.85000E-01	4.84191E-01	8.08775E-04
28	5.23000E+02	4.67000E-01	4.66704E-01	2.96414E-04
29	5.16800E+02	4.39000E-01	4.40039E-01	-1.03909E-03
30	5.15000E+02	4.31000E-01	4.31669E-01	-6.69330E-04
31	5.08900E+02	3.99000E-01	4.00651E-01	-1.65141E-03
32	5.04400E+02	3.79000E-01	3.74897E-01	4.10253E-03
33	5.00000E+02	3.45000E-01	3.47381E-01	-2.38103E-03
34	4.93800E+02	3.04000E-01	3.05326E-01	-1.32552E-03
35	4.87700E+02	2.61000E-01	2.61660E-01	-6.60419E-04
36	4.83200E+02	2.30000E-01	2.29209E-01	7.91401E-04
37	4.77900E+02	1.93000E-01	1.92081E-01	9.18955E-04
38	4.70900E+02	1.48000E-01	1.47013E-01	9.87053E-04
39	4.64700E+02	1.12000E-01	1.12566E-01	-5.65946E-04

X = Wavelength

Y = Absorbance

The same method was used for computing simulation of data collected for $[Cu(L^4)](ClO_4)_2$. The data are shown in Table 2.

TABLE 2

Number of observations = 30

Index	X	Y(Obs)	Y(calc)	Error
1	7.05100E+02	6.70000E-02	7.78206E-02	-1.08206E-02
2	6.85700E+02	9.70000E-02	9.44073E-02	2.59267E-03
3	6.72800E+02	1.26000E-01	1.18256E-01	7.74392E-03
4	6.69100E+02	1.36000E-01	1.27874E-01	8.12602E-03
5	6.56200E+02	1.80000E-01	1.73636E-01	6.36366E-03
6	6.45100E+02	2.32000E-01	2.30287E-01	1.71347E-03
7	6.34000E+02	2.99000E-01	3.03123E-01	-4.12261E-03
8	6.22100E+02	3.88000E-01	3.95162E-01	-7.16239E-03
9	6.15600E+02	4.42000E-01	4.48376E-01	-6.37606E-03
10	6.06400E+02	5.20000E-01	5.22087E-01	-2.08658E-03
11	5.98100E+02	5.83000E-01	5.81674E-01	1.32608E-03
12	5.88800E+02	6.39000E-01	6.33990E-01	5.01013E-03
13	5.82400E+02	6.63000E-01	6.58006E-01	4.99368E-03
14	5.76900E+02	6.74000E-01	6.69603E-01	4.39674E-03
15	5.70400E+02	6.73000E-01	6.72026E-01	9.73761E-04
16	5.63000E+02	6.58000E-01	6.60423E-01	-2.42323E-03
17	5.54700E+02	6.27000E-01	6.32030E-01	-5.02968E-03
18	5.44600E+02	5.79000E-01	5.83890E-01	-4.88961E-03
19	5.37200E+02	5.46000E-01	5.46608E-01	-6.07610E-04
20	5.31700E+02	5.24000E-01	5.21343E-01	2.65747E-03
21	5.20600E+02	4.88000E-01	4.82305E-01	5.69463E-03
22	5.05800E+02	4.48000E-01	4.48483E-01	-4.82947E-04
23	4.94800E+02	4.11000E-01	4.14532E-01	-3.53155E-03
24	4.90200E+02	3.90000E-01	3.93441E-01	-3.44115E-03
25	4.85500E+02	3.65000E-01	3.67140E-01	-2.14022E-03
26	4.80000E+02	3.33000E-01	3.31077E-01	1.92252E-03
27	4.73600E+02	2.89000E-01	2.84563E-01	4.43685E-03
28	4.68900E+02	2.55000E-01	2.49634E-01	5.36601E-03
29	4.60600E+02	1.94000E-01	1.92033E-01	1.96674E-03
30	4.49600E+02	1.21000E-01	1.33185E-01	-1.21850E-02

Index	Parameter	Standard Deviation
1	4.920046E+02	9.696768E-01
2	5.728387E+02	5.988908E-01
3	8.197737E-04	5.132359E-05
4	2.539289E-04	7.842775E-06
5	2.172021E-01	7.260215E-03
6	6.007763E-01	4.499583E-03
7	7.074790E-02	4.267809E-03